HAPTIC SOCIAL INTERACTION FOR AVATAR ROBOT SYSTEM: BILATERAL INTERACTION CONTROL AND USER EXPERIENCE EVALUATION

M. (Mahmoud) Barazi

MSC ASSIGNMENT

Committee:
dr. ir. J.F. Broenink
dr. ir. D. Dresscher
dr. ing. G. Englebienne

February, 2021

003RaM2021
Robotics and Mechatronics
EEMCS
University of Twente
P.O. Box 217
7500 AE Enschede
The Netherlands

Haptic social interaction for avatar robot system: bilateral interaction control and UX evaluation

Mahmoud Barazi, *m.barazi@student.utwente.nl, s2194783, Robotics and Mechatronics (RaM)*
Douwe Dresscher, *d.dresscher@utwente.nl, Robotics and Mechatronics (RaM)*
Gwenn Englebienne , *g.englebienne@utwente.nl, Human Media Interaction (HMI)*

***Abstract*—In this paper, a study is presented on social interaction through a tele-operation system, particularly handshake activity. The study includes investigation of the handshake aspects involved in the human-human handshake scenario, designing a bilateral control system, and evaluation of the developed handshake system. The proposed bilateral control scheme was tested by reusing a variable-stiffness interaction control of which the stiffness varies according to the operator anatomical arm stiffness using EMG sensor. The control design was validated by an objective transparency evaluation. The developed robotic handshake system was also subjectively evaluated through assessing the user experience about the handshake interaction. The results show that even though some hardware limitations are present, the system seems to be capable of providing the human with genuine engaging handshake experience.**

I. Introduction

The popular application of the tele-operation system is accomplishing tasks remotely such as objects manipulation and precisely positioning a needle. However, the tele-operation systems can be also used for interactional social applications [3]. The social human-robot interaction should be considered from a human-centered perspective. The social interaction includes certain aspects that needs to be taken into consideration for the interaction to be perceived as genuine. Corrupted social human-robot interaction may have negative influence on the user's experience that could even extend to the user's future of interaction with robots [11]. For a tele-handshake activity such as the one depicted in figure 1, there are two main handshake aspects that need to be taken care of in the system: handshake vigour and grasp strength [8]. The other handshake aspects are either not relevant or already taken care of. For instance, the aspects grip completeness, temperature and texture are already taken care of due to the fact that the soft hand is human-like having a complete grip, and covered with texture. Although both of these aspects grip strength and vigour are important, the focus of this work will be on the handshake vigour and the arm dynamics in handshake.

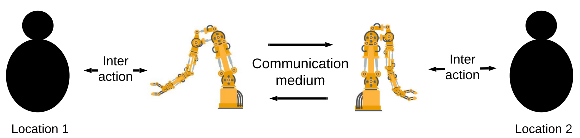

Fig. 1: A depiction for a tele-handshake system

From control point of view, a tele-handshake system should enable the handshake partners to feel each other's forces and anatomical arm stiffness. The conventional fixed-stiffness interaction control can not achieve that function as the stiffness parameter is constant, whereas the human arm stiffness is a personal characteristic, and thus differs from person to another. The human arm's anatomical stiffness can be estimated based on the arm muscle contractions using electromyograph sensors [9][1]. The approach of [9] will be applied in this work.

The goal of this work is to construct a tele-handshake system by introducing a new control architecture, namely the personalized force feedback control architecture. Additionally, the proposed architecture will be validated with using the variable-stiffness feature using EMG sensor. Finally, the UX is evaluated to investigate how natural the remote human-human interaction is through a robot system.

This paper is structured as follows: in section II, related work to haptic handshake are discussed. Section III presents the proposed control design and compares it to the conventional tele-operation control design. In section IV, the user experience components are mentioned. Sections V and VI show the obtained results. Discussion on the obtained results follows in section VII.

II. Related work

There are several handshake systems can be found in literature. These systems might differ from each other in the number of DOF that a system has, in the mechanical system design, in the human experience that the system is capable of offering to the human or in the control design of the handshake system.

(Kunii and Hashimoto, 1995) in [4] proposed a handshake system which basically allows the handshake partners to shake hands remotely. However, the system is 1-DOF system, meaning that it is able to perform only one translation, while the handshake motion is more complex than 1-DOF motion. Another system is presented by (Wang et al., 2009) in [10] that has 10-DOF, and so should be able to provide more compliance to the user, but the deficiency of this system is that it is not bilateral.

The system developed in [2] by (Alhalabi and Horiguchi, 2001) allows the handshake partners to feel forces feedback in principle. But the haptic devices used are Phantom devices which are not dedicated for handshake application, and therefore do not provide force feedback that corresponds to the human handshake vigour.

In the study [7], (Nakanishi et al., 2014) attempted to search the influence of transporting the haptic sensation channel and the visual channel in videoconferencing. Their interesting outcome, which is the designed actuated robot hand, is focused on grip force, showing the importance of grip strength on the UX. But they did not consider the arm vigor as their system is not multi-DOF; the system on the user side can only grasp the user hand but without arm motion. The importance of arm vigour will be investigated in this work.

III. Control design

In the handshake social activity, natural social interaction is the goal. This suggests using the interaction control that treats the human-robot interaction more compliantly. By using interaction control which is spring-based, the robot will have a space of compliance for interaction with human in case the human attempts to move the robot as in handshake application.

A. Interaction control

The interaction control is based on the concept that a virtual spring is connected between the mater and slave systems such that the system will behave compliantly while attempting to reach the equilibrium point where the position difference between the master and slave is zero. A simple single-degree-of-freedom interaction control-based tele-operation system is illustrated in figure 2.

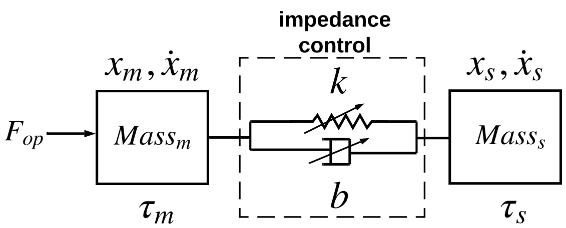

Fig. 2: An illustration for the interaction control for simple tele-operation system. $Mass_m$ and $Mass_s$ represent, respectively, the master and slave robots. Parameters k and b are stiffness and damper to be tuned. The term b is not used in this work; it is set to zero.

The control law of the interaction control is as follows excluding the damper term:

$$F_s = K\left(X_m - X_s\right) \tag{1}$$

where F_s is the force applied on the slave device, X_m is the master device position, and X_s is the slave device position. Then the force feedback is reproduced on the master device as follows:

$$F_m = -F_s \tag{2}$$

where F_m is the force feedback on the master device. The Cartesian force is mapped into the joints space by using the geometric Jacobian of the corresponding serial robot arm:

$$\begin{aligned}\tau_m &= J_m^T F_m \\ \tau_s &= J_s^T F_s\end{aligned} \tag{3}$$

where J_m ad J_s are the master and slave arms' Jacobians, respectively.

B. Variable-stiffness interaction control

The method of [9] was followed in this work. The motivation for modulating the control spring is to convey the anatomical human arm stiffness of the operator and recipient to each other so that both can feel the presence of each other. The human arm stiffness can be estimated by first measuring the muscles activity, or the EMG signals, of antagonistic muscles pair.[1] The sensor used for measuring the muscles activity is the myo armband sensor. Then the measured EMG signal is maintained to be positive by using the normalization formula written below[9]:

$$\hat{\alpha} = \max\left(0, \frac{\alpha - \alpha_{\min}}{\alpha_{\max} - \alpha_{\min}}\right) \tag{4}$$

where α_{min} and α_{max} are the maximum and minimum activation levels, which are obtained by calibration process. This calibration process is application-dependent. For handshake application, the minimum muscle activity is measured when the user is asked to perform weak handshake scenario that is sufficient to obtain minimal muscle activity from the antagonistic biceps-triceps muscles pair; and the maximum muscle activity is obtained by asking the user to perform strong handshake. Next, the muscles co-contraction level can be calculated by the following equation:

$$\eta = \min\left(1, \hat{\alpha}_{flexor}, \hat{\alpha}_{extensor}\right) \tag{5}$$

where α_{flexor} and $\alpha_{extensor}$ are the flexion and extension muscles activation of the biceps-triceps antagonistic muscles. Then the robot arm stiffness can modulated by the following formula:

$$K(\eta) = K_{\min} + \eta \cdot \left(K_{\min} - K_{\max}\right) \tag{6}$$

where K_{min} and K_{max} are the minimum and maximum sitffnesses the can be set to the robot. These values are chosen based on the requirements of the application. The values for this work were chosen based on the work of [9] with values slightly lower as handshake application requires considerable amount of compliance in the robot. The maximum and minimum stiffness are listed in table I.

	min	**max**
Trans. stiffness [N/m]	100	550
Rot. stiffness [N.m/rad]	3.5	10.5

TABLE I: Max and min stiffnesses used in the stiffness updating rule

Then the control law proposed earlier in equation 1 becomes a function of the co-contraction level:

$$F_s(\eta) = K(\eta)\left(X_m - X_s\right) \tag{7}$$

In fact the co-contraction level is filtered before being used in the control law since the EMG signals are noisy. The filtering is performed by the following equation:

$$\begin{gathered}y[n] + b_1 y[n-1] + b_2 y[n-2] = \\ a_1 x[n] + a_2 x[n-1] + a_3 x[n-2]\end{gathered} \tag{8}$$

[1]Antagonistic muscles pair means when one muscle contracts, the other one relaxes, and vice versa.

The figure 3 below shows the measurements of the muscle activity of the biceps and triceps muscles filtered at three different cut-off frequencies.

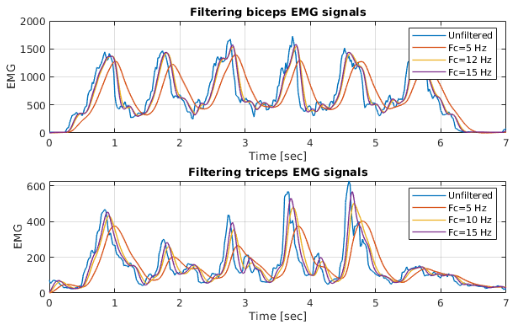

Fig. 3: The muscle activity signals measured using the myo armband sensor: filtered and unfiltered

In order to know which type of filter is required, it was found in literature that the bandwidth of electrical activity signal of human arm lies in the range of $[0, 15]Hz$ [1]. This suggests designing a low pass filter with relatively low cutoff frequency. The cutoff frequency was chosen to be $15Hz$ as choosing small frequencies leads to phase lag.

C. *Personalized force feedback control*

The proposed control design in this work is a bilateral version of the variable-stiffness control design presented in the previous section, but it is two-controller control design: The force of one spring is applied on one robot, and the force of the other spring is applied on the other robot. The design can be seen in figure 4.

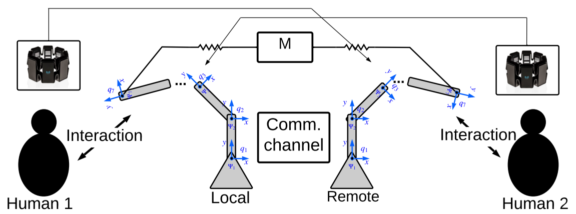

Fig. 4: Illustration of the two-spring control design.

As the figure shows, the operator's anatomical arm stiffness modulates the robot arm of the recipient, and the recipient's anatomical stiffness modulates the robot arm of the operator. With this design, operator's and recipient's handshake vigour would be transported to each other, which is a personal factor that differs according to the personality traits.

IV. Experiments and control design validation

A. *Realizability of handshake vigour*

This experiment was conducted to quantitatively measure the human handshake vigour, or shake force, during handshake. This experiment actually can be considered as an extension and completion for the experiment conducted in the work of [10] which is the only work in literature that attempted to measure the shake force to the best of the author knowledge. However, they have done the experiment with one subject only, which is slightly inaccurate, because if another person would have performed the interaction with the robot arm, different results for the shake force would be obtained. In addition, they have not mentioned any information about the stiffness of the robot arm, at which they have performed the experiment. The interaction force with the robot arm, or the shake force, changes based on the robot stiffness. That is why their results can not be generalized. To produce more reliable and accurate results, first the shake force measurement experiment was performed on a population of human subjects. Second, the experiment is done over multiple stiffness values. In this research, we performed the experiment with 12 healthy participants aged between 20 and 30 years old, including one female. Every participant was asked to shake hands with the Franka robot arm in three different scenarios, namely weak handshake scenario, normal handshake scenario and strong handshake scenario. In each scenario, the shake force was measured over three different stiffness settings, namely low stiffness, medium stiffness and high stiffness. So in total, the number of trials of this experiment was 108 trials. The experiment results are shown in figure 5.

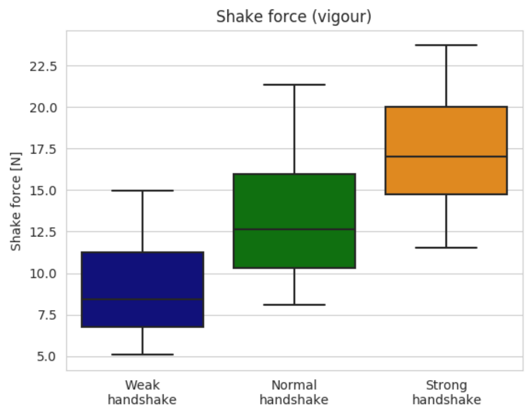

Fig. 5: The findings of quantifying the human handshake vigour. The whiskers of the a box represent the maximum and minimum. The top, the line inside the box and the bottom are respectively the 25th, 50th and 75th percentile

The figure 5 shows three categories of handshake magnitude obtained at different conditions. Each force category was found by calculating the average of the forces obtained from a certain handshake scenario over the three stiffness values. Although the interaction force is dependent on the robot properties itself such as the joints friction and perceived weight, performing the experiment at three stiffness values accounts for that effect. In other words, the figure 5 shows more reliable measurements for the interaction force during the human-robot handshake interaction, than the results of [10].

Looking at the forces in figure 5, it can be clearly noticed that the handshake strength is, as expected, proportional to the measured force, which gives more credits to the reliability of the obtained results in comparison to the results of [10]. Another result that can be derived from the figure 5 is that the handshake vigour is realizable by the Franka robot arm, because all the forces by all participants in different conditions were observed to be smaller than the maximum interaction force that the Franka robot withstands which is 30N.

B. EMG sensor calibration

Co-contraction level differs from person to another, therefore for every person who intends to wear the myo armband sensor, a calibration process should be done. The calibration is to find the maximum and minimum activation levels α_{min} and α_{max} of a particular person. The calibration of the EMG sensor is application-dependent. Two scenarios are executed to find the maximum and minimum activation levels.

1) The first scenario: weak handshake: The person hardly holds the hand of the robot arm without exerting much grasp force, and then shakes hands with the robot. It was observed that this activity is sufficient to obtain minimal muscles activation measurements from the biceps-triceps muscles.

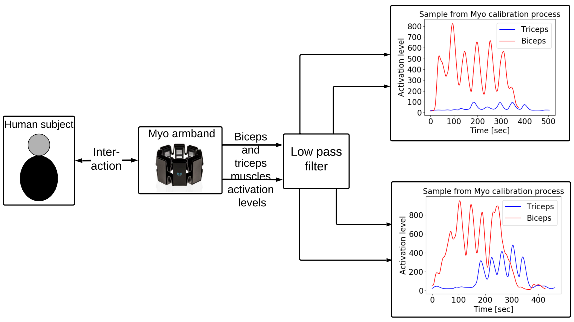

Fig. 6: The procedure of Myo armband calibration process. The lower plot was obtained from stiff handshake calibration scenario, and upper plot from a weak handshake calibration scenario

2) The second scenario: strong handshake: In this scenario, a person is required to shake hands with the robot arm slightly stronger than his normal handshake magnitude that he uses mostly so that the muscle activation corresponds to the maximum contraction level. A typical result that comes out of this calibration can be seen in figure 6 in the bottom plot.

C. Control design validation

In this experiment, the operator and the recipient perform a tele-handshake with each other remotely using the conventional and the proposed control architectures.

1) One-spring control design (conventional): As discussed before, the conventional tele-operation control architecture applies the same force feedback on the local and remote robots. For tele-handshake application, this eliminates the possibility of conveying the handshake forces of the handshake partners to each other. This is shown in figure 7 by an experiment where four participants performed handshake with operator three times each, and the average force feedback of each participant was calculated over the three trials.

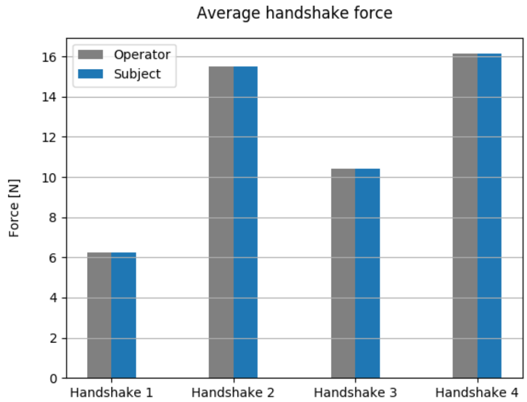

Fig. 7: The forces feedback applied on the local and remote robot are the same using the conventional control architecture disallowing to exchange the handshake forces between the handshake partners. The stiffness value was arbitrarily chosen to be $150N/m$.

The results in figure 7 shows the limitation of the one-spring control design for social interaction applications: this control design does not realize the fact that people exert different forces, where the forces are the same as can be noticed in the figure.

2) Two-spring control design (personalized): In this experiment, three participants performed tele-handshake with the operator using the proposed control architecture, where there are two controllers in the system: one applies force on the local robot, and one applies force on the remote robot system. This allows setting different stiffness values for the two robots. As can be noticed in figure 8, the forces feedback applied on the two robot arms are different. This enables transferring the impedance of the human arm to the other handshake partner. Regarding the stiffness values in this experiment, they were chosen arbitrarily to be $150N/m$ and $240N/m$ for remote and local robots, respectively. As a proof of concept, the proposed control design is validated, in the next experiment, by estimating the human arm impedance using the method of [9] in handshake application, for the purpose of transferring the handshake forces of the operator and subject to each other.

3) Proof of concept: Two myo armband sensors are used in this experiment to estimate the human arm co-contraction level for both of the handshake partners based on [9] method. Even though the handshake dynamics is non-linear, the up-down-axis motion still can be considered as the predominant motion in handshake [2]. The up-down-axis is the z-axis of the inertial frame of the Franka robot base. Therefore in figure 9 only the z-component of the Cartesian trajectory of the handshake is visualized as an indication for when the handshake partners have started the handshake motion.

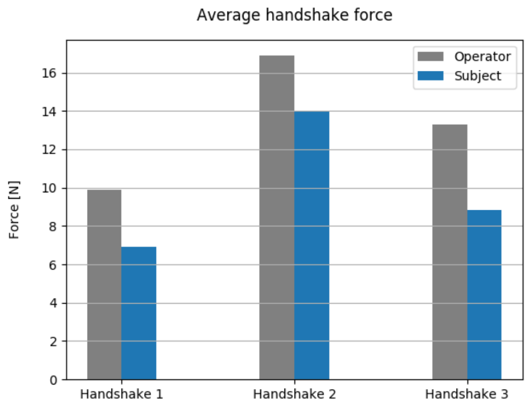

Fig. 8: The forces feedback applied on the local and remote robot are different using the proposed control architecture allowing to exchange the handshake forces between the handshake partners

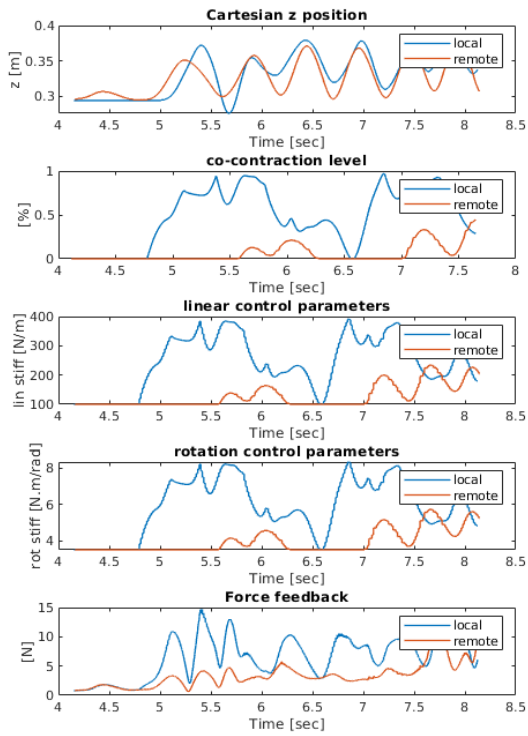

Fig. 9: Variable-stiffness control adjusts the robots' stiffnesses based on the handshake partners' muscles contractions

It can be noticed that the contraction, linear stiffness and rotation stiffness have the same pattern of variation. This is because the relationship that relates the stiffness and co-contraction level is a linear relationship as equation 6 shows. The important point to notice here is that the stiffness is modulated based on the handshake partners' interaction with the robot arms; once the motion along the z-component starts, the operator needs to contract/stiffen his arm muscles which leads to the measurements of the contraction level, and the stiffness is updated accordingly. Before and after the handshake interaction, the operator and subject muscles are relaxed, and so the contraction level is measured to be zero. As such the stiffness is not updated and it takes the value of the minimum stiffness which is 100 [N/m] for the translation stiffness, and 2.5 [N.m/rad] for the rotation stiffness. Since the force feedback is determined by the stiffness coefficient, then the force feedback that each handshake partner feels also varies accordingly. This can be seen in figure 9.
Another noticeable point in the figure 9 is that the force feedback increases with the increase of co-contraction level, which shows the effectiveness of using the EMG sensor to represent and even to reasonably quantify the human handshake vigour.

V. User experience evaluation

Following [11] the user experience should be approached from three different perspectives. One of these perspectives is the achievement of the main function which is the handshake in this case. How the user perceives the robot is another important part of the user experience. Finally, the emotional state quality that is left in the user before, during and after the interaction constitutes a significant part of the user experience. The three evaluation perspectives along with the metrics proposed in this research are shown in figure 10, and they are discussed below.

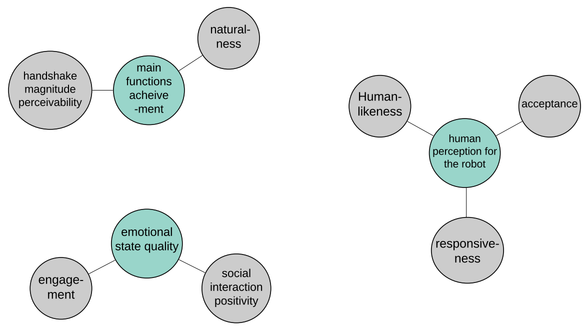

Fig. 10: Evaluation perspectives for human-robot interaction along with the elements constituting each perspective

A. Evaluation perspective I: user-perception-for-robot evaluation

The first perspective is to see how the human perceives the robot. During human-robot interaction, the user may have several impressions and feelings towards the robot. For instance, the mechanical shape of the robot whether it is human-like or machine-like, has influence on the user impression even before the interaction begins. The more the robot is human-like, the better and more genuine the human-robot interaction is [6].
Three evaluation metrics were chosen for evaluating the perception of the user for the robot. They are shown in figure 10.

The first metric is the *human-likeness* [6]. In handshake application it is important to have a robot system that is human-like that would let the user feel that he/she shakes hands with a human. The second metric is the social acceptance [6]. This metric is aimed to subjectively quantify how acceptable the robot is by the user in terms of ease-of-use. A factor that has influence on acceptance is the robot hardware complications. The complexity of the hardware is damaging for the user experience because the user usually is not familiar with robot interfaces. The third and last metric used in evaluating how the user perceives the robot is responsiveness. Responsiveness is measure of and how the robot responds in its interaction with the user. The responsiveness of the robot is an important characteristic in handshake, because it is related to vigour handshake aspect. The work of [10] has emphasized on the mutual compliance between the handshake partners. If the robot system is sluggish in its actions, then mutual compliance, or vigour, would not be achieved. Accordingly, to evaluate the aforementioned points, the questionnaire in table II was formulated.

B. Evaluation perspective II: main functions achievement

The second angle from which the human-robot interaction should be evaluated is the main functions that the robot is responsible to achieve. The evaluation metrics for the main functions are dependent on the application. For haptic handshake system, the main functions are realizing the handshake aspects, especially the grasp force aspect and vigour. The user experience evaluation regarding the vigour should be done at different stiffness values to see which one is the optimal for natural haptic handshake. So the two evaluation metrics for this aspect might be chosen to be *naturalness*, to measure how natural the perception of the handshake feels for the user, and *handshake magnitude perceivability* to measure the user's feeling about the stiffness variation and whether it corresponds to different handshake magnitudes. For these subjective metrics, the questionnaire items can be made as in table III.

C. Evaluation perspective III: emotional state quality

The last component of the user experience in human-interaction that should be assessed is the emotional quality. It is important to design robot control system that ensure the interaction experienced by the user is not only acceptable and safe, but also as positive. Because, the social robots are intended to support the humans and add positive values to the human daily live; if otherwise the user does experience the interaction with the robots as negative, the consequence might be a reluctance to interact with robots, which in turn may inhibit the acceptance of robots at all [6]. For handshake application, the system should provide the user with the social positive emotional state that humans obtain from shaking hands with each other. Two metrics could be utilized to measure the change in emotional state of the user after haptic handshake. The first might be selected to be *engagement* to see how much how exciting the handshake experience was. The second metric could be *positivity* to check whether or not the interaction of the user with robot experienced as a positive social interaction. Therefore the questionnaire items can be designed as shown in table IV.

VI. Experiments and Subjective Evaluation

In this experiment, eleven human subjects have participated in doing the experiment of tele-handshake through two Franka robot arms. The experiment was performed over three stiffness values, namely low stiffness, high stiffness and variable stiffness. The high stiffness and low stiffness values are the same as those shown in figure I. For the variable stiffness, the myo armband EMG sensor is used. Even though the experiment was done over three choices of stiffness values, some of the users' responses on the experience evaluation questionnaire are constant. Because, some questionnaire items are related to the robot itself, and not related to the stiffness or operation performance. Particularly, the user response is constant for *acceptance*, *human-likeness*, *engagement* and *social interaction positivity*. The results are shown in figure 11.

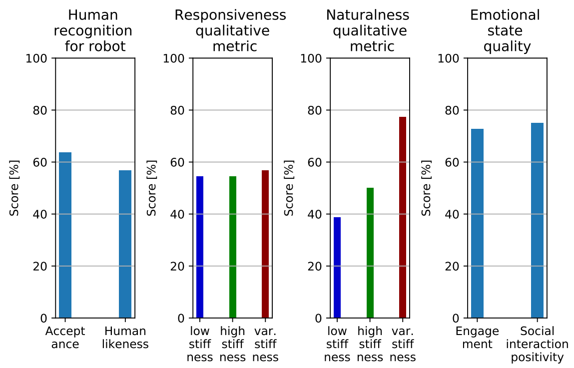

Fig. 11: The findings of the subjective evaluation. The scores are mapped into percentages. Obtaining score below 50% means the system fails in realizing the corresponding feature. Obtaining score higher than 50% means the system passes in realizing the corresponding feature.

To obtain more intuitive and interpretable insight about the performance, the total score is mapped to a percentage score using the following:

$$S = \frac{S - S_{min}}{S_{max} - S_{min}} \times 100\% \tag{9}$$

where S is the score resulted from summing the users' responses, and n is the number of participants, S_{min} is the worst score that could be obtained, and S_{max} is the best score that could be obtained. As can be seen in 11, the developed system has passed in realizing the features of human-likeness and acceptance by obtaining the scores 56.8% and 63.6% respectively. Likewise for the responsiveness metric. Observing the system's grades at naturalness, the measure of handshake vigour, it can be seen that the system has failed in realizing natural handshake in the case of low stiffness and barely passed in the case of high stiffness, where the scores are 38.6% and 50%, respectively. Whereas for variable stiffness,

Metric name	Questionnaire item	Metric qualitative values				
		-2	-1	0	1	2
Social acceptance	The robot system was socially acceptable	strongly disagree	disagree	neutral	agree	strongly agree
Responsiveness	The robot's movements were agile	strongly disagree	disagree	neutral	agree	strongly agree
Human-likeness	The robot was human-like	strongly disagree	disagree	neutral	agree	strongly agree

TABLE II: Evaluation questionnaire for the user perception about the robot

Metric name	Questionnaire item	Metric qualitative values				
		-2	-1	0	1	2
Naturalness	The manipulation experience was natural	strongly disagree	disagree	neutral	agree	strongly agree
Handshake magnitude perceivability	The handshake magnitude of the handshake partner was perceivable	strongly disagree	disagree	neutral	agree	strongly agree

TABLE III: Evaluation questionnaire about main functions achievement

Metric name	Questionnaire item	Metric qualitative values				
		-2	-1	0	1	2
Engagement	The interaction with the robots was engaging	strongly disagree	disagree	neutral	agree	strongly agree
Social interaction positivity	The handshake with the robot boosted positivity	strongly disagree	disagree	neutral	agree	strongly agree

TABLE IV: Evaluation questionnaire for emotional state quality

the handshake was reported to be the most natural, where the developed system has scored 77.3% at naturalness. For the last two evaluation metrics are the engagement and the social positivity, the scores are 72.7% and 75% respectively.

VII. Discussion

- **Human-likeness**: It was unexpected to have low score for the human-likeness metric since the robot arms that were used are 6-DOF arms having almost the same capability of the human arm in moving in 6 degrees of freedom. But obtaining the low score at human-likeness is interpretable. The Franka robot arm configuration during the experiment was not similar to the configuration of a human arm during the handshake. Because, the base of the Franka robot arm (or the shoulder) is attached on the ground, and so the robot arm is originating from a point underneath and directing upwards, whereas the human arm base (or the shoulder) is attached at the human trunk, and so the arm is originating from a point up and directing downwards. This means that during the handshake experiment, the robot arm did not mimic the human arm configuration of the handshake. That was mentioned by participants.
- **Responsiveness** It was expected for the responsiveness to obtain the highest score at the high-stiffness case (think of relatively stiff spring; even if you apply small force, then it oscillates responsively, and you feel it responds to your input; whereas if the spring is compliant, then it does not really oscillate as much as the stiff spring if input is applied). Even though the Franka robot was shown in [5] to be a suitable input haptic device in terms of transparency (or reproducing force feedback) and in terms of safety, it is still, however, not a haptic device. This means that the joints frictions might not be as low as the joint friction of haptic device such as the Virtuose 6D. Another factor is the perceived weight during the physical interaction with the robot. In comparison with the Virtuose 6D robot arm ($12kg$), the perceived weight of the Franka robot arm ($18kg$) is higher, which leads to the feeling that the robot is sluggish in its motion. This means that the human in fact does not only feel the forces of the handshake partner, but also the weight of the robot.
- **Naturalness**: For low stiffness, the operator's forces to displace the recipient arm are not effective because the local and remote robots are loosely connected, and therefore the recipients do not feel synchrony or natural handshake. For extremely high stiffness, the recipient's robot arm is not even interactional, meaning that the recipient can hardly displace the arm because of the high stiffness. Accordingly, the participants did not find this handshake natural either. Obtaining the highest score for naturalness at the case of variables stiffness case can be attributed to the fact that the handshake is a mutual process, where the handshake partners both contribute with forces and feel each other's forces, which was robotically realized by using the EMG sensor. Based on the participant's force and motion, the operator attempts to shake hands with the same force and motion, and so the participant feels a synchrony, seemingly.
- **Engagement** and **positivity**: Having the developed system passed at the *engagement* and *social positivity* metrics with sufficiently high scores means that the developed system seems to be capable of providing the user with a genuine engaging handshake experience.

VIII. Conclusion

In this work, an experimental system for haptic robotic handshake was designed and evaluated. Although, there are two important handshake aspects, namely handshake vigour and grip strength aspect, this has work focused on one of the handshake aspects: handshake vigour. In order to provide the handshake partners with realistic handshake vigour, a new interaction control architecture was proposed, consisting of two virtual springs connected between the local and remote, allowing different forces feedback to be applied on the local and remote robots. Validation for the control design was made. The effectiveness of the proposed control in offering the appropriate handshake experience was tested by subjective evaluation for the experience of human subjects. The developed system has shown quite satisfactory performance in terms of handshake human experience overall, but slightly underperformed specifically in terms human-likeness and responsiveness due to factors related to the robot itself: non-human-like kinematic configuration and relatively high perceived weight. Regarding improvements and future work, other impedance estimation method could be used, and tested on the proposed control architecture. Additionally, the passivity for two-spring design could be investigated, as well as the delay in communication channel.

References

[1] Arash Ajoudani, Nikos Tsagarakis, and Antonio Bicchi. Tele-impedance: Teleoperation with impedance regulation using a body–machine interface. *The International Journal of Robotics Research*, 31(13):1642–1656, 2012.

[2] M Osama Alhalabi and Susumu Horiguchi. Tele-handshake: a cooperative shared haptic virtual environment. In *Proceedings of Eurohaptics*, volume 2001, pages 60–64. Citeseer, 2001.

[3] Michel Franken, Stefano Stramigioli, Sarthak Misra, Cristian Secchi, and Alessandro Macchelli. Bilateral telemanipulation with time delays: A two-layer approach combining passivity and transparency. *IEEE transactions on robotics*, 27(4):741–756, 2011.

[4] Yasuharu Kunii and Hideki Hashimoto. Tele-handshake using handshake device. In *Proceedings of IECON'95-21st Annual Conference on IEEE Industrial Electronics*, volume 1, pages 179–182. IEEE, 1995.

[5] Adrian Ion Lazar. Safe use of robotic arms as input devices. Master's thesis, University of Twente, 2019.

[6] Jessica Lindblom and Rebecca Andreasson. Current challenges for ux evaluation of human-robot interaction. In *Advances in ergonomics of manufacturing: Managing the enterprise of the future*, pages 267–277. Springer, 2016.

[7] Hideyuki Nakanishi, Kazuaki Tanaka, and Yuya Wada. Remote handshaking: touch enhances video-mediated social telepresence. In *Proceedings of the SIGCHI Conference on Human Factors in Computing Systems*, pages 2143–2152, 2014.

[8] Elizabeth M Shipps and Harvey R Freeman. Handshake: Its relation to first impressions and measured personality traits. *Psi Chi Journal of Undergraduate Research*, 8(4):144–148, 2003.

[9] Kees Van Teeffelen, Douwe Dresscher, Wietse Van Dijk, and Stefano Stramigioli. Intuitive impedance modulation in haptic control using electromyography. In *2018 7th IEEE International Conference on Biomedical Robotics and Biomechatronics (Biorob)*, pages 1211–1217. IEEE, 2018.

[10] Zheng Wang, Angelika Peer, and Martin Buss. An hmm approach to realistic haptic human-robot interaction. In *World Haptics 2009-Third Joint EuroHaptics conference and Symposium on Haptic Interfaces for Virtual Environment and Teleoperator Systems*, pages 374–379. IEEE, 2009.

[11] Katharina Werner, Johannes Oberzaucher, and Franz Werner. Evaluation of human robot interaction factors of a socially assistive robot together with older people. In *2012 sixth International Conference on complex, intelligent, and software intensive systems*, pages 455–460. IEEE, 2012.

Appendix

The following table contains the results of the statistical tests on the data from the UX evaluation.

Human-likeness	-	**p-value**	**t_{crit}**	**t**
		0.17	1.81	1.00
Acceptance	-	**p-value**	**t_{crit}**	**t**
		0.025	1.81	2.21
		p-value	**F_{crit}**	**F**
Responsiveness	**low stiff.**	0.97	3.31	0.021
	var. stiff.			
	high stiff.			
		p-value	**F_{crit}**	**F**
Naturalness	**low stiff.**	0.016	3.31	4.76
	var. stiff.			
	high stiff.			
Engagement		**p-value**	**t_{crit}**	**t_{stat}**
		0.008	1.81	2.88
Social positivity		**p-value**	**t_{crit}**	**t_{stat}**
		0.0002	1.81	5.16

TABLE V: The results of the one tail t-tests and ANOVA tests

Acknowledgement

I would like to thank my supervisors, Douwe Dresscher and Gwenn Englebienne, for opening my eye on how this thesis should be done, despite some difficulties. Also, thanks to Robin Lieftink and Nimish Nadgere who have helped me in performing the experiments.

Acknowledgement

I would like to thank my supervisors, Douwe Dresscher and Gwenn Englebienne, for opening my eye on how this thesis should be finished, despite some difficulties. I will definitely not forget to thank my parents, my sisters and my brother for your continuous support. Last but not least, thanks to Robin Lieftink and Nimish Nadgere who have helped me in performing the experiments of this thesis.

Summary

Robots increasingly being utilized for social activities. Handshake is an important social interaction activity in society. Therefore it becomes important to study the handshake from robotic point of view, to investigate the feasibility of having a robot system that enables two persons to shake hands remotely.

The research group RaM of Twente University participates in the ANA Avatar XPRIZE competition. The goal of competition is to set up a tele-robotic system that should enable the operator to feel a remote environment and possibly interact with other people remotely. One of the intended interaction types to perform is the social interaction in which the operator shakes hands with another person in a way that the handshake partners feel the presence of each other. The latter interaction type, remote handshake, is the topic of this thesis. Therefore, in this work, an experimental apparatus was set up consisting of two 6- DOF robot arms and two EMG sensors, variable-stiffness bilateral interaction control was implemented enabling to apply different force feedback on the local and remote robot arms which makes the handshake partners feel the presence of each other, and finally the user experience of eleven participants was evaluated.

The obtained results show that by using the variable-stiffness control method, it is feasible to have a robot system that enables two persons to feel the presence of each other. In addition to that, the user experience evaluation shows that shaking hands remotely is sufficiently engaging and exciting as the real direct handshake between two persons, and that the remote handshake provides the user with social positivity. However, the robot system was not so responsive to the user because of the relatively high perceived weight of the robot arm. Also, robot hands were not part of the system which might have slightly influenced the user experience.

الرُوبوتَاتْ بِشَكِل مُتَصاعِد يِتِمْ الإِسْتِفَادة مِنْهَا مِنْ أَجِل نَشاطَاتْ إِجْتِماعِيّة. المُصَافَحِة هِي نَشَاطْ إِجتِماعِي تفَاعلي فِي المُجتمع. لِذلك، هو يصبح مهم دِراسة المُصافحة مِن وِجهة نظر رُوبوتِية مِن أجل التحقق مِن إمكانِية الحصول على نِظام رُوبوتي يمكِن شخصين مِن التصافح عن بعد.

المَجْمُوعَة البَحْثِيّة RaM التَابِعَة لِجَامِعَة Twente تُشَارِكْ في مُسَابَقِة ANA Avatar XPRIZE. الغَايَة النهائِيّة مِن هذه المُسابقِة هِي إِقَامة نِظام رُوبوتي الذي ينبغي أن يُمكِّن المُشغِّل مِن الإِحساس بالبِيئة البعِيدة و رُبما مِن التفاعل مع ناس آخرين عن بعد. واحِد مِن أنواع التفاعُل المستهدف تَنْفيذه هُو التَفاعُل الإجْتِماعِي، خاصةً تفاعُل التَصافُح الذي يتصافح فِيه المُشغِّل مع شَخص آخر بِطريقة أنّ المُتصافِحين يشعُرون بحضور بعضهم البعض. نوع التفاعُل الأَخير، التصافُح عَن بُعد، هو مَوضُوع هذا البَحْث. لِذلك، في هذا العَمَل، جهاز مَخبري تمّ إِعْدَاده مُؤَلّفاً مِن 6-DOF أَذْرُع رُوبوتِيّة وحسّاسات EMG، آلِيّة تحكّم ثُنَائِيّة مُتَغيِّرة الصلابة تم تنفيذها مُمَكّنَة مِن تطبيق قوة إِرتجاعِية مُتباينة على الروبوت المحلِّي والبعِيد الذي يجعل المُتصافِحين يَشْعُرون بِحضُور بعضهم البَعْض، وأخيراً تَجرُبَة المُسْتَخدِم لِأَحد عشر مُشارِك تَمّ تَقْييمها.

النَتَائِج التِي تَمّ الحُصُول عَلَيْها تُبَيّن أَنّه بِإستخدام آلِيّة التَحَكُّم الثُنَائِيّة المُتَغيّرة الصَلابة، مِن المُمكِن الحصول على نِظام رُوبوتي يمكِن شخصين مِن الإِحساس بِحضُور بعضِهم البعض عن بعد. بالإِضافة إلى ذلك، تقييم تجربة المستخدِم تبين أن المُصافحة عن بعد هِي جذابة و مُشوقة كالمصافحة الحقيقية المباشرة بين شخصين، وأنّ المُصافحة عن بعد تُزوِد المُستخدِم بإيجابِيّة إجتماعِيّة. إلّا أنّ، النظام الرُوبوتي لم يكُن مُتجاوب كثيراً للمُستخدِم بِسَبَبْ الوزن المحسُوس العالي نِسبياً للذراع الرُوبوتي. أيْضا، يد رُوبوتيّة لمْ تكُن جُزْء مِن النِظام الذي مِن المُمكِن قدْ أثّر على تجرُبة المُسْتَخدِم سلبِيّا قَلِيلاً.

Contents

1 Introduction

In this chapter the project context is clarified. Then the research questions to be answered throughout this thesis project are formulated. After that the work in literature that is relevant to the same main goals of the project is presented. Also, the main challenge faced in this project, which arises from the robotic system hardware constraints, is mentioned. Finally a layout for the report is made.

1.1 Context

Tele-operations attracted the attention in robotics research for empowering the human to accomplish complex, and possibly dangerous, activities remotely. However, the human needs do not stop at performing tasks in industrial environments. The social needs of human are also of substantial importance. Consequently, robotics research was not limited to only study the tele-operational systems performing industrial activities, but it also extended to focus on the so-called tele-presence robotics which is a robotics research area that is combination of tele-operational robotics and interaction robotics. Tele-presence aims to transport the human presence to far locations to perform sensation activities such as vision and feeling the temperature and social activities such as handshake, attempting to break the physical and time barriers. RAM and HMI labs of Twente University participate in the ANA Avatar XPRIZE competition for building a robotic avatar system that should transport the human presence to other distant locations. By this tele-robotic system, the human should be able to sense the environment that is surrounding the avatar robot and perform tele-presence social activities of which tele-handshake is the focus of this thesis.

1.2 Problem statement

Tele-handshake activity has been attempted in literature. The focus is, however, on the hand dynamics of the handshake by using robot hands as in Pedemonte et al. (2017). It is missing in literature to investigate the arm dynamics in robotic handshake activity using robot arms in both local and remote locations. Thus (1) it is missing in literature a bilateral force feedback control architecture with the ability of applying different forces feedback on each robot, and (2) it is still unknown whether a tele-handshake between two persons in distant locations through robot arms could provide a realistic handshake. These two problems will be addressed in this project.

1.3 Design goals

The ultimate goal of this project is to perform a remote handshake using two 6-DOF Franka robot arms, and to evaluate the user experience about performing handshake remotely through robot system. Consequently, the main design goals required to achieve this handshake system should revolve around the user experience (UX). They are graphically illustrated in Figure 1.1.

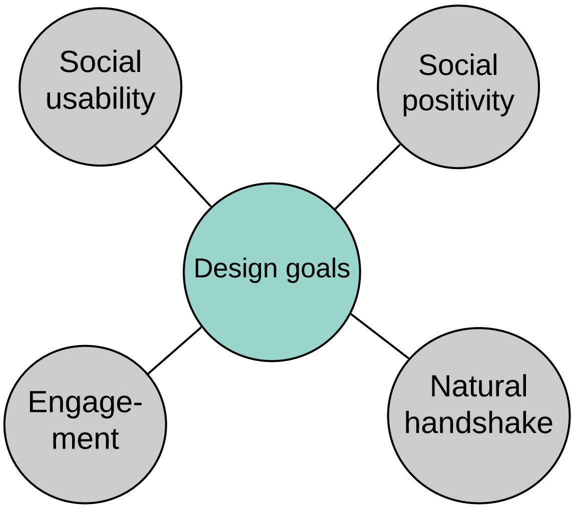

Figure 1.1: Design goals of a tele-handshake system

The design goals are listed below with more explanation:

- **Social usability** means that a robot handshake system needs to be easy to use and friendly in interaction.
- **Social positivity** means that the user interaction with the robot needs to be positive, or otherwise the result might reluctance to interact with robots anymore.
- **Engagement** means that a robotic handshake system needs to provide the handshake partners with the engaging experience similar to that obtained by real human-human handshake.
- **Natural handshake** means that the control architecture needs to enable the handshake partners to have a relatively natural handshake by feeling the presence of each other remotely.

In order to determine whether the concept of tele-handshake system could be socially usable, and that such a social activity is as positive as the real handshake between people, an experimental apparatus need to be set up. Obtaining a natural handshake is dependent on the control architecture whether it has the capability of transporting the forces and compliance of the two handshake partners to each other. This implies the need for a new control architecture that could achieve that goal. Finally, user studies need to be done on the developed control architecture to assess the user experience (UX) about performing tele-handshake, and to judge whether or not it is effective to use robotic control method for performing tele-handshake.

1.4 Related work

There are several handshake systems that were built. These systems differ from each other in the number of DOF that a system has, in the mechanical system design, in the human experience that the system is capable of offering to the human or in the control algorithm of the handshake system.
Studies of Nakanishi et al. (2014), Ouchi and Hashimoto (1997) and Jindai and Watanabe (2007) attempted to search the influence of transporting different sensation channels on the human experience. Nakanishi et al. (2014) specifically studied transporting the haptic sensation channel and the visual channel in videoconferencing, while Ouchi and Hashimoto (1997) and Jindai and Watanabe (2007) studied the combination of haptic channel and voice channel.

Kunii and Hashimoto (1995) proposed a handshake system with only 1-DOF, where the system is only able to perform one translation. This system is not capable of providing the handshake compliance that a system having 10-DOF is capable of such as the one utilized by Wang et al. (2009).
Some handshake systems were built using haptic interfaces with either fictitious artificial hands as in the work of Miyoshi et al. (2015) or other non-hand-like mechanical designs of end-effectors such as the one used by Wang et al. (2009). By using such a slave robot, this means that when the human operator shakes hand with the human subject at the other location, the human subject does not feel his hand grasped which has a large influence on his personal experience as mention by Alhalabi and Horiguchi (2001) Nakanishi et al. (2014). While other systems like the system that was built by Pedemonte et al. (2017) utilize haptic interface with a human-like robotic hand that is provided with actuators and thus capable of grasping the human subject hand.
Treatment for temperature and texture of the robotic hand was made by Nakanishi et al. (2014) as they play a role in giving the right impression to the human subject. Because shaking hands with a bare cold robot hand might give the human subject the impression that he shakes hand with a machine, which damages the tele-presence (Nakanishi et al., 2014).
Melnyk et al. (2014b) studied the handshake dynamics to quantitatively analyze some of the handshake characteristics such as handshake duration and grasp force, and the work of Tagne et al. (2016) is a continuation where it constructed more complex sensory network.
A summary for the literature that studied robotic handshake systems is provided in table 1.1 along with the main points that were addressed.

No.	Reference	Focus point
1	(Alhalabi and Horiguchi, 2001)	tele-handshake in virtual reality
2	(Pedemonte et al., 2017), (Kunii and Hashimoto, 1995), (Avraham et al., 2012), (Miyoshi et al., 2015)	tele-handshake in two distant locations
3	(Nakanishi et al., 2014), (Jindai and Watanabe, 2007), (Ouchi and Hashimoto, 1997), (Jindai and Watanabe, 2011), (Tsalamlal et al., 2015)	combining several sensation channels
4	(Miyoshi et al., 2015), (Wang et al., 2009), (Arns et al., 2017), (Papageorgiou and Doulgeri, 2015),(Pedemonte et al., 2016)	achieving handshake compliance or synchronization
5	(Orefice et al., 2016), (Orefice et al., 2018)	human characteristics recognition (gender, mood)
6	(Melnyk et al., 2014b), (Tagne et al., 2016)	quantitatively analyzing handshake aspects
7	(Melnyk et al., 2014b), (Jindai et al., 2006), (Yamato et al., 2008), (Jindai and Watanabe, 2011), (Melnyk et al., 2014a), (Jindai et al., 2015)	investigating handshake stages
8	(Knoop et al., 2017b)	haptic handshake evaluation metrics

Table 1.1: A summary of the works related to haptic robotic handshake systems

None of the work mentioned in table 1.1 paid attention to human experience taking into account all of the important aspects together. But rather, each paper has focused on one of the aspects while ignoring the others. For example, Pedemonte et al. (2017) mainly paid attention to the grip completeness aspect or in other words the human-like mechanical design of the robot hand, while Miyoshi et al. (2015) mainly focused on having consistent hand's motion, ignoring the grip completeness aspect. This work attempts to take the most important aspects together into consideration.

1.5 Problem approach

(Van Teeffelen et al., 2018)
For a system to be a tele-handshake system capable of enabling two persons of shaking hands remotely, the system has to embody the handshake characteristics explored in the Section 2.5. To achieve that ideally by a robotic system, the robotic system needs to have a substantial resemblance to the humans bodily structure by which humans perform handshake, and that is the arm and hand. A design concept for a tele-handshake system is illustrated in the Figure 1.2.

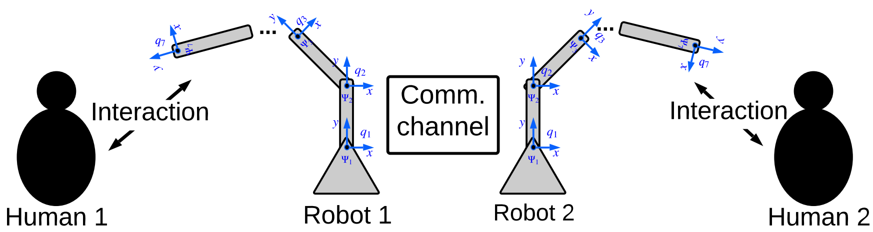

Figure 1.2: A depiction of a tele-handshake system

Several studies constructed handshake systems with a large degree of resemblance to the human arm structure such as the studies of Wang et al. (2009) and Arns et al. (2017) which use multi-DOF robotic arm. The handshake systems in the aforementioned studies consist of one robot arm only. Such a system is not a tele-handshake system, and so it does not allow remote interaction between two persons in distinct locations.
The targeted system in this project is a tele-handshake system consists of two robot arms because there are two human operators. This requires a different treatment, because the control system requires to handle two commands from the two operators. More details on control deign is found in Chapter 4.
A diagrammatic illustration of a robotic handshake system is shown in Figure 1.3.

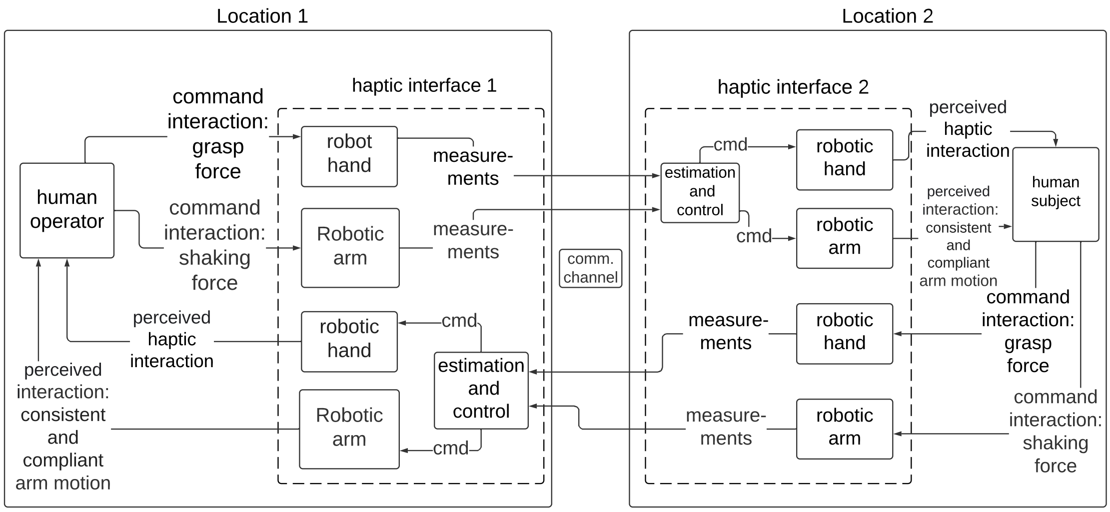

Figure 1.3: High-level design diagram for the entire tele-handshake system

As shown in Figure 1.3, there are two humans interacting with each other remotely. Consequently, the interaction of either the operator or human subject is two parts, namely command interaction and perceived interaction. This implies that the control system needs to be capable of letting the two handshake partners feel the presence of each other. This work focuses on the robot arms control system, rather than robot hands.

1.6 Report organizing

Chapter two presents background about tele-robotics and its different concepts. Chapter three talks about analysis for tele-handshake system and its design requirements as well as its evaluation methods. Chapter four shows the proposed control architecture and its difference from the conventional control architecture. After than in chapter five, the experiments are done and the control design is validated, and user studies are performed. Finally, in chapter six statistical tests are executed to assess the overall system performance, and consequently conclusions are drawn. A graphical roadmap for this report can be seen in Figure 1.4.

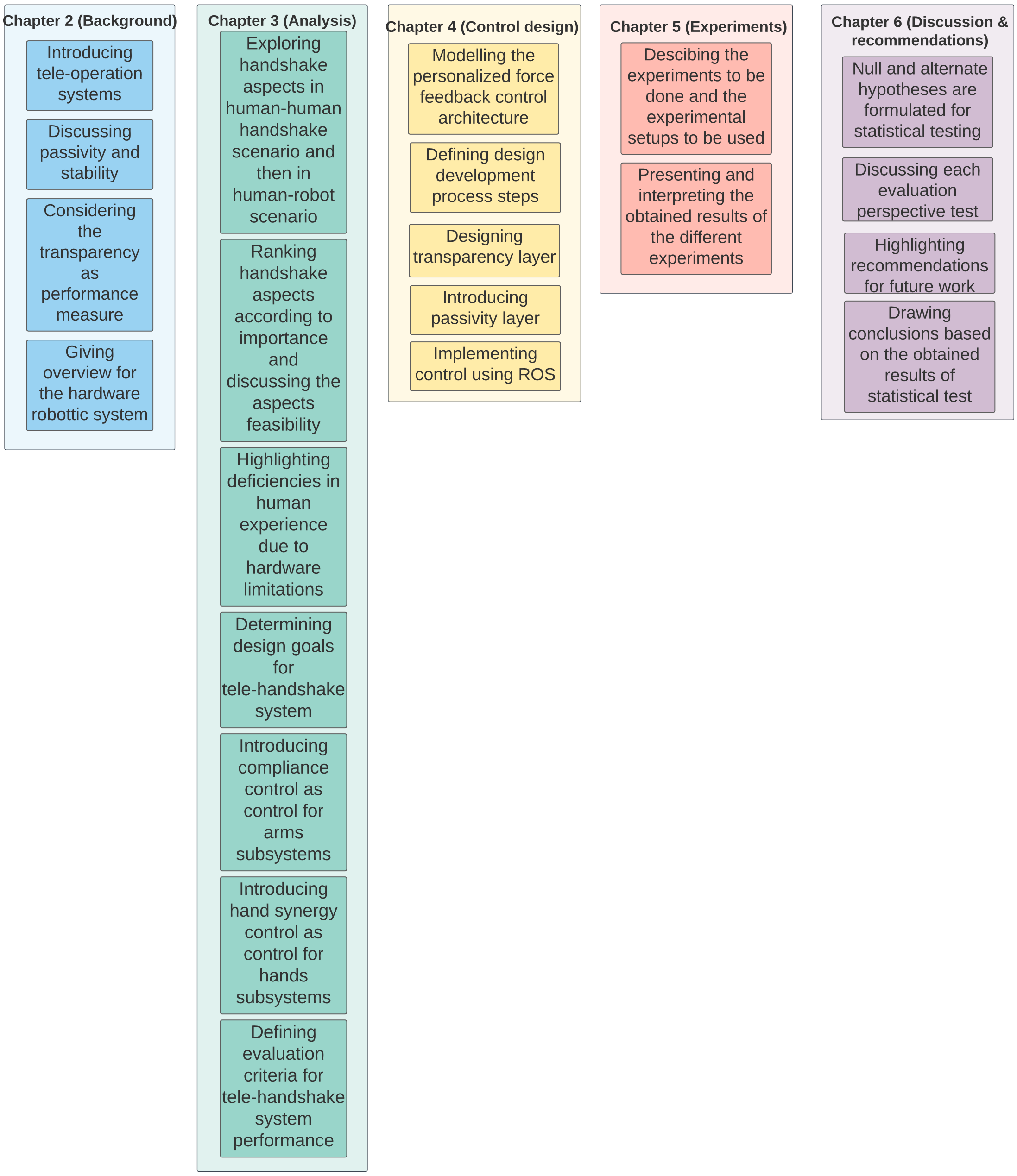

Figure 1.4: Roadmap for the entire report contents

2 Background

In this chapter, the basis for the tele-handshake system is presented. First, the teleoperation system and its ingredients is defined. Next, light is shed on passivity and transparency criteria for teleoperation systems. After that, a description for the available hardware is provided. Finally, the handshake aspects are reviewed.

2.1 Teleoperation systems

The main goal of the thesis project is to construct a haptic tele-handshake system. The essence of tele-handshake system is the teleoperation system. The tele-operation is a process that enables an operator to control a robot remotely (Franken et al., 2011). A typical tele-operational system is composed of a human operator, master system, communication channel, and slave system that is located in a remote environment. Figure 2.1 shows an illustration of such a system diagrammatically.

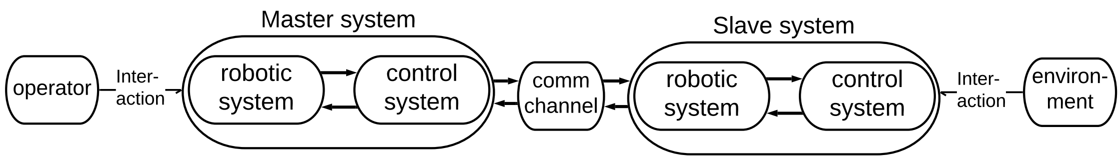

Figure 2.1: Teleoperation chain components

Note that both the master and slave systems consist of physical robotic system and a control system. Additionally, the environment can be an object that the slave robotic system interacts with, or another human. In this project the environment is considered to be another human as the goal is to perform a tele-handshake.
The teleoperation system has two main functions. The first function is to control the slave system by commands flowing from the master system to accomplish a certain task in a remote environment. The second main function is to transmit the interaction between the slave system and the environment back to the master in the form of haptic feedback, which can be force feedback only or a combination of force feedback and tactile feedback, to grant the operator a haptic sensation channel that supports him in the perception of the environment and provides him with a direct knowledge whether or not the task has been accomplished. Also, the haptic feedback increases the efficiency of accomplishing a task because it enhances the intuitiveness and dexterity of performing tasks remotely, rather than depending only on visual feedback, for example, to observe whether or not the end-effector has performed the required tasks (Franken et al., 2011).

Unilateral and bilateral notions

If the tele-operation is only aimed for controlling the slave position and guiding it to a certain position, and haptic information is not sent back to the master, then the tele-operation system is said to be unilateral (Sakow et al., 2018). However, this project attempts to build tele-handshake system which means that there is a human on the slave system side as well. Both the operator and recipient should be able to interact with each other and feel each other's forces and compliance. Such a system is said to be a bilateral tele-operation system (Mersha et al., 2013) (Franken et al., 2011) (Pedemonte et al., 2017).

2.2 Passivity

The stability property is an important property for any control system, without which the system operation becomes hazardous. However, performing stability analysis is a complicated process, especially for teleoperation systems due to the nonlinear dynamics of the human and environment (Jazayeri et al., 2013). In addition to that, there are several time-varying destabilizing factors that can potentially disturb the tele-operation system stability such as hard contact dynamics with the environment and time delays in the communication channel which is inevitable (Franken et al., 2011) (Lawrence, 1992).
The non-passive methodology of controlling robotic systems such as the use of PID joints controllers leads to a satisfactory performance in principle. However, once the robot starts interacting with the environment as in the case of haptic handshake, the interaction should be treated carefully (Folkertsma and Stramigioli, 2001), especially if the environment is unknown where the system stability becomes likely vulnerable as shown by the following theorem found in the work of Camlibel et al. (2015).

Theorem 1 *Let a non-passive system be called Σ with input-output pair (u, y), there always exists a passive system $\tilde{\Sigma}$ that when it is connected to the system Σ will give rise to unbounded behaviour of the interconnection of Σ and $\tilde{\Sigma}$.*

A direct corollary results from the above theorem as follows.

Corollary 1 *If a system is passive, then it is guaranteed to be stable.*

For the detailed proof of the theorem, refer to (Folkertsma and Stramigioli, 2001). Two important results can be inferred from the theorem and corollary. The first result is that whenever a non-passive system is in the position of interaction with an environment, the stability becomes substantially threatened. The second result is that the way to guarantee the system stability is to have the system as passive system.
It is worth mentioning that the interconnection of passive subsystems is a passive system (Schaft and Schaft, 1999).
From the aforementioned imperfections of stability property in interaction systems, the passivity becomes a more important property to have in the system, and the stability property alone is not sufficient. The concept of passivity is introduced by Willems (1972) as follows.

Definition 1 *Consider a system has input u and output y, then the system is said to be passive if a storage function $S(x)$ can be found such that the following inequality is true:*

$$S(x_0) + \int_{t_0}^{t_1} w(u(t), y(t))\mathrm{d}t \geq S(x_1) \tag{2.1}$$

where $w(u(t), y(t))$ is the energy injected to the system through its ports.

The definition means that the system is passive if the energy stored in the system is less than or equal to the initial energy in the system summed with the injected input energy. In other words, the passive system does not have the ability of generating energy.

2.3 Transparency

In the design of a tele-handshake system, the first design goal is to build a system that is able to interact safely with the human operator and the human subject without causing damages to them or to the surrounding environment, and the second design goal is to achieve the social activity handshake in an immersive way that engages both the operator and the recipient in the positiveness state-of-mind that the real handshake is capable of boosting humans with.

The first goal is obtained by targeting the passivity. But passivity does not attain the second goal. So there is a need for a performance measure that provides insights to how well the tele-operation system has preformed, and assessment on the haptic feedback whether or not it has sufficiently immersed the operator with haptic knowledge about the environment. This performance measure is called tele-operation transparency (Franken et al., 2009) (Lawrence, 1992). Ideally, a tele-operation system is transparent if the following conditions are satisfied:

$$\begin{aligned} \dot{q}_s(t) &= \dot{q}_m(t) \\ \tau_m(t) &= \tau_s(t) \end{aligned} \tag{2.2}$$

where, $\dot{q}_m$ and $\dot{q}_s$ are the velocities of the master and slave robotic systems, respectively, and τ_m and τ_s are the interaction forces between the master and the operator and the environment and the slave, respectively. The two equations above tell that if, in the ideal case, the system is transparent, then the slave system obeys the master system by moving in the same velocity and locating in the same position. Also if the system is transparent, the master will be haptically connected to the environment.

2.4 Hardware background

The robotic hardware resources from which the tele-handshake system is constructed in this project are the Virtuose 6D robotic arm, the FRANKA EMIKA-Panda robotic arm, the H-glove haptic exoskeleton and the qb robotic soft hand. In this section, a brief description for each subsystem is made.

2.4.1 qb soft hand

The qb soft hand is a commercial version of the Pisa soft hand. The main design goal behind the development of the Pisa soft hand is the construction of a robust, safe, light-weight, low-cost and simple robot hand.
The soft hand is a five-finger robot hand having 19 non-actuated degrees of freedom, 4 degrees of freedom on each finger except for the thumb which has 3 degrees of freedom, and it uses only one actuator to control the hand functions. In addition to that, there are two types of sensors integrated in the qb robot hand namely electric current sensor, and position sensor. The specifications of the qb soft hand are summarized in Table 2.1. For further details on specifications, refer to the product official specifications sheet.

Feature name	**data**
Number of DOF	19
Number of actuated DOF	1
Closure configurations	pinch grasp & power grasp
Nominal power config. grasp force	84 N
Nominal pinch config. grasp force	11 N
Effective weight	0.5 kg

Table 2.1: Summary of qb soft hand specifications

A schematics of the soft hand is shown in Figure 2.2.

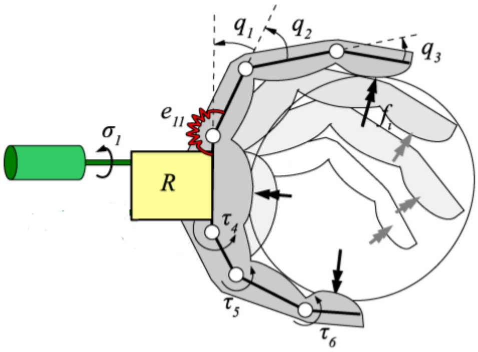

Figure 2.2: Schematics of the soft hand with adaptive synergies grasping an object. Modified from (Della Santina et al., 2018). The green is the actuator σ which generate motion acting on the joints. Those motions are mapped to the hand joint angles q_i through the matrix R, which collects the transmission ratios. The final posture of the hand depends on the external wrenches $f_{\text{ext}} = [f_1^T, f_2^T, \ldots]^T$ which is exerted by an object on the hand, the internal torques $\tau_a = [\tau_1, \tau_2, \ldots]^T$, and the springs elasticity $e_{i,j}$.

In order to achieve the low-cost, light-weight and the simple design properties of such a robotic hand, underactuation is utilized (Catalano et al., 2014), which is a technique to actuate a number of joints with less number of actuators. It is a fact in neuroscience that humans control their hands not by controlling each of its numerous degrees of freedom, but rather by coordinating them in organized motions called synergies (Catalano et al., 2014). In order to make the robotic hand adaptive with the objects that it interacts with, the adaptive synergy is utilized in the design of the soft hand (Grioli et al., 2012).

2.4.2 H-glove exoskeleton

The H-glove is a haptic device aimed for dexterous interaction applications in robotics. It mounts over the dorsal side of the hand, and connects to the fingers tips. The glove is adaptable to different sizes of hands and fingers.
The H-glove is a three-finger exoskeleton. Each finger-mechanism consists of three links, and thus has 3 degrees of freedom. So in total the H-glove has 9 degrees of freedom. The 9 joints are measurable. The force feedback is reproduced on the three fingers. However, only 2 degrees of freedom on each finger are actuated and able to reproduce the sensation of contact. A summary for the relevant and interesting specifications of the H-glove exoskeleton was made in Table 2.2.

Feature name	**data**
Number of finger mechanisms	3
Number of links per mechanism	3
DOF number per mechanism (active and non-active)	3
Active DOF number per mechanism	2
Number of position-measurable DOF per mechanism	3
Continuous force in translation	5 N
Continuous torque in rotation	0.13 Nm

Table 2.2: Summary of H-glove specifications[1]

[2]The official Haption website: https://www.haption.com/en/

The kinematics structure of H-glove exoskeleton with the joints and their rotation axes is shown in Figure 2.3. Note that in Figure 2.3 a schematics for only one of the finger mechanisms is illustrated, and that is with the gray joints. The other mechanism is a schematics for the hand finger itself. Note also that the schematics needs to be read from left to right, meaning that B_0 is the first joint which is connected to the base of the H-glove system, and B_3 is the tip of the finger mechanism.

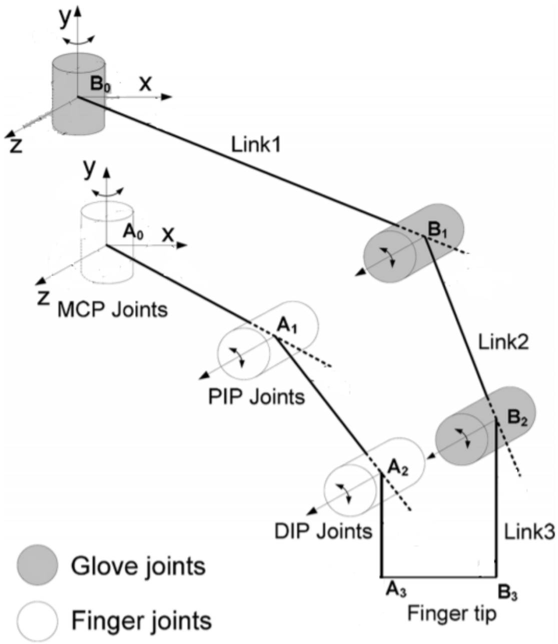

Figure 2.3: A schematics illustrates the kinematics of one finger mechanism of the H-glove exoskeleton. Modified from (Ben-Tzvi and Ma, 2014)

With the H-glove alone, the haptic feedback is created only on the fingers. In order to have the ability of 6D motion in the work space, and also to have a more immersive haptic experience, the H-glove can be attached to the haptic robotic arm "Virtuose 6D" which blocks the entire system in case of contact, providing haptic feedback to the entire arm.

2.4.3 Virtuose 6D haptic robotic arm

The powerfulness of the Virtuose 6D robotic arm is that it is a haptic robotic system capable of generating force feedback and simultaneously a robotic arm providing a 6D motion.
The Virtuose 6D consists of a fixed base and 3 links excluding the end-effector. It has 4 joints occupying the degrees of freedom as follows: the first three joints are revolute joints having 1 degree of freedom, and the fourth joint is a spherical joint having 3 degrees of freedom, totalling 6 degrees of freedom. Additionally, the Virtuose 6D is equipped with electric current sensors which are used to compute the force applied by the operator on the end-effector. A summary for the specifications of the the Virtuose 6D can be found in Table 2.3. For the complete detailed specifications, refer to the company product specifications sheet which is found on the official website.

Feature name	data
Number of links	3
Number of joints	4
Translation workspace	± 0.67 x ± 0.29 x ± 0.51 m
Rotation workspace	±165° x ±65° x ±135°
Peak force in translation	35 N
Peak torque in rotation	3.1 Nm

Table 2.3: Specifications of the Virtuose 6D robot arm

A better understanding for the kinematics structure of the Virtuose 6D can be obtained graphically. A graphical illustration of kinematics has been made which is shown in Figure 2.4.

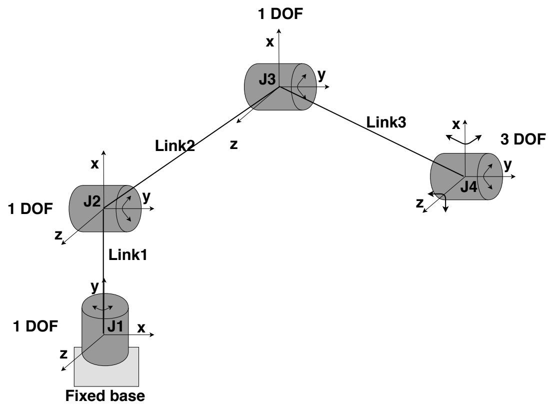

Figure 2.4: A depiction of the Virtuose 6D kinematics

The Virtuose 6D haptic arm mainly supports the impedance control mode. But it can also support a control mode that is an admittance-like control.

2.4.4 FRANKA EMIKA-Panda

The Panda is a serial robotic arm capable of 6D motion. It is composed of a fixed base in addition to six links. The Panda robotic arm has 7 joints, and so 7 degrees of freedom. All of the joints are supplied with force sensors. The Franka arm kinematics is illustrated in Figure 2.5 showing the configuration of the joints, their rotation axes and their reference frames for an arbitrary robot configuration.

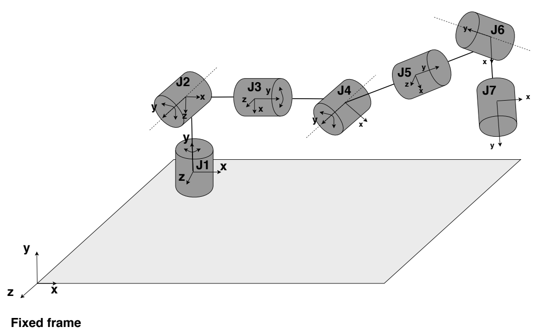

Figure 2.5: Kinematics Figure of the Franka robotic arm

Some of the relevant and interesting specifications of the Panda arm are listed in Table 2.4. In case other specifications are desired, refer to the complete company product specifications sheet.

Specification name	**data**
Number of links	6
Number of joints (DOF)	7
Number of force-measurable joints	7
Moving mass	12.8 kg
Maximal end-effector payload	3 kg

Table 2.4: Features of the Panda arm

2.5 Handshake aspects

A tele-handshake system would have a direct impact on human experience because nonverbal communication, which includes the touch and handshake, accounts for 65% of the communication between humans (Shipps and Freeman, 2003). To study the impact of robotic handshake system on the human experience, the aspects of the handshake in the social context need to be qualitatively investigated and then projected into robotics context.
In literature, there are no robotics studies that conducted comprehensive research that take all the handshake aspects into account, but instead they only objectively address some of handshake aspects such as the study of Wang et al. (2009) which addressed one handshake aspect only or the study of Arns et al. (2017) which addressed two of the handshake aspects. In order to collect a comprehensive list of handshake characteristics for this project, the aspects were investigated from either social studies explicitly addressing the handshake aspects between humans or from robotics studies. They are summarized in Table 2.5 along with the corresponding references.

No.	**Handshake aspect**	**References**
1	grasp strength	(Melnyk et al., 2014b), (Shipps and Freeman, 2003)
2	handshake vigor (shaking force)	(Miyoshi et al., 2015), (Shipps and Freeman, 2003), (Wang et al., 2009), (Melnyk et al., 2014b)
3	completeness of grasp	(Melnyk et al., 2014b), (Alhalabi and Horiguchi, 2001)
4	hand temperature	(Shipps and Freeman, 2003), (Nakanishi et al., 2014)
5	hand texture	(Nakanishi et al., 2014)
6	duration	(Melnyk et al., 2014b) (Shipps and Freeman, 2003)

Table 2.5: Summary of handshake aspects mentioned in literature

In the sequel the handshake characteristics listed in Table 2.5 are further discussed.
Grasp strength
The first aspect of handshake is the grasp strength (Melnyk et al., 2014b). Shaking hands in different grasp strengths can signal significant indications and information about the personal traits (Shipps and Freeman, 2003). A psychological study conducted by Shipps and Freeman (2003) on handshake and its relation to the personality traits reveals that grasp strength is positively correlated with rational dominance and extroversion, and negatively correlated with so-

ciability. Therefore in the context of robotics, the robotic system should be designed such that forces are exerted on the human operator and recipient hands in a certain way that corresponds to the handshake grasp.

Handshake vigor or shaking strength

The second aspect in handshaking is the handshake vigor or the shake strength (Miyoshi et al., 2015)(Shipps and Freeman, 2003). This means that in a robotic context if the human subject and the human operator move their hands in the same directions for example, then they both should feel compliance, or if they move their hands in opposite directions, they should feel resistance. Different works approached this aspect in different ways. Wang et al. (2009) present control algorithm that is capable of predicting the human intention or in other words the human next movement for the sake of having synchrony in the handshake. The work of Melnyk et al. (2014b) divides the handshake into four phases one of which is the "approaching phase" which takes place before the physical contact of hands, and they developed a sensory system to estimate the entire arm motion parameters.

Completeness of grasp

The third handshake aspect is the completeness of the grasp in handshake (Melnyk et al., 2014b). The factor that characterizes the grasp completeness aspect is the hand shape. Handshake between two humans means that the two persons enclose each other's hands and consequently they have a complete grasp of each other's hands, while handshake between a human and robot having a non-human-hand-like end-effector does not provide the human with the experience that he has grasped a complete hand. A haptic interface having an end-effector that does not resemble the human hand shape was developed by (Alhalabi and Horiguchi, 2001) and the results in terms of handshake experience was unsatisfactory. Consequently, in the robotic context, this suggests utilizing a human-like robotic hand in order to realize the experience of grasping a hand or being grasped by a hand.

Hand temperature

The fourth aspect is the temperature which can also signal information about the personality. The same study of Shipps and Freeman (2003) mentioned that shaking hands with a cold hand leads to unpleasant handshake. Nakanishi et al. (2014) also paid attention to the temperature aspect by having the capability of controlling the robot hand temperature by means of resistance wires integrated in the mechanical design of the hand so as to reduce the mechanical hand coldness.

Hand texture

The fifth handshake characteristic is the hand texture. Nakanishi et al. (2014) mentioned a treatment for the texture by wrapping the fingers and palm with certain material corresponding to an artificial skin. The reason behind this treatment is to reduce the mechanical hand hardness. Otherwise if the robot hand is left as bare mechanical hand, then the impression is damaged (Nakanishi et al., 2014).

Handshake duration

The last handshake aspect is the duration (Melnyk et al., 2014b) (Shipps and Freeman, 2003). Melnyk et al. (2014b) analyze the four handshake phases and the duration of each phase. The duration is only relevant to one-sided robotic handshake system, where the robot's handshake force and duration need to be controlled. However, in tele-handshake where there are two human handshake partners, the handshake partners are the ones who decide the handshake duration: when to start and to end the handshake. Consequently, the duration aspect is not relevant to this project.

3 Analysis

In this chapter, the handshake aspects explored in the previous chapter are ranked according to the importance and relevance Then, the suitability of the available hardware resources for realizing handshake system is discussed. Last but not least, evaluation criteria for the haptic tele-handshake system are elaborated.

3.1 Handshake aspects feasibility investigation

Since the goal of the project is to build a handshake system that should realize the handshake experiences for the operator and recipient, an investigation of the handshake characteristics between humans in the social context was required. With the discussion in the Section 2.5, the handshake characteristics have been explored. However, those characteristics need to be further investigated in light of feasibility by the available hardware resources that have been described in Section 2.4 to determine which aspects should be taken into consideration.

The tele-handshake system is a teleoperational system, and so it consists of master system and slave system. The master system is aimed to be constructed from the 6-DOF robotic arm and the H-glove, while the slave system is aimed to be construed from the Franka Emika Panda robotic arm and the qb soft hand. The handshake aspects have been investigated in social contexts as well as robotics contexts. But there are still two important tasks that need to be accomplished before thinking of the realization of the investigated aspects. The first task is to rank the found handshake aspects according to importance as some of the characteristics are not relevant for this project particularly. The second task is to investigate the suitability of the available hardware resources in realizing the nominated handshake aspects.

There are three characteristics in the Table 2.5 that are not considered explicitly, particularly the hand temperature, the texture and the handshake duration. Although the hand temperature was targeted by Nakanishi et al. (2014), it is not strict requirement that must exist in every handshake robotic systems. Because Nakanishi et al. (2014) used a bare mechanical robot hand, and so its coldness potentially damages the tele-presence. So there was a need for a special treatment for hand temperature. However, the qb soft hand available for this project is not bare, but rather stuffed with soft material and covered with fine texture disposing the potential damages that occur due to stinging coldness. Therefore the hand temperature aspect is not taken care of as it is already realized for the soft hand. The second not important handshake characteristic for this porject is the texture. As just mentioned, the qb soft hand is stuffed and covered with soft material disposing the chance of damaging the tele-presence experience due to hardness of the robotic hand. Therefore the texture aspect can be considered already realized in the qb robotic hand for the current handshake system, and as such it does not require treatment. While for the H-glove exoskeleton, the hand texture is not a concern because the operator would not grasp a real physical hand, but instead the operator relies on the haptic feedback recreated once the contact between the human subject and the soft hand occurs. The third not important handshake aspect is duration. In tele-handshake, the handshake duration should not be controllable. The tele-handshake system under study should enable two humans to shake hands realistically. This means that the operator and the recipient are the two who decide the handshake duration as the case of handshake between two humans in the everyday-life. This proposes not to control the grasp duration of the robot hand. Consequently, the handshake duration characteristic was disregarded.

Concerning the second task that should be taken care of, each of the remaining handshake aspects in Table 2.5 should be separately investigated whether or not it is feasible with these subsystems mentioned above. In addition, the aspects should be investigated from two perspectives namely the perspective of the human operator and perspective of the human subject as the human experiences of both the operator and receipt are the emphasis of this research project.

Grasp strength

As mentioned in high-level system design in Figure 1.3, the handshake consists of a grasp for a hand and a shake for an arm. The grasp strength aspect is independent of the robotic arms in both master system and slave system, and only depends on the qb robotic hand and the hand exoskeleton.
The reasoning for showing the feasibility of the grasp strength characteristic consists of two portions. The first portion is to show that it is possible to map the hand exoskeleton posture to a robot hand posture, and the second portion is to show that the qb robot hand has a reasonable grasp force, meaning it provides an acceptable comfortable grasp for a human.
Regarding the first portion of the reasoning, the position of the H-glove exoskeleton can be mapped to a position for the qb soft hand by the concept of synergy mapping which is a method of transformation from Cartesian space to the so-called synergy space, introduced by Brygo et al. (2016).
Regarding the second portion of the reasoning, the qb soft hand was already evaluated by Knoop et al. (2017a) and Knoop et al. (2017b) for human-robot handshake application to investigate whether or not the qb soft hand causes damage and pain when grasping a human hand. First, an experiment was conducted to find the handshake grasping forces by humans in three different scenarios: weak handshake, normal handshake and strong handshake. The results of these experiments are shown in Figure 3.1 which shows the grasp force interval, identifying the minimum, maximum and the median in each of the three scenarios.

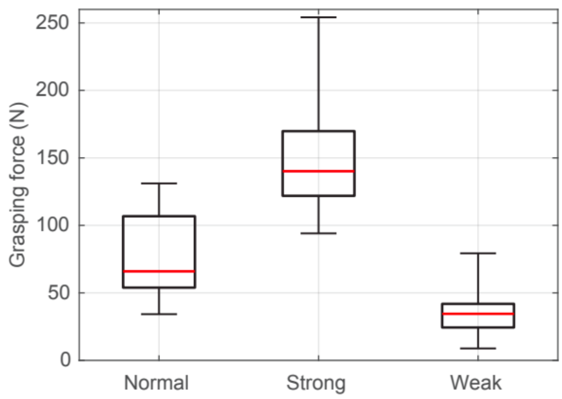

Figure 3.1: Findings of the experiment of Knoop et al. (2017b) in investigating the human handshake grasping force

After that, they performed an experiment for identifying the contact pressure distribution for a human and for the qb soft hand was done to establish a comparison between the two, to see the qb soft hand grasp whether or not is painful, and to identify the force interval to which the qb soft hand grasp force should belong to. In the experiment, the human and the qb soft hand grasped a sensorized cylinder at the maximal grasping force, and the pressure was measured by a pressure-sensitive film. Their results of the experiment can be seen in Figure 3.2.

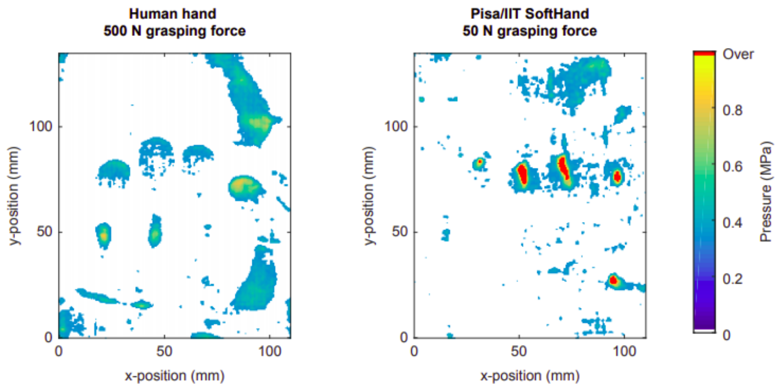

Figure 3.2: Findings of the experiment of Knoop et al. (2017a) to measure the contact pressure area

Observing the results in Figure 3.2, it can be seen that the qb soft hand can potentially result uncomfortable and painful grasp at the maximal force of 50N, because this grasp force is 10 times less than the maximal grasp force of the human, and still capable of producing higher contact pressure. This can be seen in the image on the right of Figure 3.2, where the red contact areas mean concentrated contact pressures, and the red color on the pressure scale corresponds to unknown pressure value because it is outside the measurement range of the pressure sensor Knoop et al. (2017a). However, the contact pressure requires to be significantly less than the pain threshold that is reported by Knoop et al. (2017a) to be 2 MPa. Therefore the qb soft hand can be used for realizing the grasp strength aspect in a tele-handshake system but with a strict condition being that the grasp force does not approach the maximal grasping force 50N. In other words the grasp force must belong to the weak handshake category shown in Figure 3.1 in order to avoid uncomfortable handshake that damages the recipient handshake experience. For the recipient experience about a force exerted on his hand that is belonging to the weak force category, it is unknown for the time being. It should be judged after performing experiments.
It can be concluded that it should be plausible to convey the handshake grasp force from the operator to the receipt with the available subsystems. However, it is not possible to convey the grasp force of the recipient to the operator because of two reasons. The first reason is that with this system, no knowledge can be obtained whether the environment actively interacts with the slave system. In other words, the qb soft hand is not equipped with any sensory system that is capable of measuring the grasp force of the recipient. The second reason is that the H-glove exoskeleton is not equipped with actuation system capable of providing tactile feedback to the operator's hand that could correspond to the grasp force of the recipient. In short, the handshake experience of the receipt would be complete because he could grasp the soft hand and the soft hand could grasp his hand, while the operator handshake experience is incomplete because he could have the experience of grasping a hand but he can not feel his hand grasped.

Handshake vigor

Unlike the first handshake aspect, the relevant subsystems to the handshake vigor characteristic are only the robotic arms. One key factor that affects the handshake vigor is the number of degrees of freedom of the arm systems in the master and slave systems. Because the humans' arms motion are then nearly constrained when using 1-DOF arm systems as Pedemonte et al. (2017) used, where the hands are only able to move up or down, while more freedom in arms motion and consequently more realistic handshake is attainable by a 6-DOF haptic interface as Arns et al. (2017). Therefore the more degrees of freedom the arm system has, the more reinforced the handshake vigor is. The available robotic arms in the master system and in the slave system both have 6 degrees of freedom showing the features of having spacious flexible work space for handshake.

Another key factor that characterizes the handshake vigour is the compliance of the robot arm. The compliance of the robot arm should be appropriate for the human to feel a natural handshake interaction. To show the appropriateness of the Franka robot arm, which is used as a local robot, a feasibility experiment should be done in which the human subjects shake hands with the robot at different forces and at different stiffness values. By shaking hands with the robot at a wide range of forces and under different stiffness conditions, it could be inferred if the robot has the capability to withstand different forces from different people by comparing the obtained forces with the maximum interaction force that the Franka robot can withstand which is approximately 30 Newtons, according to the specifications of the Franka robot Table 2.4. If the forces applied by different human subjects are still less than the maximum force of the Franka robot, then it could be concluded that the Franka robot is suitable for handshake application, and the vigour handshake aspect would be realized; if the forces applied by different people are greater, then the handshake application would be damaging for the Franka robot, and the vigour would be infeasible by this robot arm.

This experiment can be done using one robot Franka with the following procedure shown as a pseudo-code in Algorithm 1.

Algorithm 1: Pseudo code for the procedure of measuring the handshake vigour quantitatively

Initialization

W_{ext},τ_{ext} ,J ,J_{inv} ,q;

while *in the control loop* **do**

  measure joints positions: q;

  calculate Jacobian matrix: $J(q)$;

  calculate pseudo inverse of Jacobian matrix: J_{inv};

  measure external torques on joints: τ_{ext};

  transform external torques from joint-space to Cartesian space: $W_{ext} = J_{inv} \cdot \tau_{ext}$;

  record data using *rosbag* package

end

The findings of the feasibility experiment of the handshake vigour can be found in the chapter of experiments and results 5.1.1.

Completeness of grasp

The feasibility of the grasp completeness handshake aspect in the available hardware system can be shown by showing that both Hglove and soft hand have appropriate mechanical design capable of providing the recipient and operator with the experience that they have grasped a hand. Regarding the qb robotic hand, it is already a human-hand-like robotic hand. In addition, it is meant to be designed with a similar size to the human hand for human-robot interactions. Moreover, the qb soft hand is stuffed with soft material so that it fills up the human hand in case the human hand and the qb hand are in the position of handshake. On top of that, the qb soft hand has been used in handshake experiments in literature by Knoop et al. (2017b) and Vigni et al. (2019). Therefore the qb soft hand seems to be a proper choice for the handshake application.

Regarding the H-glove exoskeleton, it is problematic to show the H-glove suitability for handshake systems as the exoskeleton is mostly utilized for object manipulation systems and for hand rehabilitation. To the best of the author knowledge, an exoskeleton was not used for handshake robotic systems so far. The reason why it is problematic is that the operator only relies on the force feedback to have the impression that he has grasped a hand. Additionally, the H-glove is a three-finger exoskeleton, and not five-finger, which leads to an insufficiently immersive haptic feedback, and that consequently leads to incomplete grasp experience. So for the time being, utilizing the haptic feedback is assumed to correspond to grasping a hand, but the performance is left without comments until the experiments and evaluation.

3.2 Ranking handshake aspects

Based on the investigation conducted in the previous section, a ranking for the handshake characteristics is done in order to give insights about which aspects should be taken care of more than other aspects, and also insights about the performance that is expected from the tele-handshake system relying on the available hardware resources in RaM laboratory. The ranking for each handshake aspect is done based on three factors, namely relevance, feasibility and influence-on-experience. Each aspect is given a score between zero and one, where the zero is assigned if the aspect is irrelevant for this particular tele-handshake system, is unfeasible or has no influence on experience in a tele-handshake robot system; and the score one is assigned if the aspect is relevant, is feasible or has significant influence on the experience, and half score is assigned in case the aspect is partially feasible, for instance. The Table 3.1 shows the aspects, the three ranking factors and the scores for each aspect.

Handshake aspect	**relevance**	**Feasibility**	**influence-on-experience**	**Total score**
grasp strength	1	0.5	1	2.5
handshake vigour	1	1	1	3
grasp completeness	1	0.5	1	2.5
temperature	0	0.5	1	1.5
texture	0	0.5	1	1.5
duration	0	-	0	0

Table 3.1: Grading the handshake aspects

As discussed in the first section of this chapter, the temperature, duration and texture aspects are not of importance, and therefore they were given the score zero in Table 3.1. The feasibility score half was given for each of the aspects "grasp strength", "temperature", "grasp completeness" and "texture", because they are only partially feasible due to the fact that one of the hands subsystems is a hand exoskeleton which can not perform all the functions of a robot hand. All the handshake characteristics do have influence on experience except the duration, where it has influence in the case of one-sided handshake system. That is why the duration feasibility was not much investigated as it is irrelevant for the tele-handshake application. The total score could give insight on how interesting the results would be regarding the corresponding aspect. The grading of the handshake aspects is also shown in Figure 3.3 for better illustration.

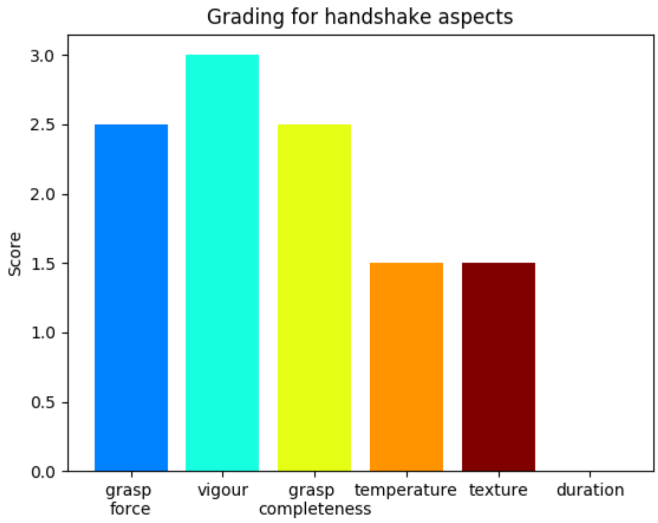

Figure 3.3: Graphical illustration for ranking the aspects

Looking at Figure 3.3, it is expected that the human handshake experience in terms of vigour is more complete than other aspects, for example, due to the fact that two 6-DOF robot arms are available in RaM laboratory which are utilized for this project, unlike all the related works who have built handshake system, where they have not used two robot arms at both local and remote sites. Similarly, the results regarding "grasp force" and "grasp completeness", although incomplete, are still better than the "temperature" or "texture", because the latter two aspects are not paid attention to.

3.3 Limitations

After analyzing the hardware robotic subsystems in Section 2.4, and analyzing the handshake aspects in Section 2.5, factors that limit the overall performance of the tele-handshake systems were found because of hardware imperfections. They are highlighted in this Section, and their influences are discussed.

3.3.1 Hardware constraints

The emphasis of this thesis is on the human handshake experience. In order to realize this experience, strict requirements for the hardware subsystems arise. As discussed in Section 2.5, the grasp force is necessary to convey from the operator to the recipient and vice versa. This requires sensory systems at both master and slave robotic systems that are able to sense and measure the operator and recipient grasp forces, and requires as well an actuation systems that apply the grasp forces on the corresponding hands. From the perspective of the recipient, as discussed in Section 2.5, the handshake experience should be complete. However, there is lack in sensory system in the slave robotic system, and lack in actuation system in the master robotic system preventing the ability of conveying the grasp force from the recipient to the operator. Therefore extensions for the hand subsystems is needed if there is need to provide the operator with handshake experience.

3.3.2 Potential solutions

A potential solution to the operator experience limitation clarified in the previous section is the tactile feedback in the master system. Tactile feedback is designed such that it provides the

operator with tactile sensation in case there is active interaction from the recipient upon the robotic hand such as a grasp. Such a feedback should sufficiently enable the operator to differentiate whether he interacts with an object or with another human since the object does not interactively grasp the robotic hand. This requires sensory system at the slave side in order to sense the interaction of the human with the robot hand. One choice for that is a force-sensitive sensors that can be placed at the soft hand where the grasp force is exerted (Vigni et al., 2019).
There are two approaches in literature to implement tactile feedback: vibro-tactile feedback (Wang et al., 2018) (Scheggi and Salvietti, 2014), and mechano-tactile feedback (Casini et al., 2015) (Ajoudani et al., 2014).
The vibro-tactile system is mainly built from coin vibration actuators. In principle, it is an effective method of providing tactile feedback. However, its effectiveness should be measured with respect to the application. Relying solely on vibro-tactile feedback in handshake application was tested in (Alhalabi and Horiguchi, 2001), and the performance in terms of handshake human experience was poor.
For the mechano-tactile system, only the electric mechano-tactile feedback systems were found in literature (Casini et al., 2015) (Ajoudani et al., 2014). Casini et al. (2015) developed a cuff to be placed around the forearm in order to render the grasp force of the soft hand when squeezing an object. The cuff is powered by DC motors that either tighten or release a strap surrounding the forearm. Their results show that such a system can reliably deliver tactile feedback to the operator, corresponding to the grasp force of the robotic hand. Therefore, mechano-tactile feedback seems to be supporting the human handshake experience more than the vibro-tactile feedback system. In some cases where a small actuator does not provide a large actuation forces, an alternative is the pneumatic mechano-tactile feedback system which should provide larger actuation forces. Such a system, which was not found in literature, consists of air source, control valve and inflatable object surrounding the arm or if possible the palm to make the experience more realistic.

3.4 Design goals for tele-handshake system

The design goals for robotic systems are dependent on the objectives. For tele-handshake system, the main goals should be to achieve a realistic handshake capable of offering the operator and the recipient with genuine handshake experiences. In other words, the design goals for tele-handshake system are to realize the handshake characteristics discussed earlier. Looking at the Table 2.5, it can be seen that the aspects that are related to the control system are grasp strength aspect and handshake vigor, because the other two aspects are hand texture and grasp completeness which is dependent on the robotic hand shape.
In control terminology, realizing the grasp strength aspect, theoretically, is achieved by proper mapping for the exoskeleton position to the robotic hand, controlling the force feedback exerted on the operator's hand, and safely controlling the force exerted on the qb robotic hand. Realizing the handshake vigor is achieved by compliantly controlling the robotic arms subsystems. The two goals are further discussed below.

3.4.1 First design goal: compliance control for arms subsystems

First of all, it should be noted that the serial robotic arms need safety considerations more than the qb soft hand and the exoskeleton because the work space of the robotic arms are relatively much larger than the work space of the exoskeleton and qb robotic hand which is only the hand grip. In other words, the arms subsystems have more potential to behave hazardously. Therefore the compliance control is discussed only for the arms subsystems.
In order to have vigorous interactive but also safe haptic handshake, an appropriate decision for the control method should be made. Since the robotic arms subsystems have relatively large work space and might act hazardously under certain conditions, then it is a good decision to choose a compliance control method rather than PID joints controllers, for instance,

that attempt to lead the joints to predefined position set points without caring whether the interaction with environment is done rigidly or compliantly.
If an energy-based method is used to represent the system, such as the port Hamiltonian modelling, that underscores the energy exchange between the subsystems, and shows the flowing of the power conjugate variables, then it would be more intuitive and more interpretable to show the need for compliance control.
Folkertsma and Stramigioli (2001) modelled each of the robot system and the control system as port Hamiltonian systems. In that case, a simplification for the entire system can be made as the Figure 3.4 shows.

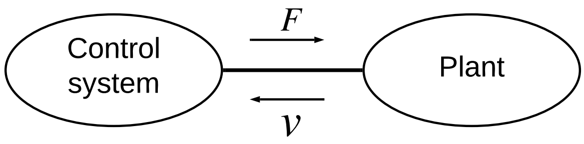

Figure 3.4: The robot and controller as port Hamiltonian systems connected by power port (Folkertsma and Stramigioli, 2001)

Note that in Figure 3.4, the connection variables are the power conjugate variables: flow and effort (or velocity and force). The direction of the force and velocity depicted in Figure 3.4 are dependent on how the plant behaves. The plant, or the robot mass, behaves like an admittance (Folkertsma and Stramigioli, 2001), and the mechanical admittance takes in force and gives out velocity. Observing this variables transfer at the control interface, it can be noticed that the definition of the impedance device applies to the control system in Figure 3.4, meaning that the input to the control system is position and the output is force. Thus, if the robot system could be modelled as port Hamiltonian system, then this shows the need for an impedance control to control the arms subsystems' compliance.

Impedance control

A tele-operation system control should make the slave robotic system position converge to the master robotic system position, and provide the operator with force feedback. A simple implementation of an impedance control is proposed by Folkertsma and Stramigioli (2001). The proposed control system is composed of virtual tunable spring and damper to achieve the desired compliance. A single-DOF teleoperational system consisting of two moving masses along one direction in addition to an impedance control can be seen Figure 3.5.

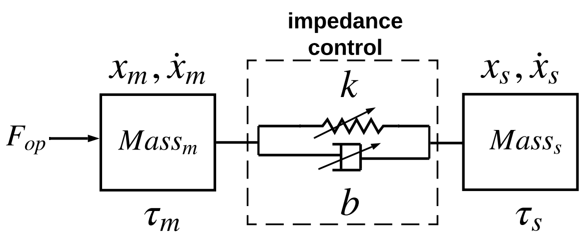

Figure 3.5: single-DOF slave robot system with an impedance controller composed of spring and damper

Where F_{op} in Figure 3.5 is the operator input interaction force that determines the master position x_m which should be sent to the slave system as set point, τ_s is the control force obtained by the virtual spring and damper and intended to be sent to the master as force feedback which is identified as τ_m. The control force produced by this controller and exerted on the master and slave systems can be expressed as follows:

$$\begin{aligned} F_m &= -k.(x_m - x_s) - b.(\dot{x}_m - \dot{x}_s) \\ F_s &= -k.(x_s - x_m) - b.(\dot{x}_s - \dot{x}_m) \end{aligned} \tag{3.1}$$

where k and b are the stiffness and friction coefficient of the virtual spring and damper respectively. In order to extend the impedance control model for the case of a multi-DOF complex robotic system, a spring matrix is defined which is composed of the linear stiffness and rotation stiffness. The spring wrench is given by:

$$W_{spting} = K \cdot X_e \tag{3.2}$$

where K is the spring matrix defined as:

$$K = \begin{bmatrix} k_{lin,x} & 0 & 0 & 0 & 0 & 0 \\ 0 & k_{lin,y} & 0 & 0 & 0 & 0 \\ 0 & 0 & k_{lin,z} & 0 & 0 & 0 \\ 0 & 0 & 0 & k_{rot,x} & 0 & 0 \\ 0 & 0 & 0 & 0 & k_{rot,y} & 0 \\ 0 & 0 & 0 & 0 & 0 & k_{rot,z} \end{bmatrix} \tag{3.3}$$

And X_e is the position error. Then the spring wrench is transformed by the robot arm Jacobian into control torques in the joints space:

$$\tau_{spring} = J^{\top} .^0 W^{ee} \tag{3.4}$$

If the dynamics of the robot demand more damped behaviour, a virtual damper on each joint with damping coefficient b can be designed. The torque resulted by such a damper for one of the joints is given as:

$$\tau_{damper} = -b \cdot \dot{q} \tag{3.5}$$

Variable impedance control

Achieving a vigorous handshake by a tele-operation system, or realizing the handshake vigor aspect, is done by conveying the compliance of the handshake partners to each other. This means that if one of the handshake partners changes the impedance of his limbs, the other partner should feel the impedance change reflected upon the stiffness of the robotic arm that he interacts with. As the human handshake experience is the emphasis of this research, the human impedance estimation method should be discussed with respect to the human convenience. Meaning that the limb impedance estimation method should not be a nuisance that disturbs the human handshake experience. This point should be discussed especially for the recipient because the recipient can be not familiar with robotic technicalities such as attaching sensors on the arm, which can be irritating.

Method 1

A method to modulate the impedance parameters of the controller is presented by Van Teeffelen et al. (2018). This method is based on the measurements of the human muscle activation levels. Accordingly, the parameters of the virtual spring and damper of the impedance control become function of the estimated muscles contraction levels. The force of the impedance control in the case of one degree of freedom system, given in equation 3.1 earlier, becomes as follows:

$$F_m = -k(\eta).(x_m - x_s) - b(\eta).(v_m - v_s) \tag{3.6}$$

where η is the estimated co-contraction level.
The co-contraction level is estimated based on the muscle activation level which is measurable by EMG. The estimation is performed as in the following relation (Van Teeffelen et al., 2018):

$$\eta = min(1, \alpha_{flexor}, \alpha_{extensor}) \tag{3.7}$$

where α_{flexor} and $\alpha_{extensor}$ are the flexor and extensor activation levels respectively. Hence the equation showing how the impedance control vary with respect to the co-contraction level is given by:

$$\begin{aligned} k(\eta) &= k_{\min} + \eta \cdot (k_{\min} - k_{\max}) \\ b(\eta) &= b_{\min} + \eta \cdot (b_{\min} - b_{\max}) \end{aligned} \tag{3.8}$$

This method was shown to be effective in estimating the human impedance and conveying it to the remote environment. But its requirement for the EMG sensors to be placed on the arm makes it only appropriate method to use for the operator, and not for the recipient. For the feasibility of this method, in RaM laboratory there is a *myo* wireless bracelet which integrates 8 EMG sensors in addition to IMU sensors. The data of EMG sensors can be processed for the purpose of impedance estimation. So, this method should be feasible.

Method 2

The authors Ajoudani et al. (2018) have introduced another method for the human limb's impedance estimation. It is also dependent on the muscle activity in the arm, which is measured by EMG sensors. In addition, it accounts for the effect of muscle-tendon lengths change when the arm configuration changes. This is accounted for by the so-called muscles Jacobian. This method is illustrated diagrammatically in Figure 3.6. The main point of this method is that the joint-space stiffness is found from the muscle activation which are measured by EMG sensors, and from the muscles Jacobian. Then the measurements of the motion capture system are used in retrieving the arm configuration to find the arm Jacobian that should transform the joint-space stiffness to Cartesian-space stiffness.

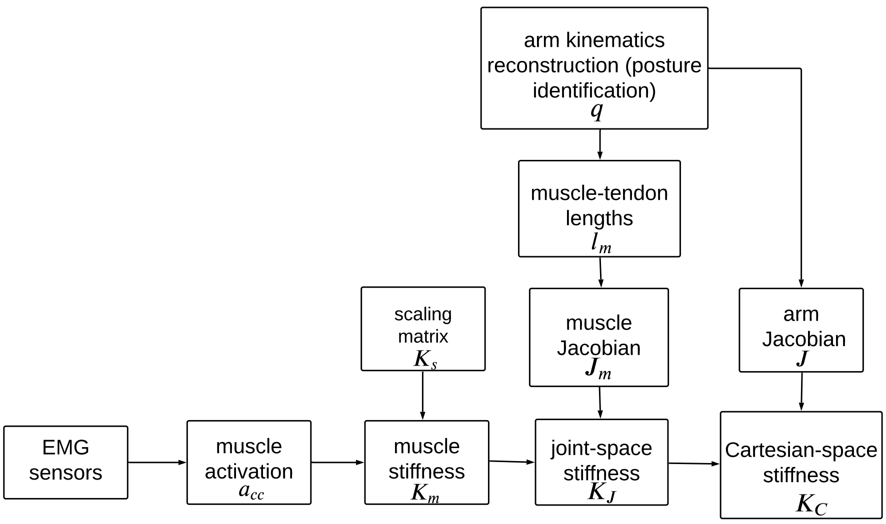

Figure 3.6: A graphical illustration for the human arm impedance estimation method of Ajoudani et al. (2018). Note that the muscle Jacobian is different from the arm Jacobian. The muscle Jacobian is obtained from the muscles lengths change w.r.t the configuration

Regarding the feasibility of the second method, there is one block in Figure 3.6 which is the "arm kinematics reconstruction" that is not feasible because it requires either inertial or optical motion tracking system that in turn requires placing IMU sensors or optical markers on the human body, which is undesirable for the human experience.

Method 3

A common method in literature for modelling the human arm is a serial manipulator of 2 DOF with the shoulder and elbow being the two joints and the wrist being the end effector (Dolan et al., 1993) (Chang et al., 2012) (Artemiadis et al., 2010). The links of this human serial manipulator are upper arm and forearm. Then the impedance is estimated by using the mechanical impedance model consisting of mass, spring and damper:

$$F = M_e\ddot{X} + B_e\dot{X} + K_eX \tag{3.9}$$

where $M_e, B_e, K_e \in \mathbb{R}^{33}$ represent the inertia matrix, damping matrix and stiffness matrix of the human arm. This requires measurements of the interaction force F and reconstruction of arm kinematics to obtain X, $\dot{X}$ and $\ddot{X}$. The interaction force could be found either by force sensor placed at the end effector to measure the human interaction force, or by estimation method. The open-source library *libfranka* of Franka robot arm seems to be containing an interaction force estimation functionality. Concerning the kinematics reconstruction of the human arm, two methods were found in literature. The first one, which seems to be the least convenient for handshake system, is kinematics reconstruction using optical motion tracking system (Fang et al., 2018). Such a motion tracking system requires placing several optical markers on the human arm and then the arm motion can be tracked by stereo camera set-up. This method might be disturbing to the recipient experience due to optical markers. The second method is reproducing the arm kinematics by inertial motion tracking system (Filippeschi et al., 2017). Instead of optical markers, this method requires the placement of IMU sensors on the human arm. For the same inconvenience reason of the optical markers, this method is not appropriate for robotic handshake system application.

In short

As can be noticed in the three methods mentioned above, sensors are required to be placed on the recipient body. Since adding extra sensory systems to the recipient's body may be damaging to his/here experience, those methods should not be utilized for estimating the arm impedance of the recipient. This implies that, for the recipient, an impedance estimation method is needed such that it does not require sensors to be directly placed on the recipient arm. Such a method was not found. So it was decided to design variable-impedance controller for the operator only, and implement the **method 1** that is based on the myo armband sensor because it seems to be the most feasible.

Myo armband calibration

Every user who aims to wear the myo armband sensor to measure the co-contraction level, a calibration process should be performed. The calibration process is to find the extremes, or the maximum and minimum, of arm muscles contraction levels. Those extreme values are used to normalize the co-contraction level by the normalization rule introduced in the work of Van Teeffelen et al. (2018). The maximum and minimum values should be defined depending on the application. For the application of handshake, two scenarios, which represent the extreme cases in handshake, were followed, and the muscles activation level was measured. In the two scenarios, the EMG-based myo armband sensor was placed on the upper arm of the participant such that the activation of the biceps and triceps antagonistic muscles are measured. The biceps and triceps are antagonistic because if the arm is in flexion configuration, then the biceps muscles become contracted and the triceps become relaxed, and vice versa if the arm is in the extension configuration. Figure 3.7 shows the two flexion and extension configurations of the arm.

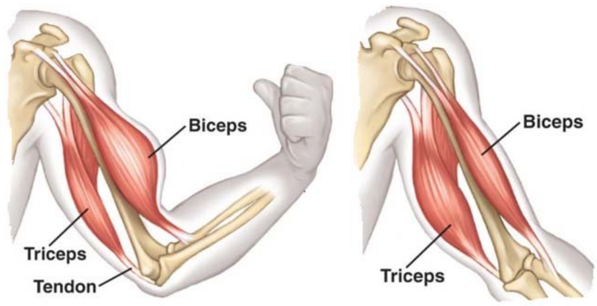

Figure 3.7: The biceps and triceps muscles. The flexion configuration is in the left, and the extension configuration in the right (Deaconescu and Deaconescu, 2018)

The results of calibration process is shown in the results chapter.

3.4.2 Second design goal: control for hands subsystems

Choosing a proper control strategy for the hands subsystems of this project particularly is an important control goal because of the large asymmetries between the master and slave. Those asymmetries are attributed to the fact that the hand system at the master system is a wearable three-fingers exoskeleton having 6 active degrees of freedom, and the robotic hand at the slave system is a five-finger underactuated robotic hand having one active degree of freedom. Refer to the description Sections 2.4.2 and 2.4.1 of each subsystem for more details about the differences. This proposes the need for expressing the hand posture by smaller number of variables, and particularly one variable as the qb soft hand has only one actuated degree of freedom. Brygo et al. (2016) presents a mapping tool that transforms the position of the hand exoskeleton finger tips from the Cartesian space to the so-called synergy space which consists of the vectors that are oriented along the grasp principal components. This mapping tool is called the synergy port. The synergy port has two functions. The first function being extracting the hand first synergy reference position from the operator's hand posture which is used then as a position command for the qb soft hand, and the second function being generating the haptic feedback by estimating the force applied by the qb soft hand along its first synergy, and then re-projecting it on the synergy space in order to obtain a force command in the operator's fingertips' Cartesian space.
Mathematically, the synergy port is a matrix that is obtained experimentally. A data set is collected from series of experiments, where the rows of the data set are number of data samples and the columns represent the number of dimensions of the space used to describe the position of each fingertip. Each data sample, or row, is the fingertips' positions with the first three components being the Cartesian position of the thumb, the second three components being the index position and the last three components being the middle position. Then the projection synergy matrix is constructed whose columns are the eigenvectors of the covariance matrix of the mean-centred data set.

3.5 Tele-handshake evaluation

For the social robotic system, system performance evaluation should be on done from two perspectives: from control engineering perspective and from user experience perspective (Alhalabi and Horiguchi, 2001) (Pedemonte et al., 2017) (Miyoshi et al., 2015) (Arns et al., 2017). First the evaluation from control engineering point of view is discussed, and after that the user experience evaluation is considered.

3.5.1 Evaluation from control engineering point of view

The objective evaluation means assessing the system performance based on physical measurements.

Grasp strength

As mentioned in Section 3.1 the operator will not feel the grasp force of the recipient due to the deficiency in the H-glove exoskeleton that it can not exert force on the operator's hand. Only the recipient would feel the grasp force of the operator. An objective evaluation for this aspect can be a hand grasping test (Pedemonte et al., 2017) which should ensure that the grasp force exerted by the qb soft hand on the recipient hand does not exceed the grasp force pain limit highlighted in Section 3.1. Such a test requires a force sensory system in order to measure the grasp strength exerted on the recipient by the qb soft hand.

Handshake vigor

This aspect is realized by the arms subsystems. Considering the arms subsystems independently, the system would be a conventional tele-manipulation system composed of a robotic arm at the master, and another robotic arm at the slave, similar to the tele-manipulation system in Lazar (2019), for which the evaluation is a transparency test described in Section 2.3 that should take care of assessing the position of the master and slave arms subsystems as well as assessing the virtual spring control force and the force feedback exerted on the slave and master robotic arms, respectively. The transparency test results are presented in the results chapter.

3.5.2 Evaluation from user experience point of view

This type of evaluation is to assess the system performance in providing a genuine human experience, especially if the human-robot interaction is present. The user experience is not fulfilled only by achieving the main function that the robot is responsible for, which is the handshake in this case. There are other factors that have influence on user experience that should be taken into account. How the user perceives the robot is also an important part of the user experience. In addition, the emotional state quality that is left in the user before, during and after the interaction constitutes a significant part of the user experience as well. Therefore, the user experience should be approached from three different perspectives (Werner et al., 2012). Figure 3.8 illustrates the three evaluation perspectives along with the metrics proposed in this research which are discussed below.

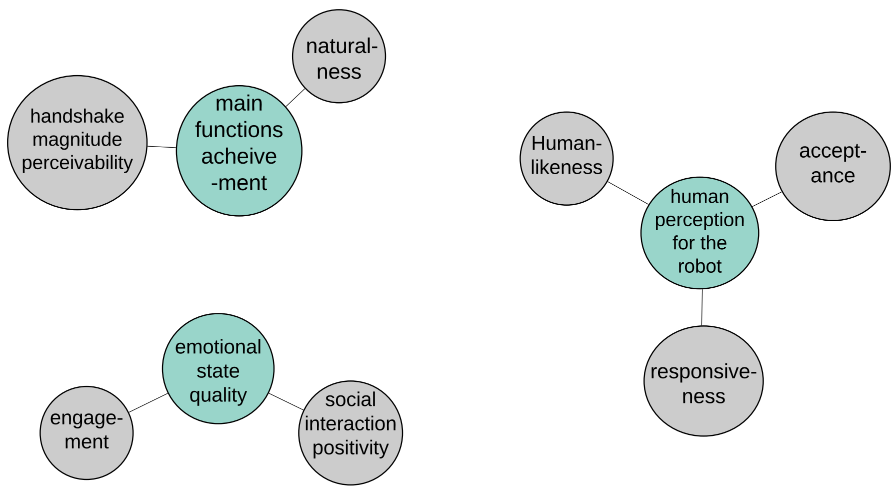

Figure 3.8: Illustration for the factors influencing the user experience

Evaluation perspective I: user-perception-for-robot evaluation

The first perspective is to see how the human perceives the robot. During human-robot interaction, the user may have several impressions and feelings towards the robot. For instance, the mechanical shape of the robot whether it is human-like or machine-like, has influence on the user impression even before the interaction begins. The more the robot is human-like, the better and more genuine the human-robot interaction is (Lindblom and Andreasson, 2016). Three evaluation metrics were chosen for evaluating the perception of the user for the robot. The first metric is the *human-likeness*. In handshake application it is important to have a robot system that is human-like that lets the user feel that he/she shakes hands with a human. Alhalabi and Horiguchi (2001) used a robot system that is not dedicated for handshake, and their UX evaluation results regarding the human-likeness was reported to be poor. Therefore there is a need for a metric to measure the user feeling regrading the shape of the robot. This metric could actually also serve as a metric evaluation for the grasp completeness aspect which is only dependent on the robot hand shape. The second metric, that is relevant to the user perception for the robot, is the acceptance. This metric is aimed to quantify how acceptable the robot is by the user in terms of ease-of-use. Factors that have influence on acceptance is the robot hardware complications. An examples of hardware complications is the robot cables that might apparent for the user and might be disturbing to the user's interaction with the robot. Another example of hardware complications is the requirement for sensory system to be mounted on the user body in order to have the entire system functioning. The hardware complication is damaging for the user experience because the user usually is not that familiar with robot interfaces. So the less easy-to-use the robot hardware is, the more damaging it is for user experience. The third and last metric used in evaluating how the user perceives the robot is responsiveness. Responsiveness is a measure of how fast the robot is in its interaction with the user. Responsiveness is also an important characteristic in handshake, and it is especially related to vigour handshake aspect. Wang et al. (2009) emphasized on the mutual compliance between the handshake partners. If the robot system is not responsive in its actions, then mutual compliance, or vigour, is not achieved. Since the UX evaluation is a self-assessment manikin (SAM) for the user, the questionnaire in Table 3.2 was formulated.

Questionnaire item	**Metric qualitative values**				
	-2	-1	0	1	2
The robot system was socially acceptable	strongly disagree	disagree	neutral	agree	strongly agree
The robot's movements were agile	strongly disagree	disagree	neutral	agree	strongly agree
The robot was human-like	strongly disagree	disagree	neutral	agree	strongly agree

Table 3.2: Evaluation questionnaire for the user perception about the robot

The user can give a response out of five possible responses with a corresponding score ranging from -2 up until 2.

Evaluation perspective II: main functions achievement

The second angle from which the human-robot interaction should be evaluated is the main functions that the robot is responsible to achieve. The evaluation metrics for the main functions are dependent on the application. For haptic handshake system, the main functions are realizing the handshake aspects, especially the grasp force aspect and vigour. The user experience evaluation regarding the grasp force should be done at different grasp forces applied by

the operator. Then the user should be interrogated about the experience whether the user has experienced and felt the difference between the applied forces. So the two evaluation metrics for this aspect are chosen to be *naturalness*, to measure how natural applying different forces is realized by the robot system, and grasp *firmness* to measure how appropriate the control design is for human-robot interaction, particularly handshake.
Concerning the vigour, the three parameters that define the handshake vigour are the number of degrees of freedom, the interaction force of the arms subsystems, and the arm stiffness as mentioned in Section 3.1. The relevant parameter to the UX evaluation is the arm stiffness. Therefore the evaluation metric for this aspect are also selected to be naturalness. So, the user should be interrogated about how natural each of the two tasks during the interaction with robot system. For these metrics, the questionnaire items can be made as in Table 3.3.

Questionnaire item	**Metric qualitative values**				
	-2	-1	0	1	2
The manipulation experience was natural	strongly disagree	disagree	neutral	agree	strongly agree
The grasping expedience was natural	strongly disagree	disagree	neutral	agree	strongly agree
The grasping was appropriately firm	strongly disagree	disagree	neutral	agree	strongly agree

Table 3.3: Evaluation questionnaire related to main functions achievement

Evaluation perspective III: emotional state quality

The last component of the user experience in human-interaction that should be assessed is the emotional quality. It is important to design robot control system that ensure the interaction experienced by the user as not only acceptable and safe, but also as positive. Because, the social robots are intended to support the humans and add new good values to the human daily live; if otherwise the user does experience the interaction with the robots as negative, the consequence might be a reluctance to interact with robots, which in turn may inhibit the acceptance of robots at all (Lindblom and Andreasson, 2016). For handshake application, the system should provide the user with the social positive emotional state that humans obtain from their interactions with each other. Two metrics could be utilized to measure the emotional equality of the user upon the interaction with the robot through a handshake. The first is selected to be *engagement* to see how much the user was engaged in the interaction, or how exciting the handshake experience was. The second metric is *positivity* to check whether or not the interaction of the user with robot has boosted with social positivity. Therefore the questionnaire items can be designed as shown in Table 3.4.

Questionnaire item	**Metric qualitative values**				
	-2	-1	0	1	2
The interaction with the robots was engaging	strongly disagree	disagree	neutral	agree	strongly agree
The handshake with the robot boosted positivity	strongly disagree	disagree	neutral	agree	strongly agree

Table 3.4: Evaluation questionnaire for emotional state quality

To obtain evaluation results that can be generalized, the experiment should be done over different behaviors of the system such as different stiffness values of the robot arms. But it is not necessary that for each run the participant has different responses. This is because some of the evaluation metrics are independent of the stiffness value, and only dependent on the robot shape, for instance. Second of all, there should be a method to map the total score to a percentage score in order to have it more readable and more interpretable. As can be noticed from the tables above, the user should report his experience by selecting a score from -2, which is the lowest score for a certain metric, up until 2, which is the highest score. It is not clear to only sum the users' scores for a certain qualitative metric to find the total score for that metric. For instance, assuming that 50 participants did the experiment, and that the total score for one of the qualitative metric was 54 which resulted from only summing the numbers corresponding to the responses. It is unclear whether this total score is sufficiently good or not. Therefore the total score is mapped using the following formula:

$$S(\%) = \frac{S - S_{min}}{S_{max} - S_{min}} = \frac{S + 2 * n}{4 * n} \tag{3.10}$$

where S is the score resulted from summing the users' responses, and n is the number of participants. With this formula, the minimum sufficient score to pass the evaluation test will be 50%; any score less than 50% then the system fails at the corresponding evaluation metric.

4 Control System Design

In the previous chapter, the control goals were formulated in addition to introducing other control concepts that were intended to use in designing the control system such as variable impedance control and human impedance estimation. In this chapter, first of all, a model for the control system is made. Then, the control system design is proposed. The designs of the transparency and passivity layers are considered. Last but not least, the Robot Operating System (ROS) is introduced as the middleware system to be used in this project.

4.1 Control system modelling

4.1.1 Conceptual system design

Figure 3.5 in the last chapter illustrates the system modelling, where the blocks of masses are the slave and master, and the spring and damper are the control. However, in the previous section, it was mentioned that for the tele-handshake system, there are two human operators and consequently there are two set points for the control system. This implies that the system design of tele-handshake system is different from that of conventional tele-operation system. Therefore a modification was made on the conceptual design of Figure 3.5, and the modified conceptual design is shown in Figure 4.1.

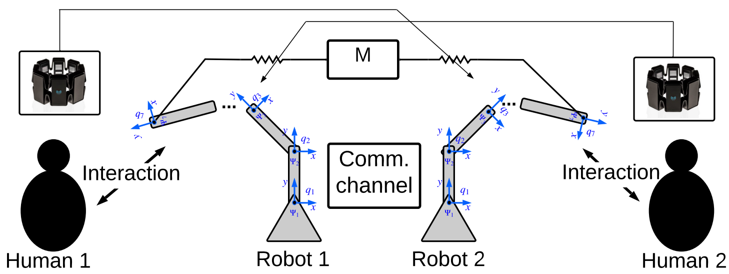

Figure 4.1: Tele-handshake control system conceptual design. The block "M" is an intermediate dummy virtual mass of which the states are considered to be measurable.

As the above figure shows, there are two springs. The spring represents a controller. Since there are two set points being given from the two handshake partners, there should be two springs representing two controllers. Each controller is modulated by the human arm co-contraction level measured by the myo armband sensor. The mass block is a dummy intermediate mass placed between the two springs to make sure that the force of one spring is applied uniquely on the neighbouring robot, not on both robots.

4.1.2 Bond graph model and verification

In order to verify that the conceptual design presented in Figure 4.1 indeed is reasonable representation for the tele-handshake system and its control, bond graph was made for the conceptual design illustrated above. The bond graph is shown in Figure 4.2.

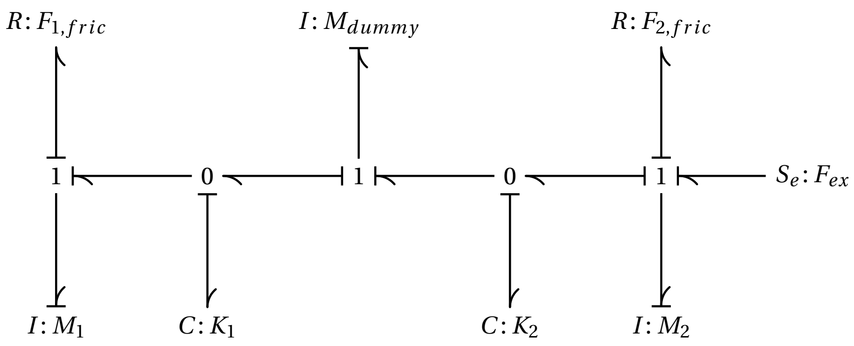

Figure 4.2: Bond graph for the conceptual design of Figure 4.1. $F_{1,fric}$ and $F_{2,fric}$ representing the friction in robot 1 and robot2. K_1 and K_2 representing the two controllers or springs. M_1, M_2 and M_{dummy} representing the two robots' masses and the intermediate mass. F_{ex} representing the external force source

The verification is to apply external force at one of the robots and investigate the state of the springs whether or not they converge to the zero equilibrium point after oscillation. The state of each of the two springs is actually the displacement between the corresponding robot position and the intermediate mass position. Therefore, when the displacements converge to the final zero state, this means that the two robots reached the same position. A simulation using 20Sim was made for the purpose of verification, and the states of the two springs are shown in Figure 4.3 after an external force is applied on the robot 2.

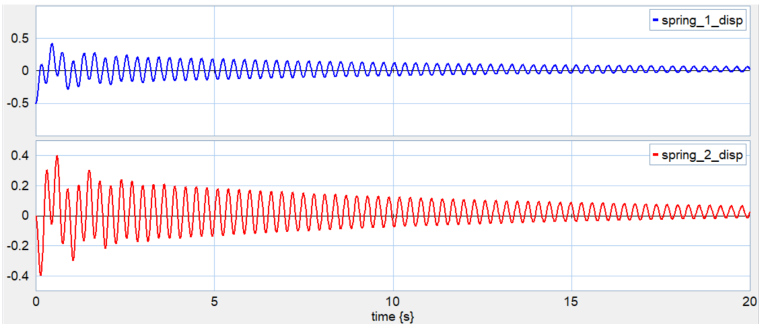

Figure 4.3: Results of applying external force on one of the robots to verify the system behavior. The force is constant and applied on robot 2 using the model in Figure 4.2

The simulation parameters are listed in Table 4.1.

	value
robot 1 [kg]	0.5
robot 2 [kg]	0.5
spring 1 [N/m]	20
spring 2 [N/m]	20
friction 1 [N.s/m]	1
friction 2 [N.s/m]	1
intermediate mass [kg]	0.1
external force [N]	1

Table 4.1: Simulation parameters of Figure 4.3

4.2 Control design

The tele-handshake system is a tele-operation system. However, there is still a difference on the control level, especially because the feature of transporting the compliance of the handshake partners to one another is an important point to be considered in tele-handshake system. In this section, an overview of the control architecture is made, and then details on the control level are later discussed in the controller's design sections.

Usually, the tele-operation system is used as an extension to the operator's capability to accomplish a certain task remotely, and to receive force feedback as a reflection for the interaction between the slave and the environment. This means that the master is the only one responsible for sending commands to the slave, and the slave follows those commands and sends force feedback to the master. That is achieved by having one controller that takes in the set point from the master, and exerts the control force on the slave device in order to make it follow the master's trajectory. But in that case, its feature of variable parameters conveys the operator's impedance to the environment only as already done by Van Teeffelen et al. (2018) and Ajoudani et al. (2012).

In this project, however, a tele-handshake system is targeted, where there are two persons to remotely shake hands, and so the two persons send commands to each other, and both should feel the compliance of each other as well. This suggests designing a control system that should enable this bilateral interaction. That is achieved by having two controllers. The first is a master controller whose set point is obtained from the master device, and whose control parameters should be modulated by the impedance of the operator. This master controller would apply its control action on the slave device. The second controller is a slave controller whose set point, this time, is acquired from the slave device, and whose stiffness parameters should be modulated by the recipient impedance. This slave controller should exert its control force on the master device. With this design, the control actions are personalized. In other words, the control actions vary based on the operator and recipient personally; another operator-recipient couple performs tele-handshake, other control actions should be computed by the controllers. This double-controller control design was thought of, because it does not make sense to modulate the stiffness parameters of one controller by two humans' impedances. Also, having two impedances measurements and one impedance controller to modulate means that the impedance of one of the handshake partners is ignored, while the tele-handshake system should actually convey the compliance of the two handshake partners to each other.

Therefore, the control of handshake system can be built on the basis of the classical control of tele-operation with some extra modifications. Figure 4.4 shows an overview of the modifications on the control transparency and passivity layer.

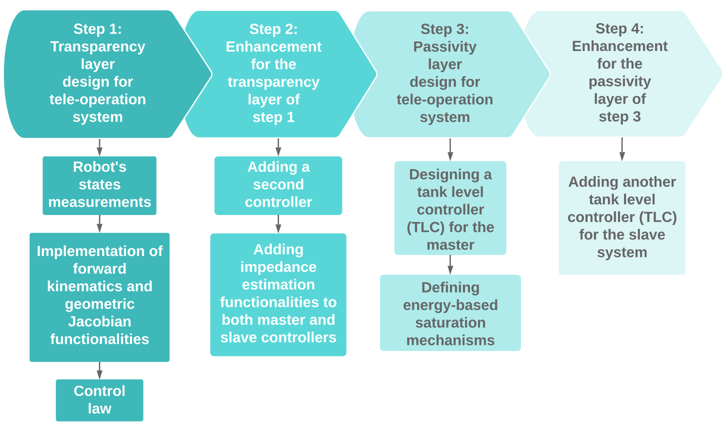

Figure 4.4: The improvements in transparency and passivity

4.3 Control design diagram

Figure 4.5 illustrates the control design of a tele-handshake system. In the sequel, the design is presented and discussed. But the passivity layer is be only introduced shortly, but not implemented because of time constraints.

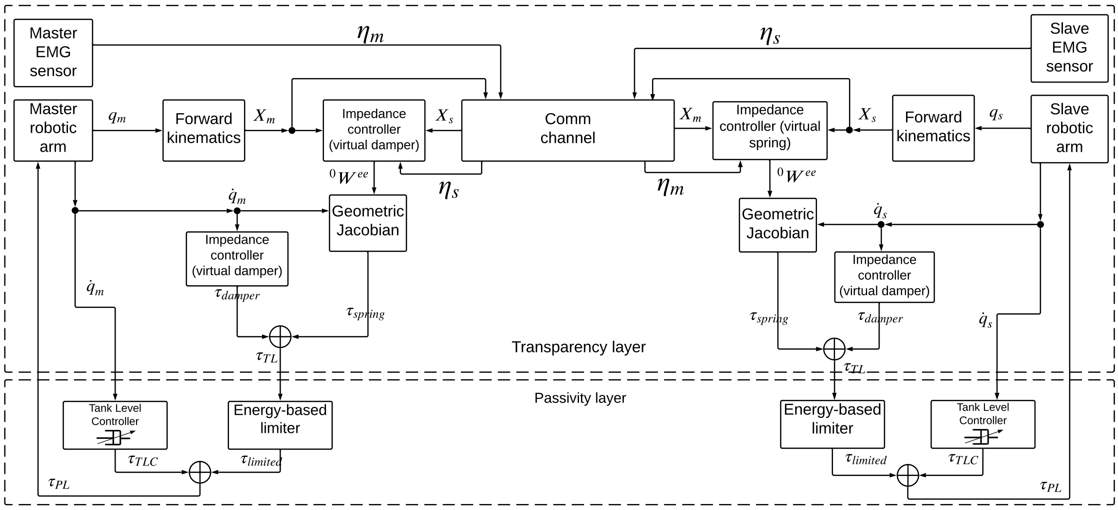

Figure 4.5: Diagram control design

4.3.1 Transparency layer

The transparency layer main function in tele-operation system is determining the control actions for the master and the slave.

Each of the block's functionality is explained below.

- **Master/slave robotic arm**
  This block represents the physical robot of the master/slave system which integrates sensors and actuators. In order to control the slave/master robotic arm, the operator/recipient should apply force to displace the master/slave physical robot, and the joints positions should be measured accordingly to use for other processes.

- **Forward kinematics**
  This block receives the joints positions measurements in order to find the pose of the robotic arm, which includes position and rotation information. These information will be used to calculate the error between the master and slave robots. The dynamics error calculation is performed in the block of *Impedance controller (virtual spring)*.

- **Geometric Jacobian**
  This block implements the geometric Jacobian which is a mapping from the joints velocities to the end-effector general twist. It is used to map the 6D vector wrench, exerted on the end-effector, into the joints torques in joints space. The computation method of the Jacobian as well as the mapping from the Cartesian space to joint space is explained in the appendix 7.2.
  It is important to distinguish between the geometric Jacobian of the master and the geometric Jacobain of the salve in case the master and slave robots are different because the geometric Jacobian is dependent on the robot configuration. In the test process, two Frank Emika Panda robots would be used for master and slave, and so the Jacobain is the same in this case.

- **Impedance controller (virtual spring)**
  As discussed in Section 3.4.1, the impedance control is composed of virtual spring and damper, that is why there are two blocks called "impedance control". Like any other control method, the impedance control requires the error between the set point position and the current position in order to stabilize the dynamics as desired. The error is calculated as follows:
  $$e = X_{sp} - X \tag{4.1}$$
  Based on this error, the control force can be calculated as:
  $$^{0}W^{ee} = K \cdot e \tag{4.2}$$
  As shown in Figure 4.5, the functionality of estimating the human impedance is integrated in the transparency layer to utilize it in modulating the controller's parameters. Hence the stiffness becomes (Van Teeffelen et al., 2018):
  $$K_{*}(\eta) = K_{*,\min} + \eta \cdot \left(K_{*,\min} - K_{*,\max}\right) \tag{4.3}$$
  Where η is the co-contraction level of the human arm given as (Van Teeffelen et al., 2018):
  $$\eta = \min\left(1, \hat{\alpha}_{flexor}, \hat{\alpha}_{extensor}\right) \tag{4.4}$$
  where α_{*} is the normalized EMG signal of the human arm during interaction, which is found as (Van Teeffelen et al., 2018):
  $$\hat{\alpha} = \max\left(0, \frac{\alpha - \alpha_{\min}}{\alpha_{\max} - \alpha_{\min}}\right) \tag{4.5}$$
  where α_{min} and α_{max} are the maximum and minimum activation levels, which are obtained by calibration process.
  Notice in the Figure 4.5 that the impedance controller located in the master acquires the set point from the slave, and its spring wrench is applied on the master robotic arm, and therefore the controller should be modulated by the recipient's impedance η_s so that the operator feels the recipient force modulated by the recipient compliance. For the impedance controller located in the slave, the same logic applies, the set point is from the master. The spring wrench is exerted on the slave robot arm and it should be modulated by the operator's impedance η_m, and that is why it is sent over the communication channel, so that the recipient feels a force from the operator modulated by the operator's impedance parameters.
  As explained in the appendix 7.2, the final control torque is given by:
  $$\tau_{spring} = J^{\top} \cdot ^{0}W^{ee} \tag{4.6}$$

- **Impedance controller (virtual damper)**
  In principle, control could be achieved by relying only on a virtual spring. But in order to reduce the oscillating behaviour of the robot, joints virtual dampers could be added. The virtual damper contribution to the control torque could be calculated by the joints velocities and the damping matrix of the joints as in the following relation:
  $$\tau_{damper} = -B\dot{q}_s \tag{4.7}$$
  where B is the diagonal damping matrix containing the damping coefficient of the virtual dampers of all the joints. Then the total control torque is the sum of the spring and damping torques as follows:
  $$\tau_{control} = \tau_{spring} + \tau_{damper} \tag{4.8}$$

Note that these joints dampers of the master and slave are not necessarily the same as the arms subsystems might be different in number of degrees of freedom. For instance, for the Franka Emika Panda robot arm, the damping matrix would be 77 matrix:

$$B = \begin{bmatrix} b_1 & 0 & 0 & 0 & 0 & 0 & 0 \\ 0 & b_2 & 0 & 0 & 0 & 0 & 0 \\ 0 & 0 & b_3 & 0 & 0 & 0 & 0 \\ 0 & 0 & 0 & b_4 & 0 & 0 & 0 \\ 0 & 0 & 0 & 0 & b_5 & 0 & 0 \\ 0 & 0 & 0 & 0 & 0 & b_6 & 0 \\ 0 & 0 & 0 & 0 & 0 & 0 & b_7 \end{bmatrix} \tag{4.9}$$

4.4 Passivity layer

The passivity layer is only introduced shortly here, but not implemented in this project. The reader is referred to the main works of passivity layer for future work perhaps.
The energy flows in the passivity layer are three parts, namely the energy to be received by a system (master or slave), the energy to be sent to a system (master or slave) and the energy exchanged with the physical surroundings (operator or recipient). As the passivity is not implemented in this work, all the energy calculations of the passivity layer can be found in the work of (Franken et al., 2011). A design hypothesis for the passivity layer of a tele-handshake system is proposed below.

Tank level controller (TLC)

In order to avoid the situation of energy depletion, or insufficient energy in the tank for accomplishing task, a tank level controller (TLC) could be further integrated in the passivity layer. This controller is aimed to monitor the energy level of the tank after the processes of sending and receiving energy has occurred. In case the tank level is insufficient relative to an energy threshold, the TLC should extract extra energy from the operator. Such a controller could be implemented by a tunable viscous damper which exerts opposing force to the operator movement to extract energy (Franken et al., 2011). The total torque exerted on the robot device would be the summation of the transparency layer torque and the TLC torque as shown in the Figure 4.5. Now for the tele-handshake, there is a modification regarding the TLC. The modifications is designing another tank level controller (TLC) for the slave system, because the handshake system have two operators to interact with since the recipient is considered as another operator who can send commands to the other side. Those two operators are seen by the system as two active energy sources that the system could extract energy from.

4.5 Implementation in ROS

The communication network is important in tele operation system, because it is the medium through which the commands of the master and the haptic information are sent. Developing robotic systems require a collection of software dependencies such software libraries, third party software components and simulation tools. Robot Operating Systems (ROS), among other robot software systems, is an open source software system that provides all the services that any other operating system does such as hardware abstraction, low-level system control, implementation of functionalities, multi-lingual communication between subsystems and package management.
Implementation-wise, each subsystem is represented by a ROS node. The different nodes, or subsystems, communicate with each other by ROS messages which are defined data type. Those messages flow through ROS topics to which a node can either publish or subscribe to send or obtain messages.
For the current system implementation, the controller for each one of the two Franka robot

arms is implemented as a ROS node, and each one of the two EMG sensors is implemented as ROS node.[1] The diagram in Figure 4.6 shows the ROS graph illustrating the nodes and the topics, and how the message flow is.

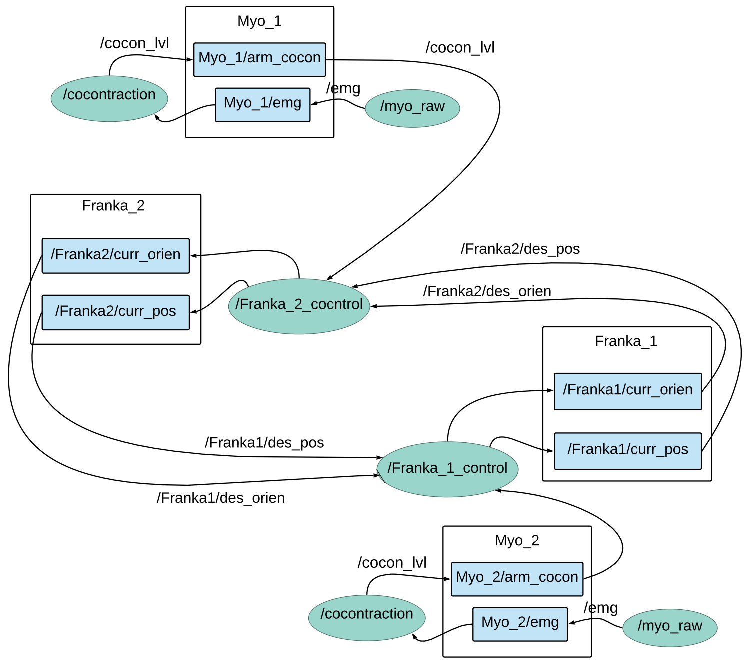

Figure 4.6: ROS graph showing the nodes and topics constituting the system. Green round shapes are the nodes, and blue rectangles are topics.

As can be seen in Figure 4.6, there are two set points (two desired positions and two desired orientations) for the tele-handshake robot system, because there are two human operators, or two handshake partners. The current pose of one of the robot arms is a set point pose for the other robot arm. This is shown in Figure 4.6 where the node of Franka1 robot, for example, subscribes to the current position and orientation topics of Franka2 robot. The first set point is given by the node "Franka_2_contol", where the set point is sent to the topic of "Franka_2", where the node "Franka_1_control" subscribes to receive the set point. Simultaneously, the node "Franka_1_control" sends its position to the topic "Franka_1", where the node "Franka_2_control" subscribes. The stiffness of one of the robot arms is modulated based on the counterpart operator arm's co-contraction level measured by the myo sensor. This is shown in the figure, where the node of "Franka_1" subscribes to the topic "Myo_2" of the measured co-contraction level of the operator2, not operator1.

[1] The implementation of the EMG myo armband sensor was reused from the code base of i-botics.

5 Experiments and results

In this chapter, a feasibility study is made for checking whether or not the Franka robotic arm is suitable for social interaction applications. Then, a transparency test for the tele-operation system is performed. Moreover, the proposed control design is evaluated by making sure that the stiffness parameter varies based on the human arm co-contraction level. Last but not least, user studies are performed to assess the user handshake experience. [1]

5.1 Experiments and set up description

5.1.1 Experiment I: feasibility experiment of realizing handshake vigour using Franak robot arm

This experiment can be considered as an extension and completion for the experiment conducted in the work of (Wang et al., 2009) which is the only work in literature that attempted to measure the shake force to the best of the author knowledge. They have done the experiment with one subject only, which is slightly inaccurate, because if another person would have performed the interaction with the robot arm, different results for the shake force would be obtained. In addition, they have not mentioned any information about the stiffness of the robot arm, at which they have performed the experiment. The interaction force with the robot arm, or the shake force, changes based on the robot stiffness. That is why their results can not be generalized. In order to have more reliable and accurate results, first the shake force measurement experiment should be done on a population of human subjects; meaning several human subjects should participate to account for the fact that different people have different handshake forces, second the experiment should be also done over multiple stiffness values. Therefore in this research, it was decided to perform this experiment with 12 healthy participants aged between 20 and 30 years old, including females and males. Every participant was asked to shake hands with the Franka robot arm in three different scenarios, namely weak-shake-force scenario, normal-shake-force scenario and strong-shake-force scenario. In each scenario, the shake force was measured over three different stiffness settings, namely low stiffness, medium stiffness and high stiffness. So in total, the number of trials of this experiment was 108 trials. The system that was used for this experiment is shown in Figure 5.1.

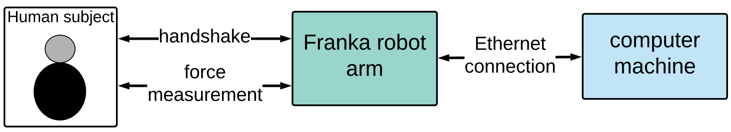

Figure 5.1: Hardware representation for the system used for measuring the handshake vigor (shake force)

Regarding the stiffness settings used for this experiment, three stiffness values were used in the experiment corresponding to very complaint arm, very stiff arm and appropriately complaint arm. The stiffness values choices were made based on work of (Van Teeffelen et al., 2018). The stiffness values are shown in Table 5.1.

[1] Due to the fact that not all the system components are available in RaM laboratory, particularly the Virtuose 6D robot arm, not the complete system was tested. Because, the H-glove exoskeleton can only be mounted on the Virtuose 6D robot arm to have the system complete. For that reason, the test experiment for the control of the robot arm subsystems was done separately without the robot hand subsystems.

	Low stiffness	Medium stiffness	High stiffness
Trans. stiffness [N/m]	100	270	550
Rot. stiffness [N.m/rad]	3.5	8.5	10.5

Table 5.1: Stiffness values used in experiment I

5.1.2 Experiment II: Transparency test or validating the control design

Because the tele-handshake is mainly a tele-operation system, a transparency experiment is required. The transparency was introduced earlier as a performance measure of how well the control system achieves the control goal, which is stabilizing the dynamics and generating force feedback. Stabilizing the dynamics can be checked by observing the error between the local and remote robots' positions, while the operator applies force on the local robot. The local and remote robots used for this experiment are two Franka robot arms available in RaM laboratory. A representation for the experimental set-up is shown in Figure 5.2.

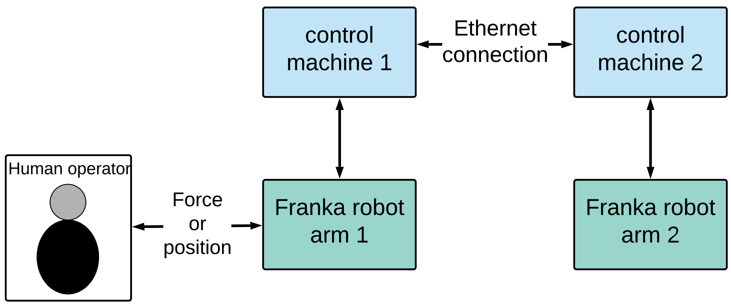

Figure 5.2: Hardware representation for the robot system used for transparency test

	Value
Trans. stiffness [N/m]	250
Rot. stiffness [N.m/rad]	6.25

Table 5.2: Stiffness values used in experiment II

It depends on the application, or the task, for which the tele-operation is used to design the robot arm compliance. For instance, for accomplishing positioning tasks, high stiffness values are used; for impact minimization tasks, low stiffness is used (Van Teeffelen et al., 2018). In this research, the task is handshake. This suggest designing considerable amount of compliance in the arm. Because, in real-life handshake between two persons, the handshake is a mutual process that is performed by the two handshake partners. Therefore, it is not an important control goal in a tele-handshake system to have the error minimized; having sufficient compliance, or realizing handshake vigour, is prioritized over minimizing the dynamics error. In fact, that comes at the cost of obtaining relatively larger error as it is well known that for low stiffness values, the stabilization error increases. However, it still can not be claimed that the low stiffness is the optimal stiffness for tele-handshake system. The stiffness of the robot arm should be determined by the human anatomical arm stiffness, which is the goal of the experiment III. The experiment II was done using the stiffness setting shown in Table 5.2

5.1.3 Experiment III: variable-stiffness control

This experiment is aimed to show that the variable-stiffness control, included in the control design of Figure 4.5, is functioning as desired. This could be checked by observing the updated stiffness of the virtual spring if it varies in accordance with the changes in the muscles co-contraction of the operator. The sensor used for measuring the operator muscles contraction is the myo armband sensor. Before using the myo armband, the EMG signals need to be filtered, and a calibration process must be done.

Part A of experiment III: Filtering of EMG signals

To reduce the noise, a filter needs to be designed. In order to know which type of filter is required, it was found in literature that the bandwidth of electrical activity signal of human arm lies in the range of $[0,15]Hz$ (Ajoudani et al., 2012). This suggests designing a low pass filter. Accordingly, a Butterworth low pass filter was designed given by the equation below:

$$y[n] + b_1 y[n-1] + b_2 y[n-2] = a_1 x[n] + a_2 x[n-1] + a_3 x[n-2] \tag{5.1}$$

where x is the unfiltered signal of the activation level, and y is the filtered version of the signal. The cutoff frequency for the biceps and triceps muscle activity was chosen to be $15Hz$ based on observations shown in the results section.

Part B of experiment III: Calibration of myo armband sensor

As mentioned in section 3.4.1, the calibration is to find the maximum and minimum muscles activation levels. Two scenarios applied to find those extreme cases activation levels. The hardware required for this experiment is shown in Figure 5.3.

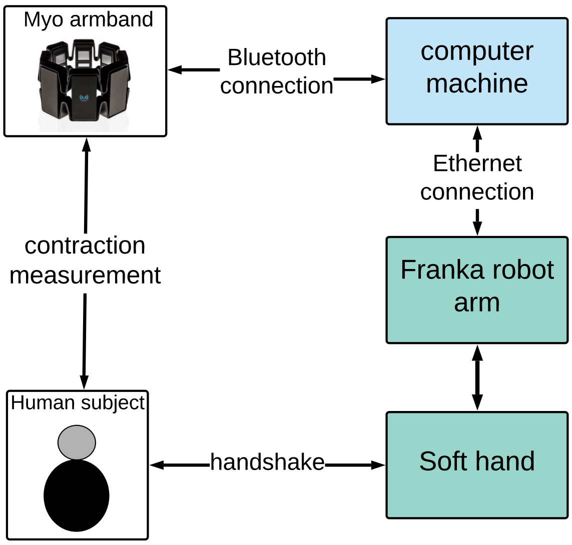

Figure 5.3: Hardware representation for the robot system used for calibration myo armband

The first scenario: weak handshake
The operator barely held the hand of the robot arm without exerting much grasp force, and then shaken hands with the robot. It was observed that this activity is sufficient to obtain minimal muscles activation measurements from the biceps-triceps muscles. That is why this scenario was chosen to define the minimal arm contraction level during handshake.
The second scenario: strong handshake
In the second calibration scenario, the experiment observer has performed a strong handshake that is slightly stronger than the normal handshake magnitude that he uses in daily live so that the muscles activation corresponds to the maximum of contraction level.

Part C of experiment III: Validating the proposed control design with human subjects

The control design of bilateral control is validated in this experiment. The operator and the recipient perform a tele-handshake with each other remotely, and the stiffnesses of the robots are modulated by the corresponding handshake partner's arm activation level. This experiment was performed to make sure that the stiffness is indeed being modulated properly based on the human muscles activation. For the maximum and minimum stiffnesses that are used in updating the stiffness, they were chosen based on previous work of Van Teeffelen et al. (2018) with slightly reducing the values, because for handshake application it is important to have significant amount of compliance in the arm even if that comes at the cost of obtaining larger error. The stiffness choices are listed in Table 5.3.

	min	**max**
Trans. stiffness [N/m]	100	550
Rot. stiffness [N.m/rad]	3.5	10.5

Table 5.3: Max and min stiffnesses used in the stiffness updating rule

In order to also make sure that this result is statistically correct, four human subjects participated in doing the experiment. One time with the classical control architecture, and one time with the proposed control design. Each experiment, the handshake partners shake hands three times, and then the force is averaged over the three trials.

5.2 Results

This section presents the results obtained from the experimental setups described in the previous section.

5.2.1 Experiment I: feasibility experiment of realizing handshake vigour using Franka robot arm

This experiment was conducted to quantitatively measure the human handshake vigour, or shake force, during handshake in order to investigate the feasibility of realizing the vigour characteristic using the Franka robot arm. The interaction force was estimated according to the pseudo code listed in Algorithm 1. The results obtained from the experiment are shown in Figure 5.4.

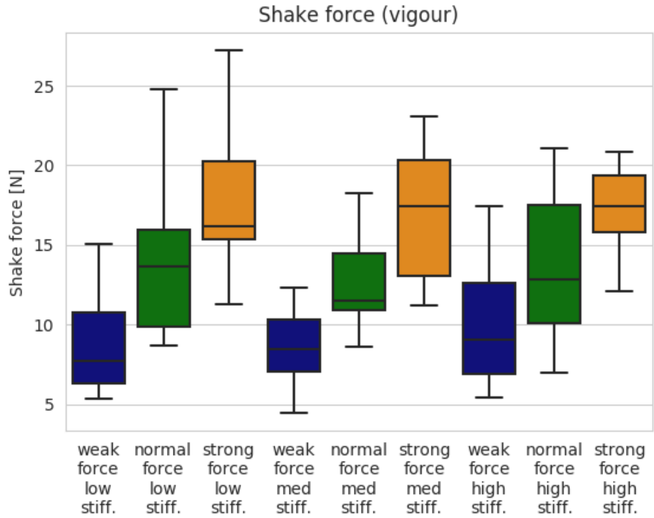

Figure 5.4: The findings of measuring the vigour quantitatively at low, medium an high stiffnesses. The whiskers of the a box represent the maximum and minimum. The top, the line inside the box and the bottom are respectively the 25th, 50th and 75th percentile

Statistical information such as mean force and variance of each handshake scenario are listed in Table 5.4. The forces of all participants in the different conditions can be found in appendix 1.4.

	Weak force		**Normal force**		**Strong force**	
	$\mu[N]$	$\sigma^2[N]$	$\mu[N]$	$\sigma^2[N]$	$\mu[N]$	$\sigma^2[N]$
Low stiff.	9	11.44	13.52	20.43	18.12	21.98
Medium stiff	8.53	6.46	12.62	8.65	17.31	17.39
High stiff.	10.27	16,96	13.39	21.83	17.19	8.57

Table 5.4: Statistics obtained from the experiment I

The conclusion of the feasibility study to draw here is that the handshake vigour seems to be realizable by the Franka robot arm, because all the forces by all participants in different conditions were observed to be smaller than the maximum interaction force that the Franka robot withstands which is 30N.
In addition to that, the findings of this experiment can provide an insight about the handshake force that the human applies in handshake activity. This is done by averaging the forces of one force category over the three stiffness values. In other words, that is done by finding the average of the three blue bars (weak force category) in Figure 5.4 together, the three green bars (normal force category) together and the orange bars (strong force category) together. This is shown in the Figure 5.5

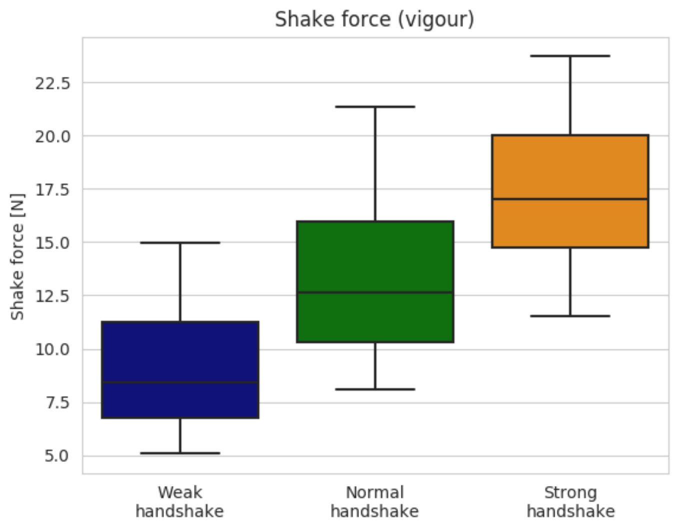

Figure 5.5: The human shake force ranges. The mean force range calculated over three different stiffness values

In comparison with the results of work (Wang et al., 2009) which is the only work in literature that attempted to quantify the handshake vigour, the findings of this experiment shown in Figure 5.5 are relatively more accurate and reliable, because the results in this work are obtained from a population of participants and account for different stiffness values (or different handshake conditions), whereas their results were obtained from one participants only and for one stiffness value only.
It is also informative to observe the mean of the forces over the same force category, which gives insight about the mean weak shake force, mean normal shake force and mean strong shake force. In addition, the standard deviation also provides important information about the variation range that the mean value can take duo to the fact that humans have different shake forces depending on the personal characteristics. The means and standard deviations for each of the three handshake scenarios are listed in Table 5.5.

	Weak handshake	**Normal handshake**	**Strong handshake**
Mean [N]	9.27	13.18	17.54
Std. dev. [N]	3.35	3.96	3.8

Table 5.5: Mean values and standard deviation found in experiment I

As mentioned by Shipps and Freeman (2003), the handshake magnitude is related to the personality traits. More specifically, the extrovert person tends to dominance and thus to have more significant handshake magnitude than the introvert. So looking at the results in Table 5.5, it can be concluded that the introvert person has a handshake force that is in the range of $9.27 \pm 3.35N$, the extrovert person has approximately a handshake force $17.54 \pm 3.8N$ and the ambivert person has a force in the interval of $13.18 \pm 3.96N$.

5.2.2 Experiment II: Transparency test or validating the control design

The operator displaced the local robot with a trajectory, and the Cartesian trajectories for the local and remote robots were recorded. The 3D Cartesian trajectories of the local and remote robot arms are shown in Figure 5.6.

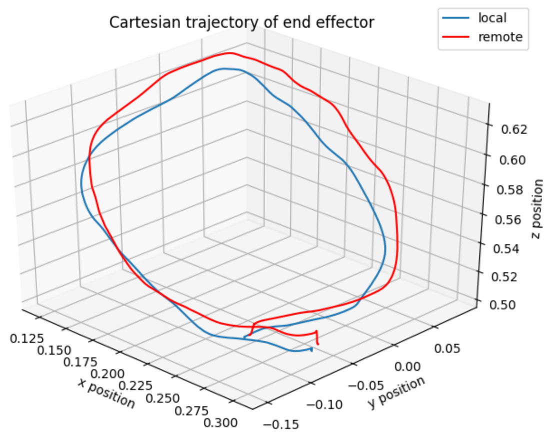

Figure 5.6: Cartesian trajectory of end effector applied by operator to test the tele-operation system transparency

In order to see the dynamics stabilization closer, the Figure 5.7 on the left shows the positions separately, and on the right it shows the corresponding control force, or force feedback or virtual spring force.

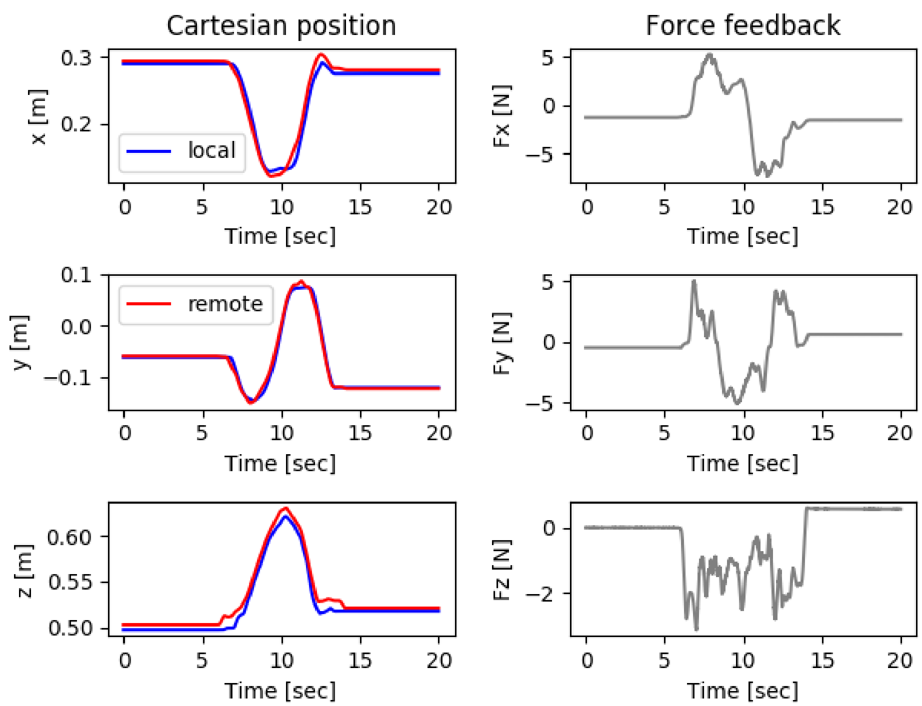

Figure 5.7: The x and y and z positions of the end effector during making the same trajectory of Figure 5.6 along with the force feedback generated

As can be observed in the Figure 5.7, the two-controller control design proposed in chapter 3.5.2 in Figure 4.5 is functioning as desired in leading the local and remote positions to the same position during a trajectory, and the force feedback is generated accordingly, which are together the main goals of this experiment. In this experiment, only the operator executed the experiment with the same stiffness, that is why the force feedback is the same for the local and remote robots. In the next experiment, a subject exists in the experiment which leads to having different forces feedback on the local and remote robots.

5.2.3 Experiment III: variable-stiffness control

Part A of experiment III: filtering the muscles activity signals

Since the EMG signals are noisy, a filter needs to be designed, because, otherwise, the co-contraction level estimation is also noisy and inaccurate, and so the stiffness. The Figure 5.8 shows filtering for the EMG signals at different cut-off frequencies.

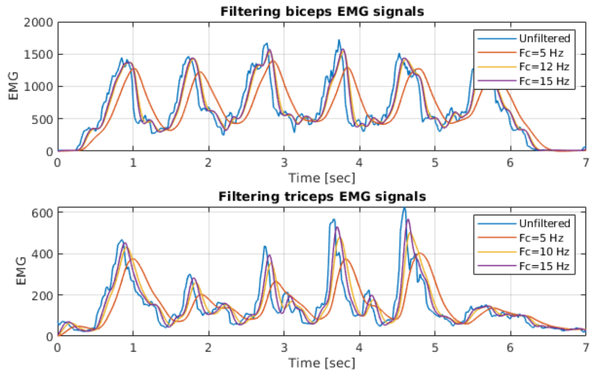

Figure 5.8: Filtering the EMG signals at different frequencies

Selecting relatively low cut-off frequencies leads to phase lag as can be seen in Figure 5.8. It is a good practice to choose close to the bandwidth of the signal, because then most of the frequency contents are passed by the filter cut-off frequency.

Part B of Experiment III: Myo armband sensor calibration

The first scenario: weak handshake

For the scenario description, you can refer to the experiment section in the previous section. The weak handshake scenario is to find the minimum co-contraction level. The calibration procedure is illustrated in Figure 5.9. Figure 5.9 shows a plot on the top for a typical output for a weak-handshake-scenario calibration.

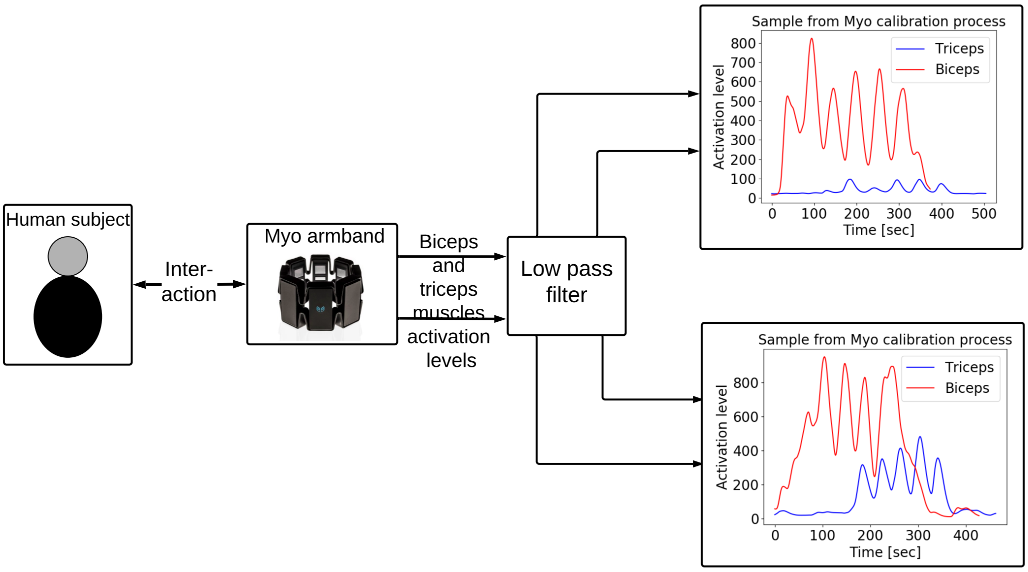

Figure 5.9: The procedure of Myo armband calibration process. The lower plot was obtained from stiff handshake calibration scenario, and upper plot from a weak handshake calibration scenario

The second scenario: strong handshake

This scenario is performed to define the maximum co-contraction level. A typical result that comes out of this experiment can be seen in Figure 5.9 with the plot in the bottom.

Part C of experiment III: Validating the proposed control architecture with modulated stiffness

This experiment's purpose is to validate of the control architecture with a subject in order to show the main feature of this control architecture which is the ability to have different forces feedback applied on the master and slave. The results are shown in Figure 5.10. It can be noticed that the contraction, linear stiffness and rotation stiffness have the same pattern of variation. This is because the relationship that relates the stiffness and co-contraction level is a linear relationship. But of course, the range of values are different. The upper and lower bounds for the contraction level are zero and one respectively, and the upper and lower bounds for the translation and rotation stiffness are shown in Table 5.3. The important point to notice here is that the stiffness is modulated based on the human's handshake interaction with the robot arm; once the motion along the z-component starts or once the handshake activity starts, the human needs to contract/stiffen his arm muscles which leads to the measurements of the contraction level, and the stiffness is updated accordingly. Before and after the handshake interaction, the muscles are relaxed, and so the contraction level is measured to be zero. As such the stiffness is not updated and it takes the value of the minimum stiffness which is 100 [N/m] for the translation stiffness, and 2.5 [N.m/rad] for the rotation stiffness.

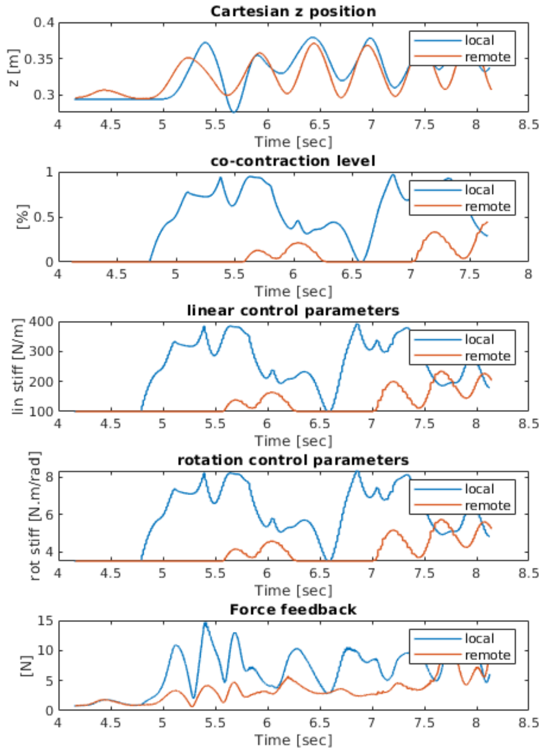

Figure 5.10: The findings of the experiment III. Variable-stiffness control adjusts the the robotic arms' stiffnesses based on the corresponding human muscles contractions

Accordingly, the force feedback that each handshake partner feels is different as the force feedback is function of the stiffness and the stiffness is being modulated by the muscle contraction level of the other person. This is shown in in the bottom of Figure 5.10. This is the difference between the proposed control, and the one-controller control design, where in the one-controller control the force feedback is the same applied on the master and slave devices, whereas in the two-controller control design, the force feedback applied on each robot is different. This means that the control design can be seen as personalized. It adjusts based on the handshake partners to give them the experience of feeling the presence of each other.

Regarding the results of the experiment with the participation of human subjects, they are shown in Figure 5.11. It shows the force feedback applied on the operator and the user.

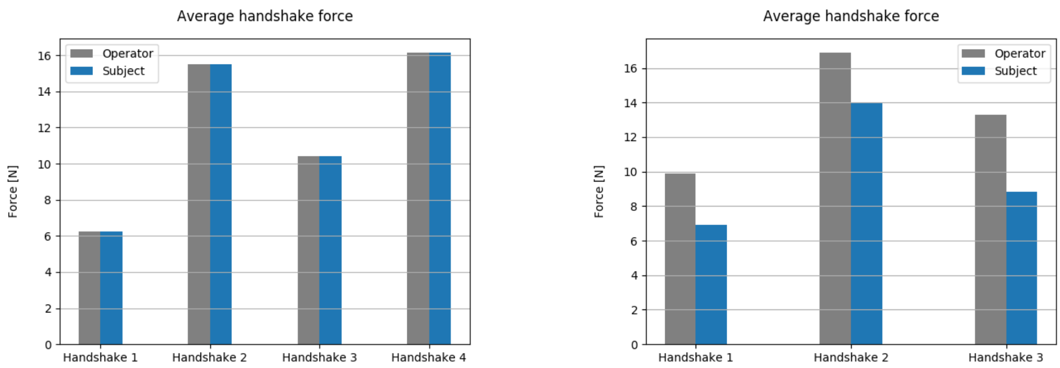

(a) Using classical control design. The stiffness value was arbitrarily chosen to be $150N/m$.

(b) Using propose control design

Figure 5.11: Force feedback using classical control architecture vs. proposed control architecture. Each handshake was performed three times, and then the average force is calculated.

It can be seen in Figure 5.11 that the forces feedback applied on the local and remote robot are the same using the classical control architecture disallowing to exchange the handshake forces between the handshake partners. On the other hand, the forces feedback applied on the local and remote robot are different using the proposed control architecture allowing to exchange the handshake forces between the handshake partners, and thus to feel the presence of each other remotely.

6 User experience evaluation and discussion

In this chapter, statistical analyses are carried out, UX evaluation is performed, and few points regarding the obtained results are discussed.

6.1 UX evaluation experiment setup description

Eleven human subjects[1] have participated in doing the experiment of tele-handshake through two Franka robot arms. The hardware representation of the experimental set-up is shown in Figure 6.1.

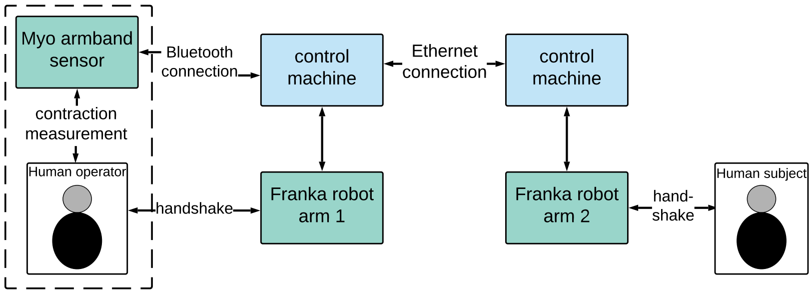

Figure 6.1: Hardware representation for UX evaluation

The experiment was performed over three stiffness values, namely low stiffness, high stiffness and variable stiffness. For the variable stiffness, the myo armband EMG sensor is used. Even though the experiment was done over three choices of stiffness values, some of the users' responses on the experience evaluation questionnaire are constant. Because, some questionnaire items are related to the robot itself, and not related to the stiffness or operation performance. For instance, whether or not the robot is human-like does not change if the stiffness value changes. The effect of changing the stiffness has influence on evaluating the main functions achievement.
The results are shown and discussed in the next section.

6.2 UX evaluation

As discussed in the analysis, the UX evaluation is in fact three parts. The first part is to evaluate the human recognition for the robotic handshake system, which includes: *social acceptance*, *human-likeness*, and *responsiveness*. The second part is evaluation for how well the robot system can achieve the main functions involved in the handshake process, which is represented by *naturalness* (feeling the handshake vigour naturally). The third evaluation part is to evaluate the user's emotion states after the interaction with handshake robot system, and that is measured by: *engagement*, and *social interaction positivity*. For the evaluation metrics of each one of those evaluation parts and for the corresponding questionnaire item, refer to section 3.5.2 for more details. The results of the user studies are shown in Figure 6.2

[1] The author is aware about the fact that the number of human subjects is slightly few. The few number is because of the restrictions on the allowed number of students who can attend in RaM laboratory duo to the health crisis.

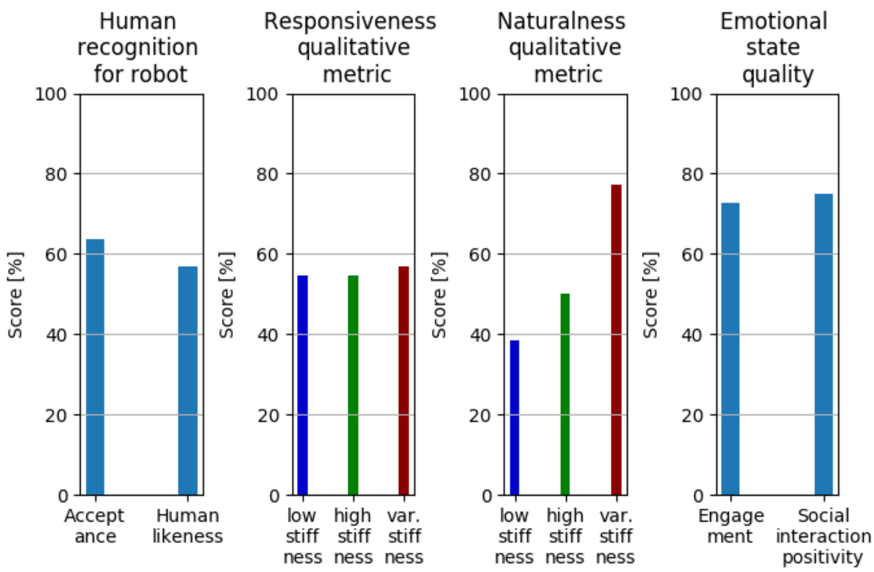

Figure 6.2: The findings of the UX evaluation. The scores are mapped into percentages. Obtaining score below 50% means the system fails in realizing the corresponding feature. Obtaining score higher than 50% means the system passes in realizing the corresponding feature.

The results of the user experience evaluation show that the system has both success and failure in matching the assessment criteria. Although the system has passed in each of the measures *engagement*, *social positivity*, *acceptance* and *human likeness*, there is variation in the obtained scores. Specifically, the system gained at *engagement* and *social positivity* the scores 72.7% and 75%, respectively, whereas at *acceptance* and *human likeness* gained the scores 63.6% and 56.8%, respectively. At the latter two evaluation measures, the system has scored lower, because the user experience at those two assessment criteria is affected by the hardware limitations which degrade the user experience further. For *naturalness* measure, the system has also passed, but only for the case of variable stiffness, because the users can feel the presence of the operator. For the *responsiveness*, the system has passed in the three values of stiffness values, but with relatively low scores, because the perceived weight of the Franka robot arm is relatively high ($18kg$), higher than the perceived weight of the Virtuose 6D robot arm ($12kg$), for example. This has the consequence of making the user not only feel the handshake partner's force, but also the perceived mass of the Franka robot itself.
These obtained results are further discussed and statistically analyzed in the next section in order to see if the system achieved the minimal acceptable performance in enabling two humans to remotely interact with each other, and in providing relatively realistic human handshake experience.

6.3 Hypotheses to test

The statistical analysis is to set up hypotheses about the obtained results and then to test them. The following table lists the hypotheses that were formulated for each one of the evaluation metrics.

Metric	Alternate hypothesis	Null hypothesis
Naturalness	The naturalness scores at the three different stiffness settings are expected to be substantially different from each other, and that the naturalness score is highest at the variable stiffness case.	The naturalness scores at the three stiffness settings are equal
Responsiveness	Score of responsiveness should be high at low stiffness case	The score of responsiveness at the three stiffness settings are equal
Social acceptance	Social acceptance score is expected to be very sufficiently high i.e above 70%	The social acceptance score is almost sufficient i.e 50%
Human-likeness	Human-likeness score is expected to be very sufficiently high i.e at least 70%	The human-likeness score is almost sufficient i.e 50%.
Engagement	The developed system is expected to gain very sufficiently high score at engagement i.e no smaller than 70%	The developed system scores at engagement almost sufficiently i.e 50%
Social interaction positivity	The system is able to provide social interaction positivity to human with a very sufficiently high score i.e above 70%	The system can almost score 50%

Table 6.1: Testable hypotheses for UX evaluation

6.4 Statistical testing and discussion

Discussion with respect to each evaluation perspective is made below.

6.4.1 Evaluation human recognition for the handshake robot system

During the human interaction with the robot, several factors can influence the user's experience. One of these factors is the shape of the robot with respect to the application that the robot is functioning for. For handshake system application, the robots should have subsystems that resemble the human limbs by which the human performs handshake. Particularly, the handshake robot should resemble the human arm and human hand. Other factors are the robot social acceptance and agility which correspond to the user-friendliness (or ease-of-use) and the robot responsiveness, respectively.

- **Human-likeness**: The human-likeness alternate hypothesis was formulated to be that it is expected to obtain a score that is above 70%. That was not obtained, as shown in Figure 6.2. A one-sample[2] statistical t-test was performed to investigate the rejection and supporting of the null hypothesis. The null hypothesis is rejected if the $t_{stat} < -t_{crit}$ or $t_{stat} > t_{crit}$ which is not the case. If the null hypothesis is not rejected, this means that the obtained score for human-likeness is not substantially different from 50%, which is correct because the obtained score is only 56%.

[2] One-sample test is chosen because there is only one group for human-likeness, as the human-likeness metric does not change according to the stiffness value.

groups	P-value	t_{crit}	t_{stat}
Human-likeness	0,17	1.81	1

Table 6.2: One-sample one-tail t-test test for human-likeness results

This result means that the developed system has barely passed in realizing the feature of human-likeness by obtaining the score 56.8%. It was actually unexpected to have low score for the human-likeness metric since the robot arms that were used are 6-DOF arms having the same capability of the human arm in moving in 6 degrees of freedom. But obtaining the low score at human-likeness is interpretable. The Franka robot arm configuration during the experiment was not similar to the configuration of a human arm during the handshake. Because, the base of the Franka robot arm (or the shoulder) is attached on the ground, and so the robot arm is originating from a point underneath and directing upwards, whereas the human arm base (or the shoulder) is attached at the human trunk, and so the arm is originating from a point up and directing downwards. This means that during the handshake experiment, the robot arm did not mimic the human arm configuration of the handshake. That was mentioned by participants. However, based on the participants' score concerning human-likeness, this experiment can give indications about the final system performance. In the final system demonstration, the local robot arm, the Virtuose 6D, will be attached upside down mimicking the human arm in handshake situation, and the remote robot is a humanoid robot that has the same bodily trunk of the human, meaning that the humanoid robot's arm should have the same configuration of the human arm in handshake. Thus, it can be inferred that the final system that is supposed to be used for the ANA XPRIZE demonstration should perform better in realizing the human-likeness feature.

- **Acceptance**: The alternate hypothesis concerning the social acceptance is that the score is expected to be at least 70%. When looking at the Figure 6.2, this score of social acceptance was not achieved by the developed system, where the obtained score is 63%. However, the one-tail t-test[3] was executed to calculate the p-value, and the p-value is smaller than the significance level 0.05, and the $t_{stat} > t_{crit}$, which means that the null hypothesis is rejected. In other words, the obtained score for acceptance can be considered to be substantially different from the minimum score of passing 50%. Practically this means that even though the obtained score is not exactly as expected, the system still has passed with satisfactory score.

groups	P-value	t_{crit}	t_{stat}
Acceptance	0,025	1,81	2.21

Table 6.3: One-sample one-tail t-test test for social acceptance results

It was predictable for the developed system to pass in acceptance, because the RaM work-space in which the Franka robots are installed is organized without many disturbances that distract the user while performing the tele-handshake experiment such as the cables between the robot and its computer machine. Additionally, the human subject was sensors-free, and that was intended from the beginning to not mount sensors on the recipient body in order for the robot system to pass in social acceptance. It is worth mentioning that the humanoid remote robot of the final system implementation is a mobile robot that does not have disturbances such as apparent cables to the user, and

[3] One-tail t-test is for inequality.

so the social acceptance score of the humanoid robot is expected to be higher than the social acceptance score for the Franka robot arm.

- **Responsiveness**: The alternate hypothesis for the responsiveness evaluation metric is that it is expected from the system to score highest responsiveness score at low stiffness. From the obtained results shown in Figure 6.2 it was not achieved where the scores at the three stiffness settings are approximately the same. By doing ANOVA test to see the difference statistically, the test results support this outcome i.e that the scores at the three stiffness values are not substantially different from each other, because the obtained p-value is not less than 0.05 as the table shows below.(The alternate hypothesis is not supported, and so the null hypothesis is accepted).

groups	P-value	F_{crit}	F
low stiff.	0,97	3,31	0,021
var. stiff.			
high stiff.			

Table 6.4: ANOVA test for responsiveness results

The scores for responsiveness in the three stiffness values can be seen in Figure 6.2 where the developed system has passed in the three cases with low scores. It was expected to obtain a higher score at the low-stiffness case, which was not obtained. Because, even though the Franka robot was shown in (Lazar, 2019) to be a suitable input haptic device in terms of transparency (or reproducing force feedback) and in terms of safety, it is still, however, not a haptic device. This means that the joints frictions might be slightly high for handshake application. So even if the stiffness parameter is low, there is the joints friction has influence on the user's interaction. Another factor is the perceived weight during the physical interaction with the robot. In comparison with the Virtuose 6D robot arm ($12kg$), the perceived weight of the Franka robot arm ($18kg$) is higher, which leads to the feeling that the robot is sluggish in its motion. In other words, the human actually does not only feel the forces of the handshake partner, but also the weight of the robot.

6.4.2 Evaluation main functions achievement

For this evaluation perspective, the difference in the stiffness of the robot arm has significant influence on the user experience, and a user's response towards the system performance varies if the stiffness changes. More specifically the users' responses about the handshake vigour, which is measured by the *naturalness* metric, will differ. The stiffness of the robot arm that interacts with the user is modulated by the operator's anatomical arm stiffness using EMG-based myo armband sensor. (Van Teeffelen et al., 2018) have already tested the effectiveness of conveying the operator's stiffness to the remote site, but that was for conveying the stiffness to a remote *environment*. In this project, the myo armband sensor is, instead, tested for conveying the operator's muscles contraction (or stiffness) to a remote *human*. Objective evaluation for the effectiveness of this method was already shown in the previous chapter in Figure 5.10. However, solely objective evaluation may not be sufficient. UX evaluation is also required to see if the human recipient indeed feels the changes in the operator's arm muscles contraction and feels the operator presence, which is one of the vital system requirement for the XPRIZE competition, and also to see if using this method leads to having a realistic handshake experience.

The alternate hypothesis of naturalness was that if the stiffness is variable and modulated based on the operator's anatomical arm stiffness, then that corresponds to more natural handshake. This can be clearly seen in the Figure 6.2. Now, in order to test how far this hypothesis is correct, a one-way[4] ANOVA repeated-measures test is executed to analyze the differences among the groups' means to investigate whether or not there is statistical significance in the obtained results.

groups	P-value	F_{crit}	F
low stiff.	0.016	3.31	4.76
var. stiff.			
high stiff.			

Table 6.5: ANOVA test for naturalness results

As can be seen form the table above, the P-value is less than the significance level 0.05. This means that the obtained results are statistically significant. The null hypothesis is rejected if the $F > F_{crit}$ which is the case. Therefore the null hypothesis is rejected, and consequently the alternate hypothesis is supported.
Observing the system's grades at naturalness in Figure 6.2, it can be seen that the system has failed in realizing natural handshake in the case of low stiffness and barely passed in the case of high stiffness, where the scores are 38.6% and 50%, respectively. For low stiffness, the operator's forces to displace the recipient's arm are not effective, because the robot arm that the recipient interacts with does not follow the set points coming from the operator if the control parameter (which is the stiffness here) is low, and therefore the recipients do not feel synchrony or natural handshake. For extremely high stiffness, the recipient's robot arm is not even interactional, meaning that the recipient can hardly displace the arm because of the high stiffness. Accordingly, the participants did not find this handshake natural either. Whereas for variable stiffness, the handshake was reported to be the most natural, where the developed system has scored 77.3% at naturalness. This can be attributed to the fact that the handshake is a mutual process, where the handshake partners both contribute with forces and feel each other's forces, which was robotically realized by using the EMG sensor. Based on the participant's force and motion, the operator attempts to shake hands with the same force and motion, and so the participant feels a synchrony, seemingly.

6.4.3 Evaluation emotional state quality

The last UX evaluation is for the emotional state of the user during the handshake activity. This evaluation process is to evaluate how positive the remote handshake interaction is for the user, and whether the remote robotic handshake provides the same emotional state that the human obtains in real handshake situations. This non-physical quantity is measured by the *engagement* and *social positivity* metrics.

- **Engagement**: For this metric, the alternate hypothesis was defined as: the developed system scores at engagement at least 70%. And the system indeed has scored beyond 70% as the Figure 6.2 shows. The t-test shows clearly that the null hypothesis is rejected, and consequently the alternate hypothesis is accepted.

groups	P-value	t_{crit}	t_{stat}
Engagement	0,008	1,81	2.88

Table 6.6: One-sample one-tail t-test for engagement results

- **Social positivity** : Regarding the hypothesis of the social interaction positivity metric, the alternate hypothesis statement is that the system is able to record a score no smaller than

[4]"One-way" or "one-factor" anova test was chosen because there is only one variable being studied which the naturalness score. And ANOVA test itself was chosen because there are 3 groups.

70%. The UX evaluation experiment with the participants has shown that the system is able to provide social interaction positivity to participants with a score higher than 70%.

groups	P-value	t_{crit}	t_{stat}
Social positivity	0,0002	1,81	5,16

Table 6.7: One-sample one-tail t-test for interaction positivity results

The null hypothesis is rejected as the p-value is smaller than 0.05 the significant level. Consequently, the alternate hypothesis is supported and confirmed by the obtained results.

7 Conclusions and Recommendations

In this chapter, conclusions are drawn, and recommendations for future work are highlighted.

7.1 Conclusions

- Having the developed handshake system passed in the evaluation element of human recognition of robots, namely *social acceptance*, indicates that human recognition for handshake robot system seems to be positive. In other words, the human, apparently, accepts to interact with another human remotely through robot system; the human seems to be not averse to interacting with robots for achieving social activities such as handshake.[1] This consequently means that the design goal of *social usability* has been achieved.

- Using the personalized force feedback control architecture and obtaining high score at *naturalness* from the use of this variable-stiffness control gives the indication that the developed system has satisfied the design goal of *natural handshake*, and that it, seemingly, enables the handshake partners to feel the presence of each other. This also implies that the experiments have also validated that the EMG myo armband sensor is a relatively effective method of modulating the stiffness for the handshake application.

- Passing at the two metrics of *engagement* and *social positivity*, is indication about the overall user experience in doing the tele-handshake social activity. These two evaluation metrics are also two of design goals defined in the first chapter. So obtaining sufficiently high scores by the developed system at those two metrics means that the developed system seems to be capable of providing the user with a genuine engaging handshake experience.

7.2 Recommendations

- A recommendation for future work is that haptic devices should be used for the robot systems that are designed for achieving social activities such as handshake. Because having the system failed in the responsiveness assessment criterion is because of the robot itself that was used in the experiment, namely Franka robot arm which is not a haptic device, meaning its joints friction and mass ($18kg$) are relatively higher than those of a haptic device such as Virtuose 6D ($12kg$).

- Another future work recommendation is that humanoid robots should be used for social interaction applications. Because human-likeness evaluation measure was not satisfied because of the hardware limitations, specifically because of the way the Franka robot installed in RaM laboratory.

- In order to have more comprehensive handshake activity, arm control and hand control should be considered together, and then the entire system including the robot hand and arm is evaluated. Because it is not sufficient to obtain impression about the handshake partner only from the arm as was attempted in this work; interaction with hands in the handshake activity is also of importance (Knoop et al., 2017b)(Melnyk et al., 2014b). The user studies were performed using only robot arms. Thus it might be a good recommendation to integrate the different subsystems of handshake system in order to obtain a more robust evaluation and a clearer insight whether or not the handshake activity can be done effectively using robot system.

[1] The author is aware that drawing conclusions from experiments that were ran over small population of participants might be slightly inaccurate.

- Another recommendation might be testing the proposed control architecture, that enables personalized force feedback, with other methods of human impedance estimation.

- The last recommendation is to investigate the changes that should be made to the passivity layer. Usually, in the passivity layer of a tele-operation system, there is one TLC (tank level controller) at the master because this is where the operator exists, but for tele-handshake system, there are two operators, which theoretically means that there should be two TLC's. This should be investigated and possibly tested.

A Motion of rigid body

The material for this appendix is from the lecture notes on geometry and screw theory for robotics (Stramigioli and Bruyninckx, 2001).

1.1 Kinematics of rigid body

Consider the rigid body in figure 1.1 with a body-fixed reference frame Ψ_1. The pose of the rigid body with respect to the inertial reference frame is expressed as a configuration matrix in the Lie group $SE(3)$ as follows:

$$H_1^0 = \begin{pmatrix} R_1^0 & p_1^0 \\ 0_3 & 1 \end{pmatrix} \tag{A.1}$$

where $R_1^0 \in SO(3)$ is the rotation matrix in of the body with respect to the reference frame, and p_1^0 is the position of the body with respect to the inertial frame. The general velocity of the rigid body with respect to the reference frame expressed in the reference frame is written as a vector in $\mathbb{R}^6$ as follows:

$$^0T_1^0 = \left[{}_x, {}_y, {}_x, v_x, v_y, v_z\right]^T \tag{A.2}$$

where w is the angular velocity and v is the linear velocity. A relation between the rigid body pose and its general velocity is in terms of the time-derivative of H-matrix:

$$^0\tilde{T}_1^0 = \dot{H}_1^0 \cdot (H_1^0)^{-1} \tag{A.3}$$

where $\tilde{T}$ is the tilde form of the twist in the Lie algebra $se(3)$.

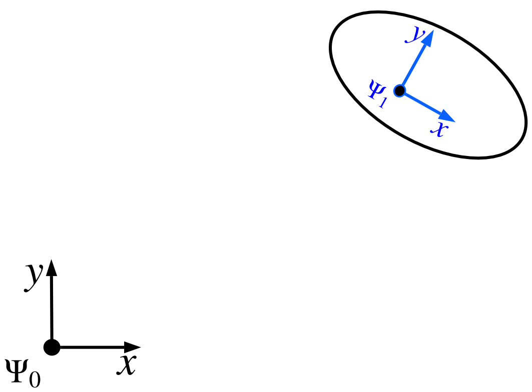

Figure 1.1: A schematic of a rigid body with showing the body-fixed frame as well as the inertial frame

1.2 Forward kinematics

Forward kinematics, or Brockett's formula, can be used to find the position of the end-effector of a serial manipulator depending on the unit twists of the joints, the joints position in the joint space and the initial configuration of the robot.

The exponential map enables calculating the joint configuration H-matrix with respect to the previous joint's frame based on the joint's tilde-form twist and the joint angle as in the following relation:

$$H_i^{i-1}(q_i) = e^{{}^{(i-1)}\tilde{T}_i^{(i-1)} q_i} H_i^{i-1}(0) \tag{A.4}$$

The chain rule can be used to find the transformation between any two joints of the serial manipulator. It is given as follows:

$$H_n^0 = H_1^0 H_2^1 \dots H_n^{n-1} \tag{A.5}$$

Substituting A.4 into A.5 the Brockett's formula for the seven-joint Franka-Panda serial manipulator to calculate the end-effector pose is obtained:

$$H_7^0\left(q_1, q_2, \dots, q_7\right) = e^{{}^0\tilde{T}_1^0 q_1} e^{{}^0\tilde{T}_2^1 q_2} \dots e^{{}^0\tilde{T}_7^6 q_7} H_7^0(0) \tag{A.6}$$

The unit twists are calculated when the robot is in the initial configuration.

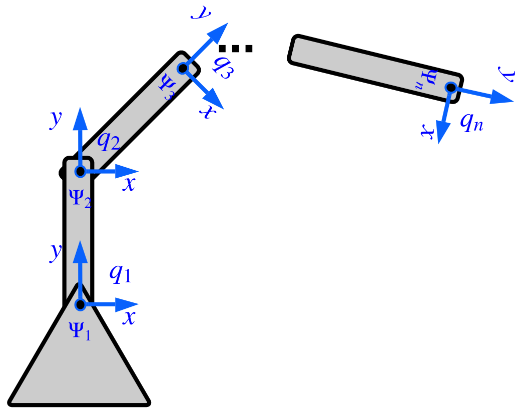

Figure 1.2: A schematics for a serial kinematic chain

1.3 Differential kinematics (geometric Jacobian)

The geometric Jacobian is a mapping from the joints' velocities to the end-effector twist of a serial manipulator, given as in the following relation:

$$ {}^0T_n^0 = J(q)\dot{q} \tag{A.7}$$

where the columns $J(q)$ are the positions-dependent unit twists of the joints expressed in the reference frame:

$$J(q) = \begin{bmatrix} {}^0T_1^0\left(q_1\right) & {}^0T_2^1\left(q_2\right) & \dots & {}^0T_n^{n-1}\left(q_n\right) \end{bmatrix} \tag{A.8}$$

where those unit twists are obtained by first finding the unit twists expressed in the previous reference frame, and then transforming that twist using adjoint matrix. So the dependency of the Jacobian on the joints positions comes indirectly from the adjoint matrix as the equation below shows:

$$ {}^0T_n^{n-1} = \mathrm{Ad}_{H_{n-1}^0(q_n)} . {}^{n-1}\hat{T}_n^{n-1} \tag{A.9}$$

where the adjoint matrix is given as follows:

$$\mathrm{Ad}_{H_{n-1}^0} = \begin{bmatrix} R_{n-1}^0 & 0 \\ \tilde{p}_{n-1}^0 R_{n-1}^0 & R_{n-1}^0 \end{bmatrix} \tag{A.10}$$

1.4 Inverse kinematics

Inverse kinematics is the problem of finding the required joints torques to set the robot in a certain configuration. For a serial manipulator, inverse kinematics is performed using the transpose of the Jacobian as follows:

$$\tau = J^T . {}^0W^{ee} \tag{A.11}$$

where ${}^0Wee$ is the wrench of the virtual spring that is assumed to be connect to the end-effector and controls the compliance of the serial manipulator.

B Human shake forces

The experiment of measuring the shake force was done with the help of 12 participants. For every participant 9 trials were performed at different conditions. The results of forces are listed in table below.

2.1 Low stiffness

Subject No.	Weak force [N]	Normal force [N]	Strong force [N]
1	5.785	10.11	14.6
2	15.05	24.78	27.23
3	9.93	15.94	25.25
4	13.36	14.06	15.38
5	6.41	9.62	15.31
6	7.04	9.53	16.16
7	9.2	16.24	15.85
8	13.7	15.96	16.17
9	8.24	13.38	22.4
10	7.13	13.97	18.23
11	6.0	10	19.58
12	5.35	8.72	11.27

Table 2.1: The subjects' forces during the condition of low stiffness

2.2 Medium stiffness

Subject No.	Weak force [N]	Normal force [N]	Strong force [N]
1	11.22	11.46	17.12
2	9.17	14.36	20.51
3	5.07	11.47	17.59
4	8.53	18.23	23.07
5	11.69	10.95	22.61
6	4.45	9.28	17.3
7	5.93	8.63	13.29
8	10.05	16.97	12.47
9	12.32	14.75	20.3
10	8.46	10.85	11.21
11	8.04	13.05	20.12
12	7.46	11.46	12.2

Table 2.2: The subjects' forces during the condition of medium stiffness

2.3 High stiffness

Subject No.	Weak force [N]	Normal force [N]	Strong force [N]
1	5.41	6.96	12.44
2	9.96	13.37	16.03
3	14.29	19.84	17.78
4	11.97	17.69	19.92
5	7.02	10	15.07
6	5.88	7.42	19.16
7	12.1	11.17	19.07
8	17.46	21.07	20.83
9	6.56	10.17	12.1
10	8.15	12.98	16.4
11	8.13	12.64	17.05
12	16.28	17.46	20.49

Table 2.3: The subjects' forces during the condition of high stiffness

Bibliography

Ajoudani, A., C. Fang, N. Tsagarakis and A. Bicchi (2018), Reduced-complexity representation of the human arm active endpoint stiffness for supervisory control of remote manipulation, in *The International Journal of Robotics Research*, volume 37, SAGE Publications Sage UK: London, England, pp. 155–167.

Ajoudani, A., S. B. Godfrey, M. Bianchi, M. G. Catalano, G. Grioli, N. Tsagarakis and A. Bicchi (2014), Exploring teleimpedance and tactile feedback for intuitive control of the pisa/iit soft-hand, in *IEEE transactions on haptics*, volume 7, IEEE, pp. 203–215.

Ajoudani, A., N. Tsagarakis and A. Bicchi (2012), Tele-impedance: Teleoperation with impedance regulation using a body–machine interface, **vol. 31**, no.13, pp. 1642–1656.

Alhalabi, M. O. and S. Horiguchi (2001), Tele-handshake: a cooperative shared haptic virtual environment, in *Proceedings of Eurohaptics*, volume 2001, University of Birmingham Press UK, pp. 60–64.

Arns, M., T. Laliberté and C. Gosselin (2017), Design, control and experimental validation of a haptic robotic hand performing human-robot handshake with human-like agility, in *2017 IEEE/RSJ International Conference on Intelligent Robots and Systems (IROS)*, IEEE, pp. 4626–4633.

Artemiadis, P. K., P. T. Katsiaris, M. V. Liarokapis and K. J. Kyriakopoulos (2010), Human arm impedance: Characterization and modeling in 3d space, in *2010 IEEE/RSJ International Conference on Intelligent Robots and Systems*, IEEE, pp. 3103–3108.

Avraham, G., I. Nisky, H. L. Fernandes, D. E. Acuna, K. P. Kording, G. E. Loeb and A. Karniel (2012), Toward perceiving robots as humans: Three handshake models face the turing-like handshake test, in *IEEE Transactions on Haptics*, volume 5, IEEE, pp. 196–207.

Ben-Tzvi, P. and Z. Ma (2014), Sensing and force-feedback exoskeleton (safe) robotic glove, in *IEEE Transactions on Neural Systems and Rehabilitation Engineering*, volume 23, IEEE, pp. 992–1002.

Brygo, A., I. Sarakoglou, A. Ajoudani, N. Hernandez, G. Grioli, M. Catalano, D. G. Caldwell and N. Tsagarakis (2016), Synergy-based interface for bilateral tele-manipulations of a master-slave system with large asymmetries, in *2016 IEEE International Conference on Robotics and Automation (ICRA)*, IEEE, pp. 4859–4865.

Camlibel, K., A. A. Julius, R. Pasumarthy and J. M. Scherpen (2015), *Mathematical Control Theory I: Non- linear and Hybrid Control Systems*, Springer.

Casini, S., M. Morvidoni, M. Bianchi, M. Catalano, G. Grioli and A. Bicchi (2015), Design and realization of the cuff-clenching upper-limb force feedback wearable device for distributed mechano-tactile stimulation of normal and tangential skin forces, in *2015 IEEE/RSJ International Conference on Intelligent Robots and Systems (IROS)*, IEEE, pp. 1186–1193.

Catalano, M. G., G. Grioli, E. Farnioli, A. Serio, C. Piazza and A. Bicchi (2014), Adaptive synergies for the design and control of the Pisa/IIT SoftHand, in *The International Journal of Robotics Research*, volume 33, SAGE Publications Sage UK: London, England, pp. 768–782.

Chang, P. H., K. Park, S. H. Kang, H. I. Krebs and N. Hogan (2012), Stochastic estimation of human arm impedance using robots with nonlinear frictions: An experimental validation, in *IEEE/ASME Transactions on Mechatronics*, volume 18, IEEE, pp. 775–786.

Deaconescu, T. and A. Deaconescu (2018), Static analysis of a torsion motor generating flexion-extension motions of the elbow, in *MATEC Web of Conferences*, volume 178, EDP Sciences, p. 07005.

Della Santina, C., C. Piazza, G. Grioli, M. G. Catalano and A. Bicchi (2018), Toward dexterous manipulation with augmented adaptive synergies: The pisa/iit softhand 2, in *IEEE Transactions on Robotics*, volume 34, IEEE, pp. 1141–1156.

Dolan, J. M., M. B. Friedman and M. L. Nagurka (1993), Dynamic and loaded impedance components in the maintenance of human arm posture, in *IEEE transactions on systems, man, and cybernetics*, volume 23, IEEE, pp. 698–709.

Fang, C., A. Ajoudani, A. Bicchi and N. G. Tsagarakis (2018), A real-time identification and tracking method for the musculoskeletal model of human arm, in *2018 IEEE International Conference on Systems, Man, and Cybernetics (SMC)*, IEEE, pp. 3472–3479.

Filippeschi, A., N. Schmitz, M. Miezal, G. Bleser, E. Ruffaldi and D. Stricker (2017), Survey of motion tracking methods based on inertial sensors: A focus on upper limb human motion, in *Sensors*, volume 17, Multidisciplinary Digital Publishing Institute, p. 1257.

Folkertsma, G. and S. Stramigioli (2001), Energy in Robotics.

Franken, M., S. Stramigioli, S. Misra, C. Secchi and A. Macchelli (2011), Bilateral telemanipulation with time delays: A two-layer approach combining passivity and transparency, in *IEEE transactions on robotics*, volume 27, IEEE, pp. 741–756.

Franken, M., S. Stramigioli, R. Reilink, C. Secchi, A. Macchelli et al. (2009), Bridging the gap between passivity and transparency., in *Robotics: Science and Systems*.

Grioli, G., M. Catalano, E. Silvestro, S. Tono and A. Bicchi (2012), Adaptive synergies: an approach to the design of under-actuated robotic hands, in *2012 IEEE/RSJ International Conference on Intelligent Robots and Systems*, IEEE, pp. 1251–1256.

Jazayeri, A., M. Dyck and M. Tavakoli (2013), Stability analysis of teleoperation systems under strictly passive and non-passive operator, in *2013 World Haptics Conference (WHC)*, IEEE, pp. 695–700.

Jindai, M., S. Ota, Y. Ikemoto and T. Sasaki (2015), Handshake request motion model with an approaching human for a handshake robot system, in *2015 IEEE 7th International Conference on Cybernetics and Intelligent Systems (CIS) and IEEE Conference on Robotics, Automation and Mechatronics (RAM)*, IEEE, pp. 265–270.

Jindai, M. and T. Watanabe (2007), Development of a handshake robot system based on a handshake approaching motion model, in *2007 IEEE/ASME international conference on advanced intelligent mechatronics*, IEEE, pp. 1–6.

Jindai, M. and T. Watanabe (2011), Development of a handshake request motion model based on analysis of handshake motion between humans, in *2011 IEEE/ASME International Conference on Advanced Intelligent Mechatronics (AIM)*, IEEE, pp. 560–565.

Jindai, M., T. Watanabe, S. Shibata and T. Yamamoto (2006), Development of a handshake robot system for embodied interaction with humans, in *ROMAN 2006-The 15th IEEE International Symposium on Robot and Human Interactive Communication*, IEEE, pp. 710–715.

Knoop, E., M. Bächer and P. Beardsley (2017a), Contact pressure distribution as an evaluation metric for human-robot hand interactions, in *HRI 2017 Workshop: Towards Reproducible HRI Experiments: Scientific Endeavors, Benchmarking and Standardization*.

Knoop, E., M. Bächer, V. Wall, R. Deimel, O. Brock and P. Beardsley (2017b), Handshakiness: Benchmarking for human-robot hand interactions, in *2017 IEEE/RSJ International Conference on Intelligent Robots and Systems (IROS)*, IEEE, pp. 4982–4989.

Kunii, Y. and H. Hashimoto (1995), Tele-handshake using handshake device, in *Proceedings of IECON'95-21st Annual Conference on IEEE Industrial Electronics*, volume 1, IEEE, pp. 179–182.

Lawrence, D. A. (1992), Stability and transparency in bilateral teleoperation, in *[1992] Proceedings of the 31st IEEE Conference on Decision and Control*, IEEE, pp. 2649–2655.

Lazar, A. I. (2019), Safe use of Robotic Arms as Input Devices, University of Twente.

Lindblom, J. and R. Andreasson (2016), Current challenges for UX evaluation of human-robot interaction, in *Advances in ergonomics of manufacturing: Managing the enterprise of the future*, Springer, pp. 267–277.

Melnyk, A., V. P. Borysenko and P. Henaff (2014a), Analysis of synchrony of a handshake between humans, in *2014 IEEE/ASME International Conference on Advanced Intelligent Mechatronics*, IEEE, pp. 1753–1758.

Melnyk, A., P. Henaff, V. Khomenko and V. Borysenko (2014b), Sensor network architecture to measure characteristics of a handshake between humans, in *2014 IEEE 34th International Scientific Conference on Electronics and Nanotechnology (ELNANO)*, IEEE, pp. 264–268.

Mersha, A. Y., S. Stramigioli and R. Carloni (2013), On bilateral teleoperation of aerial robots.

Miyoshi, T., Y. Ueno, K. Kawase, Y. Matsuda, Y. Ogawa, K. Takemori and K. Terashima (2015), Development of handshake gadget and exhibition in Niconico Chokaigi, in *Haptic Interaction*, Springer, pp. 267–272.

Nakanishi, H., K. Tanaka and Y. Wada (2014), Remote handshaking: touch enhances video-mediated social telepresence, in *Proceedings of the SIGCHI Conference on Human Factors in Computing Systems*, pp. 2143–2152.

Orefice, P.-H., M. Ammi, M. Hafez and A. Tapus (2016), Let's handshake and i'll know who you are: Gender and personality discrimination in human-human and human-robot handshaking interaction, in *2016 IEEE-RAS 16th International Conference on Humanoid Robots (Humanoids)*, IEEE, pp. 958–965.

Orefice, P.-H., M. Ammi, M. Hafez and A. Tapus (2018), Pressure Variation Study in Human-Human and Human-Robot Handshakes: Impact of the Mood, in *2018 27th IEEE International Symposium on Robot and Human Interactive Communication (RO-MAN)*, IEEE, pp. 247–254.

Ouchi, K. and S. Hashimoto (1997), Handshake telephone system to communicate with voice and force, in *Proceedings 6th IEEE International Workshop on Robot and Human Communication. RO-MAN'97 SENDAI*, IEEE, pp. 466–471.

Papageorgiou, D. and Z. Doulgeri (2015), A kinematic controller for human-robot handshaking using internal motion adaptation, in *2015 IEEE International Conference on Robotics and Automation (ICRA)*, IEEE, pp. 5622–5627.

Pedemonte, N., T. Laliberté and C. Gosselin (2016), Design, control, and experimental validation of a handshaking reactive robotic interface, in *Journal of Mechanisms and Robotics*, volume 8, American Society of Mechanical Engineers Digital Collection.

Pedemonte, N., T. Laliberté and C. Gosselin (2017), A haptic bilateral system for the remote human–human handshake, in *Journal of Dynamic Systems, Measurement, and Control*, volume 139, American Society of Mechanical Engineers Digital Collection.

Sakow, M., A. Parus, M. Pajor and K. Miadlicki (2018), Unilateral hydraulic telemanipulation system for operation in machining work area, in *Advances in Manufacturing*, Springer, pp. 415–425.

Schaft, A. v. d. and A. Schaft (1999), *L2-gain and passivity in nonlinear control*, Springer-Verlag.

Scheggi, S. and G. Salvietti (2014), Haptic guidance in urban search and rescue scenarios with reduced visibility, in *Proc. 20th IMEKO TC4 Int. Symp. and 18th Int. Workshop on ADC Modelling and Testing Research on Electric and Electronic Measurement for the Economic Upturn, Benevento, Italy*.

Shipps, E. M. and H. R. Freeman (2003), Handshake: Its relation to first impressions and measured personality traits, in *Psi Chi Journal of Undergraduate Research*, volume 8, pp. 144–148.

Stramigioli, S. and H. Bruyninckx (2001), Geometry and screw theory for robotics, *Tutorial during ICRA*, **vol. 2001**, p. 75.

Tagne, G., P. Hénaff and N. Gregori (2016), Measurement and analysis of physical parameters of the handshake between two persons according to simple social contexts, in *2016 IEEE/RSJ International Conference on Intelligent Robots and Systems (IROS)*, IEEE, pp. 674–679.

Tsalamlal, M. Y., J.-C. Martin, M. Ammi, A. Tapus and M.-A. Amorim (2015), Affective handshake with a humanoid robot: How do participants perceive and combine its facial and haptic expressions?, in *2015 International Conference on Affective Computing and Intelligent Interaction (ACII)*, IEEE, pp. 334–340.

Van Teeffelen, K., D. Dresscher, W. Van Dijk and S. Stramigioli (2018), Intuitive Impedance Modulation in Haptic Control using Electromyography, in *2018 7th IEEE International Conference on Biomedical Robotics and Biomechatronics (Biorob)*, IEEE, pp. 1211–1217.

Vigni, F., E. Knoop, D. Prattichizzo and M. Malvezzi (2019), The role of closed-loop hand control in handshaking interactions, in *IEEE Robotics and Automation Letters*, volume 4, IEEE, pp. 878–885.

Wang, F., W. Zhang and W. Luo (2018), An Empirical Evaluation on Vibrotactile Feedback for Wristband System, *Mobile Information Systems*, **vol. 2018**.

Wang, Z., A. Peer and M. Buss (2009), An HMM approach to realistic haptic human-robot interaction, in *World Haptics 2009-Third Joint EuroHaptics conference and Symposium on Haptic Interfaces for Virtual Environment and Teleoperator Systems*, IEEE, pp. 374–379.

Werner, K., J. Oberzaucher and F. Werner (2012), Evaluation of human robot interaction factors of a socially assistive robot together with older people, in *2012 sixth International Conference on complex, intelligent, and software intensive systems*, IEEE, pp. 455–460.

Willems, J. C. (1972), Dissipative dynamical systems part I: General theory, in *Archive for rational mechanics and analysis*, volume 45, Springer, pp. 321–351.

Yamato, Y., M. Jindai and T. Watanabe (2008), Development of a shake-motion leading model for human-robot handshaking, in *2008 SICE Annual Conference*, IEEE, pp. 502–507.